ACOUSTIC EMISSION VIS-À-VIS ELECTROCHEMICAL TECHNIQUES FOR CORROSION ASSESSMENT IN RC ELEMENTS

Thesis

Submitted for the award of

DOCTOR OF PHILOSOPHY

by

SHILPA PATIL

(Regd. No 950902007)

Under the supervision of

Dr. Shweta Goyal
Associate Professor
Thapar University
Patiala-147004

Dr. Bilavari Karkare
Professor & Principal
Vishwakarma Inst. of Information Tech.
Pune-411048

CIVIL ENGINEERING DEPARTMENT

THAPAR UNIVERSITY, PATIALA - 147004

MAY - 2015

CERTIFICATE

This is to certify that the work presented in the thesis titled, **"ACOUSTIC EMISSION VIS-À-VIS ELECTROCHEMICAL TECHNIQUES FOR CORROSION ASSESSMENT IN RC ELEMENTS"** which is being submitted by **Mrs. Shilpa Patil, Regd. No 950902007**, in fulfillment of the requirement for the award of the degree of **'Doctor of Philosophy'** in the Department of Civil Engineering, Thapar University, Patiala, is an authentic record of the candidate's own work. . Mrs. Shilpa Patil has worked under our guidance and supervision. To the best of our knowledge, the thesis has reached the requisite standard. The matter presented in this thesis has not been submitted for the award of any other degree in any other university.

Dr. Shweta Goyal
Assistant Professor
Dept. of Civil Engineering
Thapar University
Patiala - 147004
India

Dr. Bilavari Karkare
Professor and Principal
Dept. of Civil Engineering
Vishwakarma Inst. of Information Tech.
Pune - 411048
India

ACKNOWLEDGEMENTS

The Almighty has provided me the cherished opportunity to express my heartfelt gratitude to my guides for their invaluable guidance and constant encouragement throughout the period of doctoral programme. I am cherished to express my thankfulness to my mentors Dr. Shweta Goyal, Assistant Professor, Civil Engineering Department, Thapar University, Patiala, and Dr. (Prof.) Bilavari Karkare, Principal and Professor, Civil Engineering Department, Vishwakarma Institute of Information Technology, Pune. I will always remain indebted to them for their meticulous guidance, constructive criticism, clear thinking and constant encouragement till the completion of the work. Their systematic approach and unconditional co-operation made me work hard. Indeed, I shall remain grateful to them forever.

I am thankful to Dr. C. S. Garde, Department of Applied Science and Engineering, Dr. H. B. Dhonde and Dr. M. A. Mahajan, Department of Civil Engineering, Vishwakarma Institute of Information Technology, Pune as well as Dr. S. G. Karkare, expert in the field of corrosion science for their unconditional support during my experimental work.

I also put on record my sincere thanks to Dr. R. D. Angal, Retired Professor, Department of Material Science and Metallurgical Engineering, IIT Bombay and the expert in the field of corrosion science for his valuable guidance and constant assistance in my research work.

I greatly acknowledge “Board of College and University Development”, Savitribai Phule Pune University and “Rajiv Gandhi Science and Technology

provided a great financial help for my research work. I would also like to thank the authorities of Vishwakarma Institute of Information Technology for providing me the financial assistance as and when required.

I am also thankful to Mr. V. N. Rao (Physical Acoustics India Private Ltd.) and Mr. Vinay Achawal (Crest Technology, Pune) for providing constant support during the development of experimental setup through imparting the knowledge about equipment used in the research work.

I am highly obliged to my colleagues in the Department of Civil Engineering, for constantly encouraging me during my tenure of work. Along with this, the active support and enthusiasm provided by non-teaching faculty of Workshop Department, Vishwakarma Institute of Information Technology, Pune, during preparation of experimental set up is greatly acknowledged.

I thank my parents, Mr. Manikrao Chivate and Mrs. Bharati Chivate, as well as my in-laws Mr. Dilip Patil and Mrs. Vijayshree Patil whose love and affectionate blessings help me in achieving all my goals in life. The blessings of my brother Mr. Sachin, sister in-law Mrs. Milan, Sister Mrs. Roopali, friends and relatives helped a long way in achieving my objective.

Above all, a word of admiration to my husband, Mr. Vishal Patil, without whose inspiration and strength, I would not have been able to achieve this pursuit. My son Mihir always kept my morale high with his ever smiling and cheerful face.

Patil

(Mrs. SHILPA PATIL)

ABSTRACT

Reinforced concrete (RC) structures have the potential to be very durable and capable of withstanding a variety of adverse environmental conditions. However, failures in the RC structures still occur due to adverse effects of external or environmental agencies. One of the main causes leading to degradation of RC structures is the corrosion of steel reinforcement.

Corrosion of steel rebar in concrete is an electrochemical process and it has been widely studied using various non-destructive techniques. Half-cell potential measurement is one of the most widely used, practical and standardised non-destructive method which provides an indication of the likelihood of corrosion activity at the time of measurement. The other electrochemical methods such as linear polarisation resistance, electrochemical impedance spectroscopy etc. provide corrosion rate, but the calculations are based on certain assumptions of degree of polarization of the embedded bar. Another non-destructive technique widely used in practice is ultra-sonic pulse velocity measurement. Ultrasonic guided waves at high frequencies can be effectively used to distinguish between the loss of bar cross-sectional area and changing interface conditions. However, to produce guided waves in the rebar embedded in concrete, it is necessary to attach two transducers at the ends of the rebar projected out of concrete specimens, which is not possible in actual structural element. All these techniques cannot be called truly non-destructive techniques as these methods require either electrical or physical contact with steel embedded in concrete. Thus, to overcome all these difficulties, there is a need to develop a non-destructive methodology, which will assess the corrosion of steel

embedded in RC element effectively without physical contact with the rebar. The researchers have reported that acoustic emission (AE) technique is suitable for failure monitoring of various structures and can also identify onset of corrosion without physical contact with the rebar.

AE technique has been widely used to monitor and examine the behaviour of variety of materials. This technique is unique in the sense that it literally records the signals emitted from different sources within the structure under service loads. AE technique makes it possible to measure the ultrasonic elastic waves generated within a material by local micro displacements and is a tool which allows early detection of any mechanical, physical or chemical damage, as source of energy. These elastic waves or elastic energy generated within the structure at the location of distress, propagates as a stress wave in the structure and is detected by one or more AE sensors. By separating the back-ground noise from AE data and through detailed study of various parameters of AE, the physical phenomena or damages in different materials can be evaluated.

The earlier research reported that AE technique can be used for detecting onset of corrosion. AE technique is a qualitative method which can find the initiation of corrosion of steel embedded in concrete by identifying developed cracks in concrete, however it has not been used to quantify the rate of corrosion. Thus, it is necessary to develop a method to quantify the losses due to corrosion of rebar using AE technique. Hence, current research work aims to assess the corrosion of steel embedded in concrete using AE technique quantitatively.

In the present work, applicability of AE technique was studied vis-à-vis electrochemical techniques (half-cell potential measurement and Tafel extrapolation

technique) for corrosion assessment in RC elements. To achieve sufficient degree of corrosion in laboratory within limited time period, impressed current technique was used for accelerating corrosion process. Different variables used in the study include three bar diameters, two types of steel and two types of cement. A statistical tool (ANOVA) was used to study the effect of these variables on corrosion and hence on AE measurements. The result obtained from AE technique is correlated with the result of destructive technique i.e. actual gravimetric mass loss of steel embedded in concrete to develop a mathematical model. SOLVER function was used for the development of mathematical model. Further, the developed mathematical model was validated for realistic corrosion exposure conditions in the laboratory using internal chloride exposure.

The results of experimental work concluded that cumulative signal strength (CSS) parameter of AE technique is a promising parameter for corrosion monitoring studies as the variation of CSS w.r.t. time has shown a specific trend indicating active corrosion which is similar to the curve of typical phenomenological corrosion loss of steel due to seawater immersion. Chloride induced corrosion of steel embedded in concrete can be classified in two different stages. Both these stages are well identified by electrochemical techniques as far as corrosion process of steel embedded in concrete is concerned, whereas AE technique can identify the corrosion process of steel reinforcement as well as damage to concrete due to subsequent cracking.

The results of ANOVA using CSS values for all material variables viz. cement type, steel type and rebar diameter proved that there is not enough evidence to reject the null hypothesis which indicates that the effect of variables on magnitudes of CSS is not significant. Similarity in the results of ANOVA obtained for magnitudes of

corrosion current densities and CSS values satisfactorily validated the results of AE measurements.

The results of SOLVER confirmed that a non-linear relation exists between max CSS value and gravimetric mass loss. The relation between the two parameters is analogous to natural exponential growth function. From the results of experimental work conducted using internal chloride exposure, it is concluded that the developed mathematical model is well validated and can also be used appropriately for realistic corrosion exposure conditions in the laboratory.

Thus, AE technique proves to be a powerful and truly non-destructive technique for corrosion assessment and can be successfully used for quantification of corrosion of steel embedded in concrete without having physical/electrical contact with the steel, which is required in electrochemical techniques.

LIST OF PUBLICATIONS

1. Patil, Karkare & Goyal, "Acoustic Emission Technique for Damage Assessment of RC Structures", *International Journal of Research in Engineering Science & Technology*, Special Issue 1, Jan 2011, Civil Engg. 46-53.
2. Patil S., Karkare B., Goyal S., "Acoustic emission vis-à-vis electrochemical techniques for corrosion monitoring of reinforced concrete element", *Construction and Building Materials*, 2014; 68: 326-332.
3. Patil S., Karkare B., Goyal S., "Influence of material properties of reinforced concrete element on acoustic emission due to corrosion" *Concrete Research Letters,* 6(1), 11-20.
4. Patil S., Karkare B., Goyal S., "Quantitative interpretation of corrosion of steel rebar in concrete using acoustic emission technique", *communicated to "Measurement".*
5. Patil S., Karkare B., Goyal S., "A Novel Acoustic Emission based mathematical procedure for quantification of rebar corrosion in reinforced concrete", *communicated to "Current Science".*
6. Patil S., Karkare B., Goyal S., "Performance evaluation of accelerated corrosion techniques", *Under Preparation*

ABBREVIATIONS

Abbreviation	Word(s)
AE	Acoustic Emission
ANOVA	Analysis of Variance
C/D	Cover to rebar Diameter
CRS	Corrosion Resistant Steel
CSS	Cumulative Signal Strength
df	Degrees of Freedom
MS	Mean Squares
OPC	Ordinary Portland Cement
PPC	Portland Pozzolana Cement
SCE	Saturated Calomel Electrode
SS	Stainless Steel
SS*	Sum of Squares
TMT	Thermo Mechanically Treated

CONTENTS

LIST OF FIGURES

LIST OF TABLES

Table Caption **Page No.**

CHAPTER 1

INTRODUCTION

1.1. GENERAL

Reinforced concrete structures are generally durable under moderate environmental conditions. However, failures in the reinforced concrete structures do still occur due to adverse effects of external as well as internal factors causing deterioration and subsequent loss in service life. One of the most important causes for deterioration of reinforced concrete structures is corrosion of steel reinforcement. The common causes of corrosion initiation of reinforcing steel are the ingress of moisture, chloride ions and carbon dioxide to the steel surface. After initiation of corrosion, the corrosion products (iron oxides and hydroxides) are deposited in concrete pores around the rebar. This deposition within the restricted space sets up expansive stresses and results in cracking of concrete and spalling of concrete cover, thus resulting in progressive deterioration of the concrete *(Song & Saraswathy, 2007)*. Along with unpleasant appearance it weakens the concrete structure to a high degree. Moreover, bond strength between the steel and the concrete is also reduced (Fig. 1.1).

In a tropical country like India, that has more than 3000 km of coastline where approximately 80% of the annual rainfall takes place in the two monsoon months, corrosion related problems are alarming *(Gadve et al. 2009)*. In metro cities, the carbon and nitrogen oxide emissions aggravate the situation further by neutralizing the concrete cover. Hence, a reinforced concrete structure requires major restoration work within 15 years of its construction *(Gadve et al. 2009)*. The failure of structures due to reinforcement corrosion, in most of the cases, is manifested by loss of structural serviceability, characterized by concrete cracking and delamination. The concrete cracking and delamination not only impair the appearance of the structure

but also weakens its serviceability. Thus corrosion is of great importance while considering the safety and durability of reinforced concrete structures. This problem has reached alarming proportions in the past three decades, leading to very high repair costs, sometimes above the initial construction cost or in extreme situations leading to the final collapse of the structure *(Montemor et al. (2003))*

(a) Corrosion of beam

(b) Corrosion of column

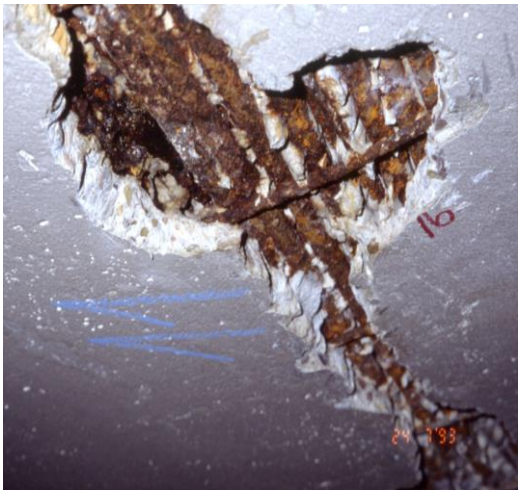

(c) Corrosion of slab

Fig. 1.1. Corrosion in reinforced concrete structures

1.2. CORROSION OF STEEL EMBEDDED IN CONCRETE

The corrosion of steel embedded in concrete is an electrochemical process that requires a flow of electric current and several chemical reactions forming a galvanic corrosion cell. The three essential components of this cell are,

(a) Anode,

(b) Cathode and

(c) Electrolyte.

Fig. 1.2 illustrates the reactions taking place during corrosion of steel embedded in concrete.

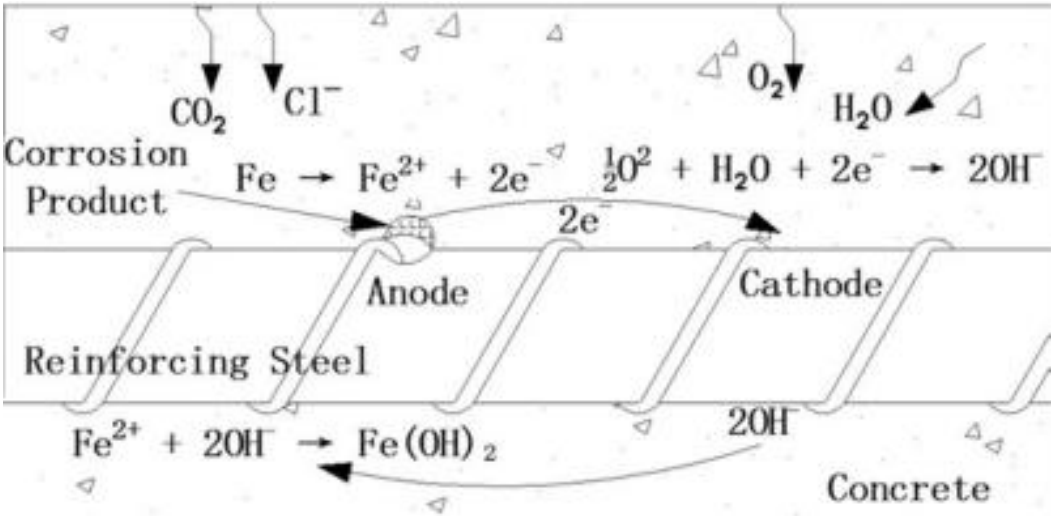

Fig.1.2. Corrosion cell in reinforced concrete *(mdpi.com)*

In reinforced concrete, the anode and the cathode of galvanic corrosion cell are on the same steel bar. At the anode, corrosion is taking place and metal is being lost where, the iron atoms lose electrons to become iron ions (Fe^{++}). This oxidation reaction is referred to as the anodic reaction as given below *(Broomfield, 2007).*

$$Fe = (Fe^{++}) + 2e^- \quad (1.1)$$

At the cathode, oxygen in the presence of water, accepts electrons to form hydroxyl ions $(OH)^-$. This reduction reaction is referred to as the cathodic reaction as:

$$2e^- + H_2O + \frac{1}{2} O_2 = 2OH^- \quad (1.2)$$

These hydroxyl ions then combine with the ferrous ions to form ferrous hydroxide:

$$Fe^{++} + 2OH^- = Fe(OH)_2 \quad (1.3)$$

In the presence of water and oxygen, the ferrous hydroxide is further oxidized to form Fe_2O_3 as below:

$$4Fe(OH)_2 + O_2 + 2H_2O = 4Fe(OH)_3 \quad (1.4)$$

$$2Fe(OH)_3 = Fe_2O_3 . H_2O + 2H_2O \quad (1.5)$$

The flow of electrons (electric current) between the anode and the cathode takes place through the electrolyte solution. In reinforced concrete, the electrolyte solution is provided by the pore fluid of concrete surrounding the steel *(Broomfield, 2007).*

In a good quality concrete, the risk of corrosion is minimal as it normally provides good chemical and physical protection to the embedded steel reinforcement. Concrete is alkaline due to the presence of hydroxides of Calcium, Potassium and Sodium and the alkalinity typically ranges from pH 12 to 13. Due to the high alkalinity of the concrete pore water, the steel reinforcing bars are passivated by an iron oxide film (Fe_2O_3). This thin chemical oxide film around the embedded steel protects the steel from corrosion. Through intact cover the concrete provides physical protection to steel by retarding the access of oxygen, moisture and various aggressive species to the steel/concrete interface. The alkaline condition due to formation of dense and impermeable passive layer, if fully established and maintained, prevents further corrosion of the steel. However, the passivating environment is not always maintained. Two conditions can break down the passivating environment in concrete

without damaging the concrete. One is carbonation and other is chloride attack *(Broomfield, 2007).*

When carbon dioxide (CO_2) from the atmosphere penetrates concrete and dissolves in the pore solution, carbonic acid is formed. This acid reacts with the alkali in the cement to form carbonates and lower the pH of concrete to a level (pH below 10) where steel will corrode. When the alkalinity reaches an enough low level, the steel reinforcing bar becomes depassivated and in the presence of sufficient water and oxygen corrosion is initiated and propagated. Similarly, when chloride ions reach the reinforcing steel by penetrating the concrete through the pore water and cracks in the concrete, they destroy the passive oxide film surrounding the steel and initiate the corrosion *(Broomfield, 2007).* Corrosion of steel in concrete in the presence of chlorides, but with no oxygen (at the anode), takes place in several steps. At the anode, iron reacts with chloride ions to form an intermediate soluble iron-chloride complex:

$$Fe + 2Cl^- = (Fe^{++} + 2Cl^-) + 2e^- \quad (1.6)$$

When the iron-chloride complex diffuses away from the bar to an area with higher pH and concentration of oxygen, it reacts with hydroxyl ions to form $Fe(OH)_2$. This complex reacts with water to form ferrous hydroxide:

$$(Fe^{++} + 2Cl^-) + 2H_2O + 2e^- = Fe(OH)_2 + 2H^+ + 2Cl^- \quad (1.7)$$

The hydrogen ions then combine with electrons to form hydrogen gas:

$$2H^+ + 2e^- = H_2 \quad (1.8)$$

As in the case of corrosion of steel without chlorides, the ferrous hydroxide, in the presence of water and oxygen, is further oxidized to form Fe_2O_3 as shown in Eq. 1.4 and 1.5.

These corrosion products resulting from the corrosion of steel reinforcing bars occupy a volume several times than that of the original steel *(Gadve et al. 2009)*. This increased volume induces expansive stresses in the concrete resulting in cracks, delamination and successive spalling of concrete cover. This provides further an easy pathway for water and chlorides to reach the steel, thus accelerating the corrosion process and deteriorating the reinforced concrete structure.

1.3. NON-DESTRUCTIVE EVALUATION

Due to the large extent of corrosion problems encountered in reinforced concrete structures all over the world, the durability of the concrete structures exposed to aggressive environments has become a problem of major importance. Quality control, maintenance and planning for the restoration of such structures requires non-destructive inspections and monitoring techniques to detect the corrosion at an early stage. Properly monitoring the structures for corrosion performance and taking suitable measures at the appropriate time could result in enormous saving in maintenance related costs.

Corrosion monitoring can give complete information of changing condition of a structure in time. Usually the condition of the structures is monitored by visual inspection and remedial measures are resorted to only when the condition becomes very serious due to heavy rusting of steel reinforcement followed by cracking and spalling of concrete. It is desirable to monitor the condition of such strategic structures right from the construction stage by carrying out periodic corrosion surveys and maintaining a record of data *(Song & Saraswathy, 2007)*. Many non-destructive techniques for assessment of cracks developed in concrete and many electrochemical techniques for measurement of the corrosion rate of reinforcing steel in concrete are available. The commonly used non-destructive as well as electrochemical techniques

along with their uses and limitations are summarized in Table 1.1 and Table 1.2 respectively. From the tables it is clear that for simultaneous assessment of cracks developed in concrete and corrosion of steel embedded in concrete, combination of two or more non-destructive and electrochemical techniques is required. Thus, there is a need for development of methodology which will assess the damages in concrete as well as corrosion of steel in concrete using single non-destructive technique.

Table 1.1. Various Non-destructive Techniques for assessment of cracks in Concrete *(Mehta and Monteiro, 2006)*

Method	Detects	Limitations
Ultra Sonic Pulse Velocity Method	Presence of voids, cracks / Concrete Properties	Presence of reinforcing bar increases the wave velocity giving wrong results
Ground Penetrating Radar	Delamination/ Rebar Depth	Effective when spacing between rebar > 7cm and concrete cover> 40cm
X-Ray computed Tomography	Cracks / Rebar Depth	Not suitable for thin structures
Acoustic Emission	Presence of Fractures	Method is not quantitative

Table 1.2. Various Non-destructive / electrochemical Techniques for Corrosion Assessment of steel embedded in concrete *(Mehta and Monteiro, 2006; Song and Saraswathy, 2007)*

Method	Detects	Limitations
Half-Cell Potential Measurements	Corrosion Probability	Method is not quantitative
Linear Polarisation Resistance Method	Corrosion Rate	Measures average value of corrosion rate along the steel reinforcement
Concrete Resistivity Method	Corrosion Risk	Presence of reinforcing bars affects the measurements
Electrochemical Impedance Spectroscopy	Corrosion Rate	Measures average value of corrosion rate along the steel reinforcement
Ultra Sonic Pulse Velocity Method	Surface Defects like notches, pitting corrosion etc.	Requires physical contact with steel reinforcement
Acoustic Emission	Onset of corrosion	Method is not quantitative

1.4. SCOPE AND OBJECTIVES OF THE PRESENT RESEARCH WORK

It is observed that corrosion of steel rebar in concrete has been widely studied using various electrochemical as well as non-destructive techniques (as is critically reviewed and is presented in Chapter 2). Half-cell potential measurement is one of the most widely used, practical and standardised non-destructive method which provides an indication of the likelihood of corrosion activity at the time of measurement. However, it does not furnish direct information on the rate of corrosion of reinforcement. The other electrochemical methods such as linear polarisation resistance method, electrochemical impedance spectroscopy etc., though provides corrosion rate, the calculations are based on certain assumptions about how much of the underlying bar is polarised during the test. As a result, different devices are likely to give different corrosion rates even if testing were done at the same point *(Carino N. J., 1999)*. Also, these electrochemical techniques require localized damage to concrete cover to enable an electrical connection to be made to the reinforcing steel.

Another non-destructive technique widely used in practice is ultra-sonic pulse velocity measurement. But, the presence of reinforcement increases the apparent wave velocity of the concrete which affects the ultra-sonic pulse velocity measurements in concrete and may give erroneous results *(Mehta and Monteiro, 2006; Song and Saraswathy, 2007)*. Ultrasonic guided waves at high frequencies can be effectively used to distinguish between the loss of bar cross-sectional area and changing interface conditions *(Ervin et al. 2008)*, but to produce guided waves in the rebar embedded in concrete, there is a need to attach two transducers at the two ends of the rebar projected out of concrete specimens. This set-up for acquiring data is not possible for structures in practice.

All above mentioned techniques cannot be called truly non-destructive techniques as these methods require either electrical or physical contact with steel embedded in concrete. Thus, to overcome all these difficulties, there is a need to develop a non-destructive methodology, which will assess the corrosion of steel embedded in reinforced concrete element effectively. From the literature review, it is found that acoustic emission (AE) technique can be used for finding damages in concrete as well as for detecting onset of corrosion. Current research states that AE technique is a qualitative method which can find the initiation of corrosion of steel embedded in concrete by identifying developed cracks in concrete but can't find the extent or rate of corrosion.

Looking at this gap in research identified through the literature review, the objectives of the present research work are formulated as follows:

1. To carry out corrosion assessment of steel in RC elements using acoustic emission vis-à-vis electrochemical techniques.
2. To study the effect of cement type, steel type and bar diameter on corrosion and hence on acoustic emission measurements.
3. To develop mathematical model to assess the corrosion of steel embedded in concrete by co-relating non-destructive test results and destructive test results of specimens.
4. To validate the developed mathematical model for natural exposure conditions.

1.5. LAYOUT OF THE THESIS

The thesis presentation has been organized in seven chapters. In the **First Chapter**, the scope and objectives of the research work have been presented.

In the **Second Chapter**, a comprehensive and critical review of the relevant literature justifying the objectives of the research work is presented.

A pilot study is carried out to establish experimental set-up for accelerated corrosion using impressed current technique in laboratory. The details of these tests along with details of materials are presented in **Chapter Three**.

Chapter Four elaborates the experimental results for corrosion measurement of steel embedded in concrete under accelerated conditions using AE technique and electrochemical techniques and their comparison with each other.

Chapter Five deals with the overall influence of various materials used in research on corrosion and on AE measurements. The analysis of variance for identifying the factors affecting AE measurements is also presented in the fifth chapter. In addition, the chapter also explains the development of mathematical model for quantification of corrosion using AE technique.

Chapter Six explains methodology used for validation of impressed current technique and developed mathematical model for realistic corrosion exposure conditions.

Chapter Seven briefly summarizes the entire work. The conclusions drawn from the investigation are reported and the scope for future investigations in the area is highlighted in this chapter.

At the end, references cited in the entire work have been presented.

CHAPTER 2

LITERATURE REVIEW

2.1. INTRODUCTION

The objective of this chapter is to review the existing literature for corrosion assessment of steel embedded in concrete using electrochemical and AE technique. Exhaustive literature is available on corrosion process and its monitoring in reinforced concrete structures using various non-destructive techniques. The scope of this review is restricted to corrosion assessment using half-cell potential, Tafel extrapolation technique and AE technique. The natural corrosion process is usually slow and takes a long time to initiate. Hence to enable corrosion monitoring and its further investigations rapidly in laboratory, the specimens are usually subjected to accelerated corrosion. The different techniques for inducing and accelerating corrosion in laboratory have also been discussed in the present chapter.

2.2. ACCELERATED CORROSION TECHNIQUES

The first step towards investigating any corrosion related problem experimentally is to subject the specimens to accelerated corrosion. The accelerated corrosion technique is used for degradation of fresh reinforced concrete specimens to the condition that is expected to achieve after years of exposure to corrosive environment. Selection of an appropriate method for inducing corrosion into the test specimen is quite challenging *(Gadve 2008)*.

One of the effective method of inducing corrosion into RC specimens is alternate immersion into and removal from NaCl (Sodium Chloride) solution of concrete specimens, simulating alternate drying and wetting cycle *(Kawasaki et al.*

2010; Ohtsu and Tomoda 2008). Though the method is effective, it involves lots of practical difficulties in handling the samples for repeated drying and wetting cycles and the time required to achieve severe corrosion level is normally several weeks.

Another method of adding chlorides artificially to the concrete in situ can initiate the corrosion by depassivating steel rebars and corrosion can be further propagated by curing the RC specimens in salt water *(Pradhan & Bhattacharjee, 2009).* Acceleration of corrosion by this method can achieve severe corrosion level in a short period. Though this is a completely acceptable method, the research *(Poursaee and Hansson 2009)* suggested that there are extraneous effects of chlorides on the concrete itself. Therefore, exposure to concrete or pore solution containing chlorides should be avoided unless the goal is to determine the influence of contaminated mixture components. Instead, sufficient time should be allowed for steel to passivate before exposure to chlorides. Also, the method does not seem to be realistic taking into account the fact that in practical situations no concrete is deliberately cast or cured in salt water *(Gadve et al. 2009).*

The corrosion process can also be accelerated by impressing a positive direct current into the reinforcing steel bar to act as anode and negative current into some external inert cathode, using external DC source thereby developing a corrosion cell. Previous studies (*Yoon et al. 2000; Idrissi and Limam, 2003; Caré and Raharinaivo, 2007; Ohtsu and Tomoda 2008; Gadve et al. 2009*) confirmed that impressed current technique is a valid method to study the corrosion process of steel in concrete and showed similarities to natural corrosion pattern when solutions contain chlorides. The method suits very well to laboratory experimentation as it is very fast. Therefore, this method for accelerated corrosion is used in a variety of corrosion experiments

(Maaddawy and Soudki, 2003; Spainhour and Wootton, 2008; Gadve et al. 2009; Yoon et al. 2000; De Benedetti et al. 2013; Ing et al. 2005; Austin et al. 2004, Masoud and Soudki, 2006; Idrissi and Limam, 2003). Hence in the present experimental investigation, it was decided to use impressed current technique for acceleration of corrosion.

The detailed literature for all these methods used for accelerating corrosion is presented as below.

Kawasaki et al. (2010) conducted alternate dry-wet test on reinforced concrete beams and applied AE technique for corrosion assessment of steel embedded in concrete. The work confirmed that both the onset of corrosion and the nucleation of concrete cracking are clearly observed by AE technique. From the results, a great promise for AE techniques to monitor the corrosion process in RC structures was clarified.

Pradhan & Bhattacharjee (2009) illustrated the findings of an experimental investigation carried out on large number of specimens for evaluating the performance of different types of rebar in chloride contaminated concrete made with different types of cement through different corrosion rate techniques. For accelerating corrosion they admixed chloride in concrete with different concentration.

Ohtsu and Tomoda (2008) conducted experimental work to identify corrosion process using continuous acoustic emission (AE) monitoring. The tests were performed on reinforced concrete beams using accelerated corrosion test by impressed current technique and a cyclic wet and dry test. They found similar variation of AE activities in both the corrosion tests with the difference that the first AE activity in cyclic wet and dry test was observed on 40^{th} day while in impressed current test it was found on 4^{th} day.

Poursaee and Hansson 2009 described some of the pitfalls in assessing chloride-induced corrosion of steel in concrete by comparing the accelerated laboratory tests such as admixed chlorides and applied anodic current, electrochemical methods such as linear polarisation resistance and cyclic polarisation methods, macro vs. micro-cell corrosion along with half-cell potential. The study of the influence of surface finish of the reinforcing steel as well as different grades of steel on its corrosion was also carried out. The results concluded that accelerating the corrosion by applying an anodic current to rebar should be avoided unless the goal is to assess circumstances in which this happens in practice, such as stray current corrosion. Exposure to concrete or pore solution containing chlorides should be avoided unless the goal is to determine the influence of contaminated mixture components. Instead, sufficient time should be allowed for the steel to become passivated before exposure to chlorides. It is important to consider both microcell and macrocell corrosion. Ignoring the microcell component will underestimate the degree of corrosion. In interpreting the data obtained by half-cell potential measurements, environmental factors should be taken into account and, wherever possible, repeated condition analyses should be conducted at the same time of the year. Except for fundamental research on the corrosion processes, the type of reinforcing bar and its surface conditions should be representative of those used in practice, in order to evaluate field performance.

Care and Raharinaivo (2007) carried out accelerated corrosion tests by impressing current between steel embedded in mortar and a counter-electrode to study the process of corrosion leading to cracking in mortar. The specimens made of mortar reinforced with steel, were immersed in two types of solutions viz. solution containing chloride and solution without chlorides. The results obtained provided information on corrosion kinetics of embedded steel when corrosion is accelerated by impressed

current and show the similarities to natural corrosion pattern when solutions contain chlorides. The study concluded that accelerated corrosion test by impressed current is a valid method to study the corrosion process of steel in mortar, and its effects on the damage of mortar cover.

Maaddawy and Soudki (2003) investigated experimentally the influence of varying the impressed current density level to accelerate steel reinforcing corrosion in concrete structures. The study evaluated the concrete side strain behaviour, the crack width, and the mass loss due to uniform corrosion under different levels of corrosion rates. The study concluded that on the basis of mass loss and within the limits of the current density levels and the percentages of mass loss used, impressed current is a reliable technique to simulate the corrosion of steel reinforcement in concrete.

Ahmad Shamsad (2009) briefly addressed all the aspects of the impressed current technique and also provided a brief description of some of the alternative techniques for accelerating corrosion of steel in concrete. The study also investigated the relationship between theoretical and actual corrosion mass loss based on Faraday's law and commented that actual corrosion current density can be calculated using applied current density.

Thus, form the literature, it can be concluded that impressed current technique is a valid and reliable method to simulate the corrosion of steel reinforcement in concrete. Many researchers have used impressed current technique to accelerate the corrosion and to monitor corrosion using various non-destructive techniques. The literature on the same is presented in subsequent sections.

2.3. ELECTROCHEMICAL TECHNIQUES

Rebar corrosion is an electrochemical process which involves the transfer of electrically charged ions between two locations on the reinforcing bar with different potentials (anode and cathode) through the electrolyte solution provided by the pore fluid of concrete surrounding the steel *(Pradhan and Bhattacharjee, 2009; El-Gelany, 2001; Di Benedetti et al. 2013)*. To assess the corrosion of rebar, various electrochemical techniques are used which estimate corroded condition of rebar from the electrical data. The most widely used, practical and standardized electrochemical method is half-cell potential measurement which is a qualitative method providing an indication of the likelihood of corrosion activity at the time of measurement. Electrochemically, the corrosion rate measurement is based on the determination of anodic or cathodic corrosion current at the half-cell potential in the absence of any applied potential. The determination of anodic or cathodic currents separately in the absence of any applied potential is not possible in practice because the production of electrical charges at the anode is exactly equal to its consumption at the cathode to maintain equilibrium of the charges with a zero net current *(El-Gelany, 2001)*. Hence, the polarization resistance techniques are used for this purpose. Amongst various techniques, Tafel extrapolation technique is widely used method in practice. The detailed information of two techniques viz. half-cell potential and Tafel extrapolation technique are presented in subsequent sections.

2.3.1. Half-cell potential measurements

When there is active corrosion of steel rebar in concrete, current flow (ion migration) through the concrete between anodic and cathodic sites is accompanied by an electric potential field surrounding the corroding bar. These potential lines intersect the surface of the concrete and the potential at any point can be measured

using the half-cell potential method. By mapping equipotential contours on the surface, those portions of the structure where there is a high likelihood of corrosion activity are identified by their high negative potentials *(Carino N. J., 1999)*.

In principle, the half-cell potential of an electrode can be measured by coupling it with the hydrogen electrode which is in the standard state. However, in practice, it is rather cumbersome to use the hydrogen electrode and difficult to fabric as well. Hence it is preferable to use secondary electrodes which are easy to prepare and are quite reproducible. One such electrode is the calomel electrode in which mercury metal is reversible with mercurous ions produced by mercurous chloride. Since this salt of mercury is sparingly soluble, the activity of mercurous ions and hence the half-cell potential changes with the activity of the chloride ions. It is convenient to use saturated solution of potassium chloride. Thus, the cell is called as saturated calomel electrode (SCE) *(Angal R.D. 2010).*

In the present study, SCE is used for half-cell potential measurements. During the half-cell potential measurements, the positive terminal of the voltmeter is attached to the reinforcement and the negative terminal is attached to the reference electrode. A high-impedance voltmeter (normally >10 mV) is used so that there is very little current through the circuit. The electrical contact of reference electrode with the concrete is achieved through a porous plug. If the bar were corroding, the excess electrons in the bar would tend to flow from the bar to the half-cell and the voltmeter indicates a negative voltage. This half-cell potential is also called open-circuit potential. A more negative voltage reading means that the embedded bar has more excess electrons and hence a higher likelihood that the bar is corroding. Thus, the half-cell potential method provides an indication of the likelihood of corrosion

activity at the time of measurement. However, it does not furnish direct information on the rate of corrosion of the reinforcement *(Carino N. J., 1999).* As per *ASTM C 876-91* standard, the probability of reinforcement corrosion is as given in Table 2.1.

Table 2.1. Corrosion condition related with half-cell potential measurements *(Song and Saraswathy, 2007)*

Half-cell potential values		**Corrosion condition**
(mV vs SCE)	**(mV vs CSE)**	
< -426	< -500	Severe corrosion
< -276	< -350	High (<90% risk of corrosion)
-126 to -275	-350 to -200	Intermediate corrosion risk (uncertain)
> -125	> -200	Low(10% risk of corrosion)

2.3.2. Tafel extrapolation technique

Tafel extrapolation technique is a well-established electrochemical technique based on polarisation resistance method. The technique basically involves measuring the change in the open-circuit potential of the short circuited electrolytic cell when an external current is applied to the cell *(Carino N. J., 1999).* This can be accomplished potentiostatically by changing the potential of the reinforcing steel by a fixed amount and monitoring the current decay after a fixed time *(Song and Saraswathy, 2007).* Thus, a potential scan is applied to the specimen starting from open-circuit potential (E_{corr}) and extending to a few hundred millivolts (about 250 mV) either in the cathodic or anodic direction. The applied potential forces the specimen to assume a potential other than open-circuit potential. The current measured in this case is the difference between anodic and cathodic currents and is nonzero. The potential is

plotted against the measured current and the resulting potential-current diagram is referred to as the Tafel plot. Fig. 2.1 shows an idealized Tafel plot.

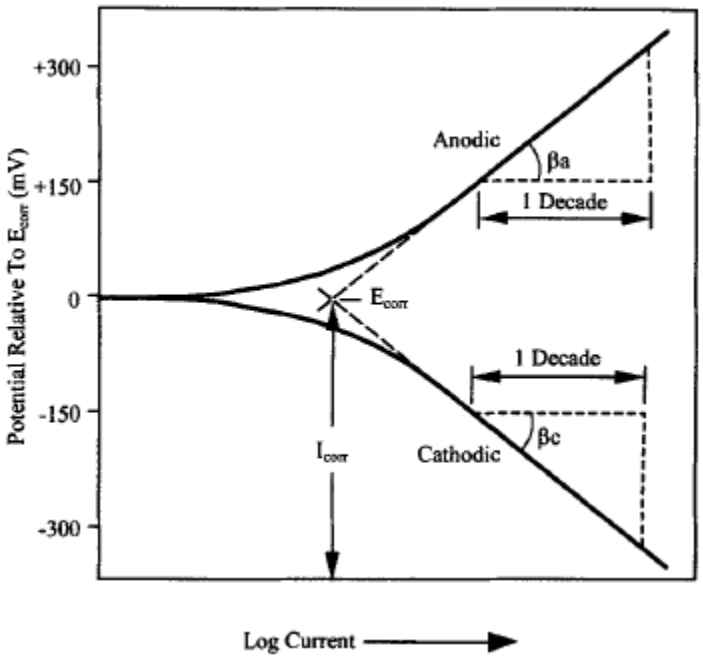

Fig. 2.1. Idealized Tafel plot *(El-Gelany, 2001)*

This plot exhibits a linear region, the slope of which is known as Tafel constant (anodic Tafel constant and cathodic Tafel constant). The intersection of the projection of the linear region of the plot with E_{corr} gives corrosion current (I_{corr}) *(El-Gelany, 2001; Song and Saraswathy, 2007; Kelly et al. 2002).* Once I_{corr} is determined, the following equation, derived from Faraday's law, can be used to calculate the corrosion rate as per *ASTM G102-89*.

$$\text{Corrosion rate (mm/year)} = \frac{(0.00327 \times i_{corr} \times EW)}{d} \quad (2.1)$$

Where:

EW = equivalent weight of steel in grams,

d = density of reinforcing steel bar in g/cm^3,

i_{corr} = corrosion current density ($\mu A/cm^2$)

It is obtained as:

$$i_{corr} = \frac{I_{corr}}{A}$$

Where, A = Exposed surface area of steel in cm^2

Many researchers have used the above mentioned electrochemical techniques for corrosion assessment. The detailed literature for the same is presented as below.

Song and Saraswathy (2007) reviewed all the electrochemical and nondestructive techniques from the point of view of corrosion assessment and their applications to bridges, buildings and other civil engineering structures.

Pradhan and Bhattacharjee (2009) proposed a laboratory methodology for identification of indicating parameter for rebar corrosion initiation using half-cell potential. The laboratory experimentation demonstrated that the half-cell potential is a suitable and stable determining parameter indicating rebar corrosion initiation in chloride contaminated concrete. Through this work it was also reconfirmed that the critical chloride level leading to corrosion initiation is not a unique value and varies with steel type, cement type, and w/c ratio.

Pour-Ghaz et al. (2009) presented a quantitative interpretation of half-cell potential measurements in concrete structures. The half-cell potential measurement was modeled numerically and the effect of resistivity, cover thickness, oxygen availability and anode–to-cathode area ratio on the half-cell potential mapping was investigated.

Carino N. J. (1999) provided an overview of the corrosion of steel in concrete and presented three different nondestructive electrochemical tools viz. the half-cell potential method, the concrete resistivity test and the linear polarization method that are commonly used in corrosion investigations. The study emphasized the principles

of operation and the inherent limitations of these methods as well as reviewed the electrochemical principles involved in the corrosion of steel in concrete.

El-Gelany M. A. (2001) presented the results of a laboratory investigation in which the applicability of Tafel plot and linear polarization techniques in short-term corrosion rate measurement of reinforcing bar in concrete were studied. The investigation concluded that both the Tafel plot and linear polarization resistance techniques can be used conveniently and effectively to evaluate the corrosion rate of reinforcing bars in concrete with certain advantages and disadvantages over each other. The Tafel plot technique determines the corrosion rate independently but the main disadvantage is that the potential perturbation of the reinforcing steel due to the large applied potential makes the specimen unsuitable for sensitive electrochemical measurements. Whereas in Linear polarization technique, the specimens quickly recover their original open circuit potential after the test and can be reliably used for other tests. The disadvantage of this technique is that it is depends on the Tafel plot technique for the Tafel constants.

2.3.3. Application of electrochemical technique for monitoring of accelerated corrosion using impressed current technique

The application of different electrochemical techniques for monitoring accelerated corrosion using impressed current technique in different materials is presented below:

Spainhour and Wootton (2008) investigated the corrosion performance of steel reinforcement embedded in concrete samples encased by carbon fiber reinforced polymer (CFRP) wraps experimentally. To accelerate corrosion, the samples were subjected to an impressed current and a high salinity solution. Corrosion activity

during exposure was monitored by measuring current flow and reinforcement mass losses following exposure.

Ha et al. (2005) investigated a systematic study on the influence of mineral admixture, namely fly ash (FA) on the corrosion resistance of steel in concrete by electrochemical technique using accelerated short-term techniques in 3% NaCl solution. Electrochemical techniques such as open circuit potential measurements and anodic polarization studies were carried out. An impressed voltage technique and macrocell corrosion study was also carried out to understand the optimum level of replacement of FA with better corrosion resistance properties. Results were compared with conventional gravimetric weight loss measurements. Results showed that fly ash up to 30% replacement level improved the corrosion resistance properties of steel in concrete, improved the permeability characteristics of concrete, delayed the initial corrosion time and decreased corrosion rate.

Gadve et al. (2009) investigated the progression of corrosion of steel in concrete after it was treated with surface bonded FRP (CFRP and GFRP). Concrete cylinders with embedded steel bars were immersed in salt water and anodic current was passed through the reinforcement to initiate cracking in concrete due to accelerated corrosion of steel. Pull out strength, mass loss, half-cell potential of steel and cell voltage were reported as metrics of performance of the samples.

Wootton et al. (2003) presented the results of experimental study on the corrosion performance of embedded steel reinforcement in cylindrical reinforced concrete specimens with different surface treatment options. Samples were subjected to impressed current and a high salinity solution. Test variables included the types of epoxy, wrap fiber orientation, and the number of wrap layers. Samples were evaluated

for corrosion activity by monitoring corrosion potentials and impressed current flow levels, and by examining reinforcement mass loss and concrete chloride content among samples. Test results indicated that FRP wrapped specimens had prolonged test life, decreased reinforcement mass loss and reduced concrete chloride content.

Masoud and Soudki (2006) presented an experimental study to evaluate the corrosion activity in reinforced concrete beams repaired with FRP sheets. Constant current was impressed in the specimens to accelerate the corrosion activity. The corrosion activity was evaluated using non-destructive technique which included half-cell potential measurements and destructive technique which included evaluation of the mass loss of the main reinforcing bars. The experimental results showed that the corrosion potential decreased with the progress of corrosion and the FRP repair caused a higher rate of decrease in the corrosion potential with time than that observed when FRP was not provided. Results also showed that mass loss of the main reinforcing bars due to corrosion was reduced by up to 16% because of FRP repair.

2.4. ACOUSTIC EMISSION TECHNIQUE

Acoustic Emission (AE) is defined as "The class of phenomenon whereby transient elastic waves are generated by the rapid release of energy from localized sources within a material, or the transient waves so generated" *(ASTM E1316, 2010)*. Acoustic activity may be observed both in highly elastic as well as brittle materials. The common sources of acoustic emissions are defect-related deformational processes such as crack nucleation/growth and plastic deformation. In metals, acoustic emission sources include yielding, corrosion and crack growth. In composites, matrix cracking, fiber breakage and fiber debonding are common sources of emission *(Degala et al. 2009)*. Its unique ability to passively record the events at the moment of their

occurrence is definitely the main reason for the wide use of this technique for structural health monitoring. The elastic waves generated in the structure during the deformation of material, propagates as a stress wave in the structure and is detected by one or more AE sensors mounted on the surface of the material. By separating the background noise from AE event, the ongoing condition of a structure can be monitored *(Rens et al. 1997, Degala et al. 2007)*. Figure – 2.2 represents the general working principle of an AE monitoring system.

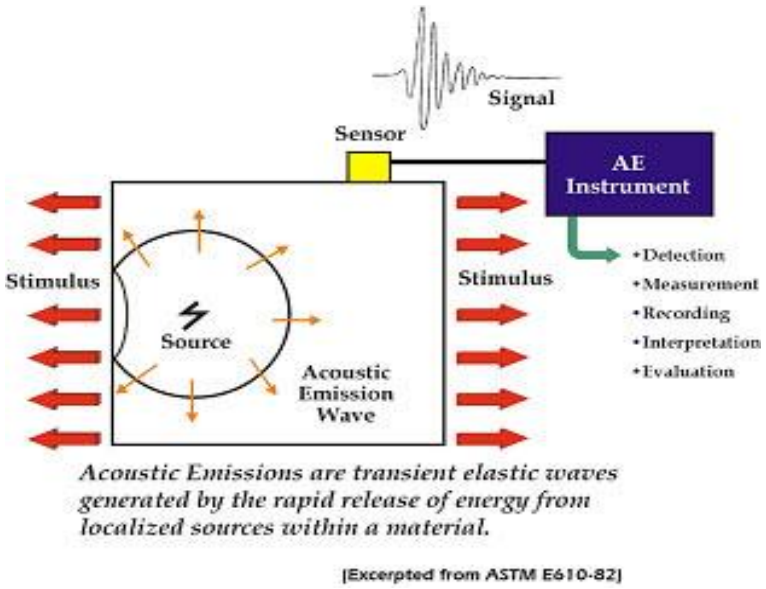

Fig. 2.2. Principle of AE technique *(www.mistrasgroup.gr)*

AE differs from most other non-destructive testing methods in two key aspects. First, the signal has its origin in the material itself, not in an external source. Second, AE detects release of energy, while most other methods detect existing geometrical discontinuities. The consequences of these fundamental differences are summarized in Table 2.2. AE equipment is highly sensitive to any kind of movement in its operating frequency range (typically 20 to 1200 kHz). The equipment can detect not only the crack growth and material deformation, but also the processes such as solidification, friction, impact, flow and phase transformations. Therefore, AE technique is valuable

for monitoring chemical reactions, including corrosion process, liquid-solid transformations and phase transformations *(Pollock, 2003)*.

Table 2.2. Characteristics of acoustic emission inspection compared with other inspection methods *(Pollock, 2003)*

Acoustic Emission	Other Methods
Detects movement of defects	Detect geometric form of defects
Requires stress	Do not require stress
Each loading is unique	Inspection is directly repeatable
More material-sensitive	Less material-sensitive
Less geometry-sensitive	More geometry-sensitive
Less intrusive on plant/ process	More intrusive on plant/ process
Requires access only at sensors	Requires access to whole area of inspection
Tests whole structure at once	Scan local regions in sequence
Main problems: noise related	Main problems: geometry related

The advantages of AE technique over other non-destructive techniques are listed as *(Grosse and Ohtsu, 2008)*:

1. Acoustic emission is generated by the material itself. In contrast, other types of stress-wave nondestructive testing methods, such as impact echo and ultrasonic, need an external input source.
2. Damage processes in materials being tested can be observed during the entire load history, without any disturbance to the specimen.
3. AE technique is a global test which covers a large area with one test, whereas the other methods cover a very limited area and are referred to as local tests. AE sensors can be fixed to the surface of the specimen for the entire duration of test and is not required to be moved for scanning the whole structure point by point.

Access to both sides of an object, which is necessary for all through-transmission methods, is not required in AE technique.

4. AE is applicable for local, global, remote and continuous monitoring purposes and is advantageous in case of bridge monitoring which can be conducted without hindering traffic over the bridge structure.

A drawback of acoustic emission is that it depends on the applied load. As a result, some discontinuities may not emit detectable acoustic emission under a particular load, thereby making a particular test effect non-repeatable due to the nature of the signal sources. Also, quantitative AE analyses are still difficult for applications to actual structures.

2.4.1. AE equipment used in monitoring

The measurement of AE essentially involves three basic components: recording of generated AE wave, processing of the collected data and its interpretation. These are accomplished with the use of an array of instruments. Each component has a unique role to play and is essential for proper monitoring. A brief description of each component is given below *(Grosse and Ohtsu, 2008)*.

- **Sensors:** Most traditional AE sensors consist of piezoelectric elements. Their primary function is to detect transient elastic mechanical waves generated within a structure and convert them into electrical AE signals. The appropriate transducers needed for data acquisition are chosen based on the purpose and sensitivity required for the investigation. The sensors are usually mounted on the structure by using adhesives or by holders. The Fig 2.3 shows various kinds of sensors available in today's market.

Fig. 2.3. Common types of sensors available in the market *(www.pacndt.com)*

- **Couplants and holders:** AE sensors are fixed on the surface of material to be monitored using various Couplants. These are mainly used to aid in easy and complete conduction of acoustic waves generated from the source. Commonly used, couplants are oil, glue, high vacuum grease, etc. Along with the use of couplants, most field tests require additional holders to hold the sensors in place.
- **Preamplifiers:** Preamplifiers are available either separately or integrated with the sensors. The main purpose of this device is to improve the signal-to-noise ratio and effectively filter and reject noise from areas outside the sensor operating range.
- **Data acquisition system**: Modern AE systems use computers and appropriate software for qualitative real-time assessment of the collected AE data. All the signals received at the sensor are acquired and stored in the acquisition system. The new generation systems also enable extensive post-processing facilities.

2.4.2. AE data analysis

Traditionally, two different approaches are used for recording and analyzing AE signals: (a) Parameter-based analysis and (b) Signal-based analysis *(Grosse and Ohtsu, 2008).*

(a) Parameter-based analysis: In parameter based analysis, the AE events are recorded with sensors and a set of parameters are extracted from the signal which

are stored and further used to assess the extent of damage. Fig. 2.4 shows a typical AE signal with commonly used parameters which are described below *(ASNT Volume 6, 2005)*.

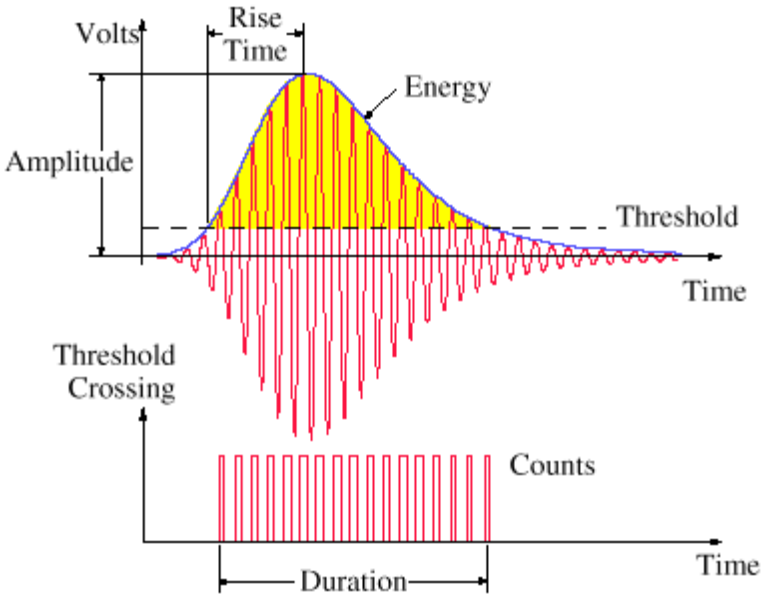

Fig. 2.4. Typical AE signal *(Nair and Cai, 2010)*

- **Threshold:** The AE recording is triggered, once the signal crosses a set threshold value. This value of voltage is set for the discrimination of AE signals from running waves and eliminate as much noise as possible. The care should be taken while setting the threshold so that weak signals are not missed by setting too high threshold.
- **Hit:** A signal that exceeds the threshold and causes a system channel to accumulate data. One waveform correspond one "hit".
- **Counts:** It is the number of times one signal exceeds the set threshold within the duration. Counts are used as a practical measure of acoustic emission activity.
- **Amplitude:** It is the maximum (positive or negative) AE signal excursion during an AE hit. Amplitude is directly related to the magnitude of source event. It is expressed in volts or in AE decibel scale using the relation:

$$dB = 20 \log\left(\frac{V_{max}}{1\mu V}\right) - Preamplifier\ gain\ in\ dB \quad (2.2)$$

Where 1µV at the sensor is defined as 0dB.

- **Duration:** A time interval between the triggered time of one AE signal and the time of disappearance of the signal. Analogous to counts, this parameter measures the source magnitude. It is expressed in microseconds and particularly useful for noise filtering and other kinds of signal qualification.
- **Rise time:** A time interval between the triggering time of AE signal and the time of the peak amplitude of waveform. This parameter is often useful in problems involving time dependent processes such as dynamic loading or vibration of structures.
- **Energy:** It is defined as a measured area under the rectified signal envelope which is gain dependent. Energy of the signal is another parameter that conveys information about the strength of the AE source. The energy is preferred to interpret the magnitude of source event over counts because it is sensitive to the amplitude as well as the duration and less dependent on the voltage threshold and operating frequencies.
- **Signal strength:** It is defined as the integral of rectified voltage signal over the duration of AE waveform packet. The signal strength normally includes the absolute area of both the positive and negative envelopes. This feature is similar to energy except that it is calculated over entire AE signal dynamic range and is independent of gain. It is also a function of both the amplitude and duration of the signal. It is sometimes referred as relative energy which relates to the amount of energy released by the material or structure. Signal strength is often used to specify the overall cumulative acoustic emission activity.

(b) Signal-based analysis: In parameter based analysis, various parameters of the signal are recorded, but the signal itself is not recorded. This minimizes the time and the storage space of data recorded. The waveform based approach offers better data interpretation capability than parameter based approach by allowing the use of signal processing techniques. One of the biggest advantages of signal-based analysis is the capability of signal-to-noise discrimination based on waveforms. Analysis of recorded waveforms generally provide information about the nature of the source and help in distinguishing different sources of AE. Frequency analysis of recorded waveforms is the most commonly used tool. Two basic types of signals are usually seen: burst and continuous signal, as shown in Fig. 2.5.

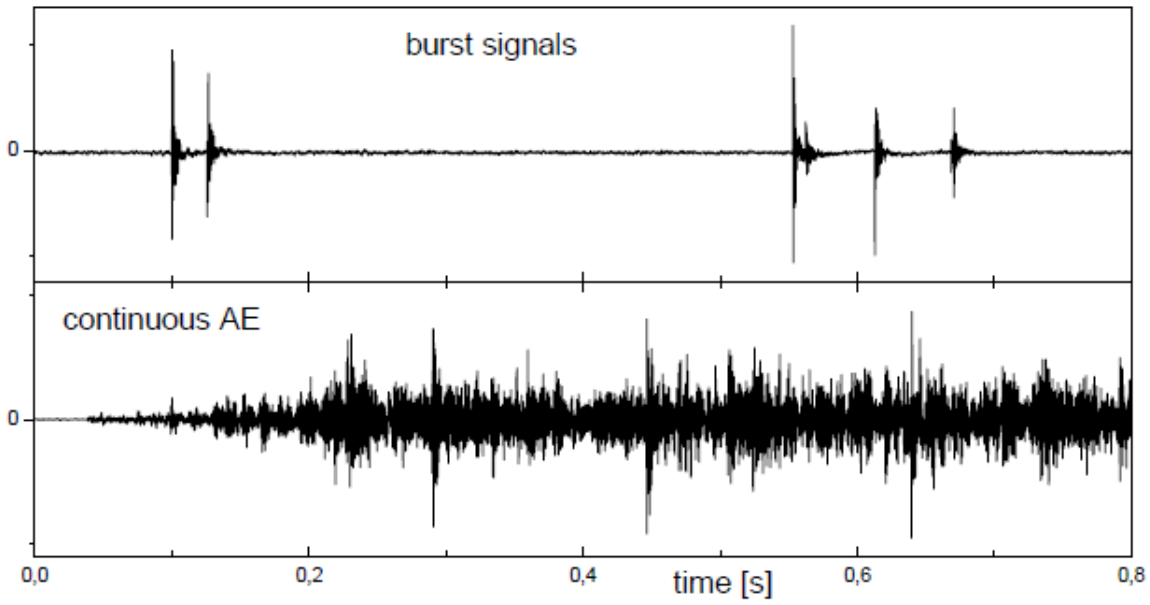

Fig. 2.5. Burst and continuous AE signal *(Grosse and Ohtsu, 2008)*

The burst signal occurs only for a short duration while continuous signals occur for longer period of time. Burst signals often arise from fracture or crack growth and continuous signals are mainly noise signals. The main disadvantage of signal based approach is the generation of large volume of data. In order to ensure all frequencies

are recorded, the sampling is kept higher. Because of the high sampling rates, signal of even small duration will be of large data size. Despite, this drawback the signal based approach is still widely used because of the advantages it offers in signal processing.

2.5. AREAS OF APPLICATION OF AE TECHNIQUE

The primary goal of AE monitoring in structures is to detect, locate and assess the intensity of damage. Thus, indicators of structural damage such as cracks, corrosion and de-lamination that warn impending failure have become the focal point of any AE study *(Nair and Cai, 2010)*. The literature for the same is explained in following sections.

2.5.1. Application of AE for concrete in laboratory and field

Numerous laboratory studies have been conducted to demonstrate the ability of AE to detect various properties and damages in concrete and RC elements. The applicability of AE technique to concrete of early age has been also studied.

Lura et al. (2009) investigated the acoustic emission activity of cement pastes during the first day of hydration. Fresh cement pastes were cast in sealed sample holders designed to minimize friction and restraint. It was observed that the majority of acoustic emission events occurred in lower water to cement ratio pastes, while cement pastes with higher water to cement ratios showed significantly less acoustic activity. These acoustic events occurred around the time of setting. A layer of water on the surface of the cement pastes substantially reduced acoustic emission activity at the time of setting. According to these experimental results, the acoustic emission measured around setting time was attributed to cavitation events occurring in the pores of the cement paste due to self-desiccation.

Kunisue et al. (2002) measured AE activities during dynamic compaction to estimate the degree of compaction. During measurement, AE sensor was attached to the outer surface of mold. Three types of concrete with three water-cement ratios were studied. In the ordinary concrete cases (W/C = 45% and 60%), both AE count rate and energy shifted from the active state to the steady state at around 100 seconds elapsed. In the case of non-slump concrete, the stable state was later reached than ordinary concretes after 400 seconds. Thus, it was demonstrated that fully compacted state could be estimated by observing AE activity during dynamic compaction.

In hardened concrete, AE technique has been used for studying the fracture process. The parameters like shape of aggregates, strength of cement matrix, ratio of volume of aggregate to the total volume of specimen has influence on fracture energy and hence on AE energy.

Raghuprasad and Vidyasagar (2008) measured AE energy released during fracture process of plain concrete beams to investigate the relation between AE energy and fracture energy. The experimental study consists of use of AE technique on series of concrete specimens with geometrically similar notched plain concrete, three-point bend specimens of different sizes during testing of fracture energy. Acoustic emission energy release was monitored while testing concrete specimens for fracture energy. The study observed size effect on the strength of concrete beams. The study found the linear relationship between AE and fracture energy.

Shah and Chandrakishen (2010) used AE technique for studying the fracture behaviour of concrete interfaces. The experimental study analyzed the AE data in terms of the number of events to obtain the size of fracture process zone and the damage zone. The width of fracture process zone and damage zone were computed

using AE data and were found to be independent of size. It was observed that as the difference in compressive strength of concrete on either side of interface increased, the load carrying capacity, number of AE-events, AE-energy, width of fracture process zone and damage zone decreased.

Muralidhara et al. (2010) estimated the fracture process zone size for which AE energy was utilized instead of the event and concluded that the absolute energy of AE signals describes an AE event better than the peak amplitude.

Chen and Liu (2007) applied AE technique with three dimension orientation feature to study the effect of maximum aggregate size on fracture properties and the fracture process zone at the crack tip. It was concluded that AE hits has a potential to measure inner damage of concrete during cracking.

Ranjith et al. (2008) studied the effect of displacement rate and moisture content on mechanical properties of concrete, using AE technique along with volumetric stiffness-stress and volumetric strain-stress curve methods. AE technique was used to identify crack propagation in concrete. AE results identified three crack propagation zones as crack initiation, secondary cracking and crack damage.

AE technique has been extensively used for damage assessment of concrete and RC structures. Various researchers have implemented different tools of AE technique such as parameter-based or signal-based analysis for damage assessment of structures.

Yoon et al. (2000) investigated the acoustic emission behaviour of reinforced concrete beams tested under flexural loading to characterize and identify different sources of damage including micro crack development, localized crack propagation and de-bonding of the reinforcing steel by testing plain, notched-plain, reinforced and

corroded-reinforced specimens. Both AE parameter analysis and waveform analysis exhibited a favorable correlation with the condition of damage in the RC beams. It was concluded that AE may provide a promising method to estimate the damage of RC structures.

Kocur and Vogel (2010) addressed the parameter-based AE technique for damage evaluation of RC slabs. Through the experimental work, damage classification such as flexural cracks and shear cracks were identified successfully by reconsidering the definitions of load ratio and calm ratio associated with Kaiser Effect.

Colombo et al. (2003) utilized AE technique for monitoring damages in RC beam by laboratory experiment and found good relationship between the trend of b-value and the microcracking and macrocracking appearing during test. The parameter, b-value is defined as a relation between the number of AE hits and the maximum amplitudes. Results suggested that b-value analysis of AE signals could be used to interpret data obtained by local monitoring of concrete bridges.

Benavent et al. (2010) investigated applicability of AE for assessing low-cycle fatigue damage in RC exterior beam-column sub- assemblages. They observed significant increase in AE activity when the steel reinforcement begins to undergo plastic deformations. The microstructure process was also well defined by AE improved b-value method.

In addition to laboratory studies, AE technique has also been used successfully for source location and damage intensity predictions in numerous field applications.

Shigeishi et al. (2001) used the AE technique to monitor integrity of an existing bridge which was representative of both masonry and reinforced concrete construction. The results demonstrated that AE can be applied to condition assessment

of bridges and can be useful in detecting crack growth and determining the position of the crack tips at a much earlier stage in their development, before they are noticed during visual inspection.

Fricker and Vogel (2007) installed acoustic monitoring system on an existing bridge. It was concluded that continuous acoustic monitoring was able to record, analyze, classify and locate wire breaks in grouted and partially grouted tendons even in a noisy environment. Invasive inspections confirmed spontaneous wire breaks that were also detected during the monitoring.

Yuyama et al. (2007) showed that AE is a very useful technique to detect and evaluate failures of high strength steel tendons in prestressed concrete bridges. Through intensive analysis of the detected AE signals, they showed that meaningful AE events from the failures are clearly discernable from other sources as traffic noises and hammering.

Carpinteri et al. (2007) applied AE technique for health monitoring of different structures like masonry and concrete building, concrete viaduct etc. and showed the effectiveness of AE technique to ascertain stability or instability conditions and to forecast the extent of damage in structures characterized by the propagation of discrete cracks.

Nair and Cai (2010) conducted case studies of existing prestressed concrete slab-on-girder bridge as well as steel bridge with a concrete deck by applying AE technique. They utilized intensity analysis technique for damage quantification and concluded that AE technique has a promising future in becoming an integral part of any structural health monitoring system.

2.5.2. Application of AE for corrosion assessment in reinforced concrete

Reinforcement corrosion and resulting cracking are considered as major damage mechanism that requires long term condition assessment of RC structures. In this regard, the researchers have employed AE technique effectively to detect concrete cracking due to corrosion of reinforcement.

Assouli et al. (2005) applied AE technique to provide a mechanism of corrosion of reinforcement and to quantify its severity by reproducing the carbonation of the concrete through application of heating-cooling cycles to the concrete samples. The study found three different acoustic signals corresponding to the infiltration of the medium through porosity, compressive forces and micro cracks. The study proposed a physical model of the reinforcement-electrolyte interface to describe the behavior of the reinforcement against corrosion in chloride solution before and after carbonation.

Idrissi and Limam (2003) presented the results of experimental investigation on the use of acoustic emission coupled with electrochemical techniques during the accelerated corrosion of steel rebar embedded in mortar and immersed in sodium chloride solution. The result showed a perfect correlation between the evolution of the AE activity and the corrosion current density. They also underlined that AE activity depends on porosity of mortar.

Ohtsu and Tomoda (2008) conducted AE monitoring in an accelerated corrosion test using cyclic wet and dry method to identify corrosion process in reinforced concrete. They observed two periods of high AE activity. To elucidate these two activities, AE waveform parameters and the slope gradient of AE amplitude distribution were investigated. They concluded that both the onset of reinforcing bar corrosion and the nucleation of concrete cracking can be detected using AE technique. The study also

compared the total number of AE hits with phenomenological model of steel embedded in concrete subjected to marine environments and showed that the two curves are in remarkable agreement.

Kawasaki et al. (2010) obtained similar results during cyclic wet-dry test of RC beams. They implemented Ib-value analysis to identify the transition period from the dormant stage to initiation stage of corrosion and SiGMA analysis to identify concrete cracking. The Ib-value is calculated using averaged amplitude and standard deviation whereas SiGMA analysis consists of 3-D AE source location procedure and moment tensor analysis for AE source. The researchers also compared half-cell potential results with AE results and indicated that the technique can give an early warning of corrosion than the established electrochemical technique.

Leelalerkiet et al. (2005) experimentally studied the deterioration of reinforced concrete due to corrosion of rebar under chloride environment with AE technique and compared the results with half-cell potential and polarization resistance. The study concluded that AE technique gives an earlier warning of corrosion than half-cell potential measurement. In addition crack types at onset of corrosion and nucleation of cracking are identified from AE parameter. The work also estimated the corroded area by inverse boundary element method which was found in remarkable agreement with visual inspection, whereas results of electrochemical techniques were marginally successful.

Di Benedetti et al. (2013) studied the effectiveness of AE in detecting and characterizing the initiation of corrosion process coupled with electrochemical techniques for pre-cracked RC specimens. The experimental study on corrosion monitoring was conducted during initiation period of corrosion, focusing the study to

onset of corrosion and showed that when cumulative signal strength is plotted versus time, it increase sharply at a certain time which can be correlated to damage and corrosion.

Di Benedetti et al. (2013a) in another work presented an accelerated corrosion test set-up and AE monitoring methodology based on the historic index, for laboratory experiments on RC specimens. Accelerated corrosion was attained by increasing the capillarity suction of RC exposed to chlorides. The frequency spectrum of the AE signals before and after the initiation of corrosion was investigated to isolate the frequency components associated with corrosion. It was shown that the AE signals generated by early corrosion excite a well-defined narrow band of the frequency spectrum.

Noorsuhada et al. (2011) reviewed the relationship between acoustic emission signal strength and damage evaluation. To get information on this relation, several case studies were referred. The study reported that damage in concrete can be evaluated using AE signal strength analysis. The graph of signal strength versus time can be used to visualize the condition of structural element.

Ing et al. (2005) identified the influential cover zone factors that affect the magnitude of the AE measurements per gram of steel loss. Prisms with various concrete strength, cover thickness, aggregate and rebar diameters were studied to ascertain the important variables likely to be encountered on reinforced structures. The experimental results confirmed that early corrosion can be detected by AE before any external signs of cracking and it was verified by internal visual inspection and mass loss. They also showed that concrete strength, being exponentially related to the AE energy, was the most influential parameter affecting the AE measurement. The rebar diameter

indicated a promising relationship with AE energy per gram of steel loss, whereas cover thickness had a negligible effect on AE energy. The researchers tried to establish a relation between total absolute energy parameter of AE technique and mass loss. However, the analysis was not successful to establish a promising relation.

2.6. GAP IN THE RESEARCH AREA

From the literature review, it can be concluded that AE technique can be used for finding damages in concrete as well as for detecting onset of corrosion. The technique is able to identify onset of corrosion earlier than well-established electrochemical techniques. However, AE technique is a qualitative method which can find the initiation of corrosion of steel embedded in concrete by identifying developed cracks in concrete, but it has not been used to quantify the mass loss of steel embedded in concrete due to corrosion and rate of corrosion.

Thus, in practice, for complete condition monitoring of reinforced concrete structures or structural elements, along with AE technique, a suitable electrochemical technique is also required to assess the rate of corrosion. As discussed earlier, all the electrochemical techniques require electrical/physical contact with reinforcing steel necessitating local damage to the existing structural element. This can be avoided, if both the requirements viz. initiation and growth of crack in concrete due to corrosion as well as rate of corrosion of steel embedded in concrete can be assessed using truly non-destructive technique like AE technique. Thus, there is need to develop a method to quantify the mass loss due to corrosion of rebar using AE technique. Hence, current research work aims to assess the corrosion of steel embedded in concrete using AE technique quantitatively.

2.7. CLOSING REMARKS

Based on the literature review and gap in research area, in the present research work, applicability of AE technique is studied vis-à-vis electrochemical techniques (half-cell potential measurement and Tafel extrapolation technique) for corrosion assessment in RC elements. To achieve sufficient degree of corrosion in laboratory within limited time period, impressed current technique is used for accelerating corrosion process. The effectiveness of impressed current technique is further verified by using alternate dry-wet method which represents real life corrosion process. Different variables used in the study include three bar diameters, two types of steel and two types of cement. A statistical tool (ANOVA) is used to study the effect of these variables on corrosion and hence on AE measurements. The result obtained from AE technique is correlated with the result of destructive technique i.e. actual mass loss of steel embedded in concrete to develop a mathematical model. Regression analysis is used for development of mathematical model. Further, the developed mathematical model is validated for realistic corrosion exposure conditions in the laboratory using internal chloride exposure.

To fulfil these requirements, preliminary experimental investigations are conducted to design the experimental programme. The details of these investigations are presented in Chapter 3.

.

CHAPTER 3

PRELIMINARY EXPERIMENTAL INVESTIGATIONS AND FINAL TEST PROCEDURE

3.1. INTRODUCTION

The objective of research work is to monitor and quantify corrosion of steel embedded in concrete using AE technique. Therefore, experimental program necessitates creation of laboratory conditions to set corrosion into the specimens. Corrosion of steel in concrete is a process that requires several years and decades to set in. Preparation of samples that imitate the field conditions would be a long procedure and their performance would be required to monitor over several years. Therefore, it is prudent to devise a pilot test that introduces rapid corrosion and provides quick results to enable corrosion monitoring and its further investigations.

Various methods of inducing and accelerating corrosion process in laboratory specimens have been discussed in Chapter 2. Out of the methods discussed, impressed current technique is employed in the present experimental programme. This chapter describes the preliminary investigations carried out to set corrosion rapidly in laboratory conditions in different stages. These tests helped to decide the basic parameters of test procedure, viz. the final dimensions of specimen, sodium chloride (NaCl) concentration, methodology for impressed current technique and input value of voltage for accelerated corrosion.

3.2. PRELIMINARY EXPERIMENTAL DETAILS

Before starting the experimentation for corrosion monitoring by acoustic emission, it was extremely important to decide certain parameters of accelerated corrosion technique adopted. The objective of the experimental plan was to obtain

corrosion results within reasonable period of time. Therefore, the dimensions of the specimen and the level of impressed current were to be finalized. For finalizing these parameters, a detailed preliminary experimentation was carried out. The preliminary experiments were divided into three stages. The details of the three stages are described in the following sections:

3.2.1. Stage-I

In the beginning of the experimental programme, the use of basic materials, mix design and specimen dimensions were to be decided. The initial choice of materials, specimen size and the experimental procedure is described in the subsequent sections:

3.2.1.1. Material System

In the preliminary testing, M20 grade of concrete was prepared using 53 grade Ordinary Portland Cement (OPC), natural river sand confirming to zone I as per *IS: 383-2002* as fine aggregates and crushed stone of nominal size 20 mm as coarse aggregates. The specific gravity of fine and coarse aggregates were 2.75 and 2.70 respectively. The water absorption for coarse aggregate was 1% while moisture content for fine aggregate was 2%. The ratio of cement: sand: coarse aggregate was 1: 2.23: 3.14 (by weight) with water-cement ratio of 0.55. Cubes of size 150 mm were cast to measure the compressive strength of the mix designed. The cubes were cured for a period of 28 days at the temperature of 27 ±2 ºC and relative humidity of 100%. The temperature of the curing tank was maintained by thermostats. The average compressive strength of the cubes at 28 days of curing was measured on 2000 kN capacity compression testing machine and was obtained to be 20 MPa. The chemical composition and physical properties of cement as obtained from manufacturer are shown in Table 3.1 and Table 3.2 respectively, whereas Table 3.3 and Table 3.4

reports the results of sieve analysis for fine and coarse aggregates used in Stage-I of preliminary experimental work respectively.

Table 3.1. Chemical composition of cement (OPC)

Compound	Percentage (%)
CaO	63.2
SiO_2	21.40
Al_2O_3	5.00
Fe_2O_3	3.60
MgO	0.8
SO_3	2.2
LOI	1.5

Table 3.2. Physical Properties of cement (OPC)

Fineness	
Specific Surface	306 m^2/kg
Soundness	
By Le – Chatelier Method	0.8 mm
Setting Time	
Initial Setting Time	140 minutes
Final Setting Time	190 minutes
Compressive Strength	
i) 3 days	38.2 MPa
ii) 7 days	48.3 MPa
iii) 28 days	66.4 MPa
Temperature during Testing	27^0C
Standard Consistency	29 %

Table 3.3. Results of sieve analysis for fine aggregates

Sr. No.	I.S. Sieve size.	Weight retained on each sieve	Cumulative weight Retained	Cumulative percentage weight retained	Cumulative percentage weight passing
01.	10mm	3	3	0.32	99.68
02.	4.75mm	121	124	13.36	86.64
03.	2.36mm	174	298	32.11	67.89
04.	1.18mm	218	516	55.60	44.40
05.	600µ	149	665	71.66	28.34
06.	300µ	186	851	91.70	8.30
07.	150µ	57	908	97.84	2.16
	Total	**1000 g**			

Table 3.4. Results of sieve analysis for coarse aggregates (20 mm)

Sr. No.	I.S. Sieve size.	Weight retained on each sieve	Cumulative weight Retained	Cumulative percentage weight retained	Cumulative percentage weight passing
01.	80mm	0	0	0.00	100.00
02.	40mm	0	0	0.00	100.00
03.	20mm	539	539	26.95	73.05
04.	12.5mm	632	1171	58.55	41.45
05.	10mm	814	1985	99.25	0.75
06.	4.75mm	12	1997	99.85	0.15
07.	2.36mm	3	2000	100.00	0.00
08.	1.18mm	0	2000	100.00	0.00
09.	600µ	0	2000	100.00	0.00
10.	300µ	0	2000	100.00	0.00
11.	150µ	0	2000	100.00	0.00
12.	< 150µ	0	2000	100.00	0.00
	Total	**2000 g**			

Thermo mechanically treated (TMT) reinforcing steel of grade Fe 500 having length 400 mm and diameter 16 mm was used. The chemical composition of TMT steel as obtained from manufacturer is presented in Table 3.5.

Table 3.5. Chemical composition of TMT steel

Element	Percentage (%)
C	0.25
Mn	0.90
S	0.035
P	0.035
Si	0.45

3.2.1.2. Specimen Preparation

Cylindrical specimens with standard dimensions of 300 mm height and 150 mm diameter as specified in *IS: 5816 - 1999* were cast with transverse clear cover of 67 mm and bottom cover of 50 mm as shown in Fig. 3.1.

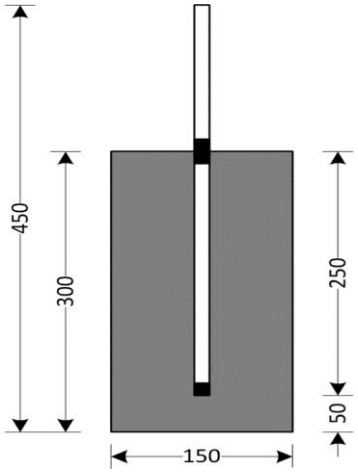

Fig. 3.1. Cylindrical reinforced concrete specimen

Before casting, the steel bar was drilled and threaded at one end to accommodate the threaded copper screw for electrical connections (Fig. 3.2).

Fig. 3.2. Threaded end of steel rebar with screw for electrical connection

The bar was then cleaned with wire brush to remove any surface scale. Each reinforcing bar was then weighed to 0.1 g accuracy. Teflon tape was wound around the bar at two locations – bottom edge and at the steel-concrete interface to serve as a bond breaker and to avoid crevice corrosion. This also helped to maintain the embedded length of bar in concrete precisely at 210 mm. The protruded part of the steel bar was coated with white oil paint for protecting this portion from corrosion (Fig. 3.3).

Fig. 3.3. Steel reinforcing bars before casting

Then, the cylindrical specimens of dimensions 300 mm x 150 mm were cast with the concentric steel bar. Fig. 3.4 shows the specimens after casting. After casting, all specimens were cured at temperature of 27 ±2 ºC and relative humidity of 100% for 7 days. The specimens were then kept immersed in 3.5% NaCl solution on 8^{th} day for 24 hours to ensure full saturation and on 9^{th} day, the specimens were subjected to accelerated corrosion using impressed current technique.

Fig. 3.4. Specimens after casting

3.2.1.3. Inducing Corrosion in Steel rebar

The objective of inducing corrosion to the reinforcing bar is to simulate the corrosion damaged concrete. The quickest method of inducing corrosion is by impressing anodic current. In this method, the specimen is immersed in NaCl solution

and a direct current is passed making the reinforcement bar as an anode and another metal nobler than steel in electro-chemical series as cathode.

In this investigation, a stainless steel (SS) mesh rolled into a hollow, open cylinder was used as cathode. The cathode and the specimen were placed in NaCl solution of known concentration. The level of NaCl solution was kept 3 cm below the top surface of the specimen to alleviate corrosion at the steel-concrete interface. The DC regulated power supply having capacity of 200 mA DC at 30 V was used in the present study. The reinforcing steel bar was connected to the positive terminal of the external DC source and negative terminal was connected to the SS mesh. The direct electrical constant current was impressed between reinforcing bar and the SS mesh (Fig. 3.5).

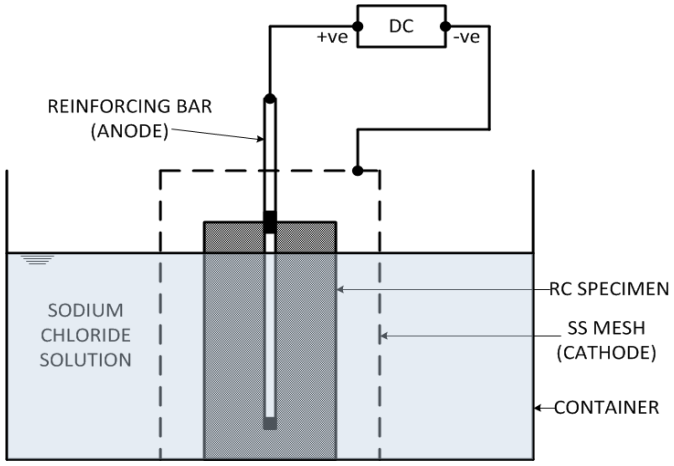

Fig. 3.5. Schematic representation of Accelerated Corrosion set-up

Figure 3.6 shows the laboratory set-up for inducing accelerated corrosion by impressing constant anodic current into the steel rebar. Initially, a total of four specimens were cast and subjected to different levels of accelerated exposure by varying the imposed current and concentration of NaCl. Anode to cathode voltage corresponding to constant current was monitored daily for all specimens. The testing

was terminated when specimens showed large amount of oozing of corrosion products. All the specimens were then broken, the steel rebar was extracted and cleaned with wire brush to calculate the mass loss. Table 3.6 gives the details of corrosion exposure and mass loss for these specimens. Table 3.7 gives the details of anodic current and the corresponding voltage for all specimens

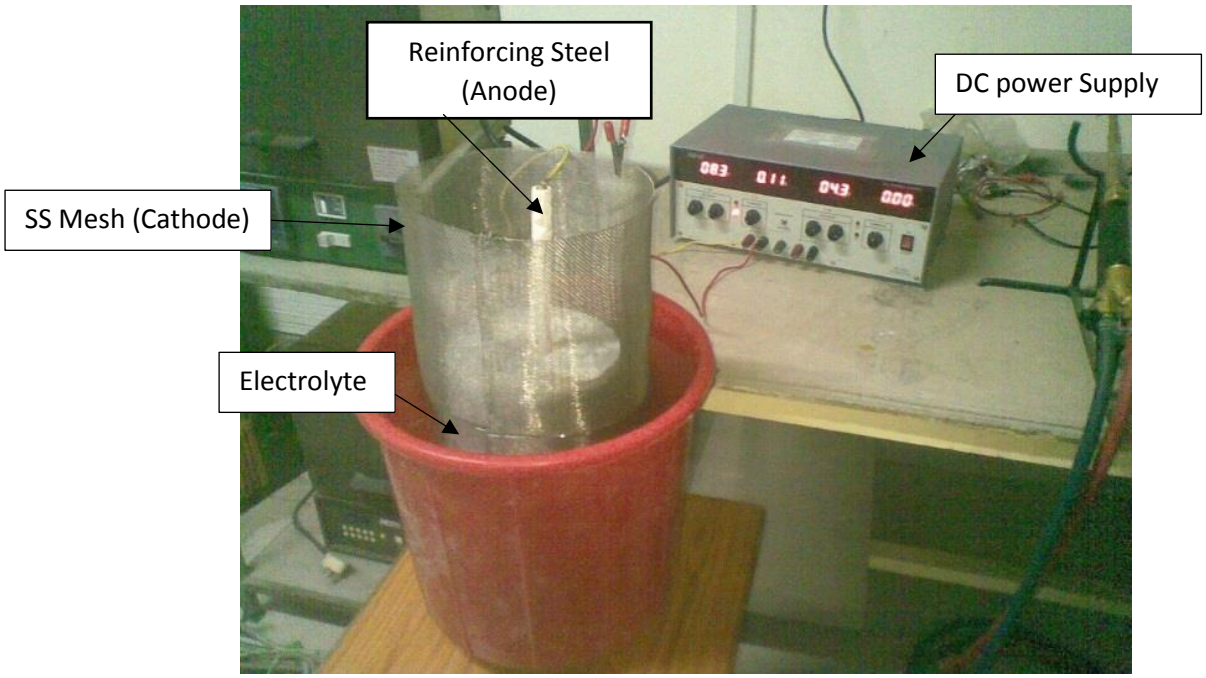

Fig. 3.6. Laboratory Set-up for Stage-I

Table 3.6. Corrosion Exposure Details (Stage-I)

Test Specimen	NaCl Concentration (%)	Anodic Current (mA)	Duration of exposure (Days)	Wt. of bar before corrosion (g)	Wt. of bar after corrosion (g)	% Mass Loss
Specimen 1	5	300	8	650.5	633.0	2.690
Specimen 2	3.5	300	8	652.5	627.0	3.908
Specimen 3	3.5	100	12	626.0	620.0	0.958
Specimen 4	3.5	100	12	627.0	625.5	0.556

Table 3.7.Corrosion monitoring results for specimens in Stage-I

Days	Specimen 1		Specimen 2		Specimen 3		Specimen 4	
	Current (mA)	Voltage (V)	Current (mA)	Voltage (V)	Current (mA)	Voltage (V)	Current (mA)	Voltage (V)
1	300	25.7	300	29.5	100	10.8	100	8.5
2	300	26.1	270	29.3	100	11.5	100	9.1
3	300	26.4	270	29.4	100	11.7	100	9.6
4	300	26.7	270	29.7	100	11.8	100	9.9
5	300	27.1	290	29.6	100	12.0	100	10.1
6	300	27.4	320	29.6	100	12.1	100	9.8
7	300	25.7	330	29.6	100	12.2	100	9.8
8	300	26.5	310	29.5	100	12.4	100	9.8
9	--	--	--	--	100	12.5	100	10.3
10	--	--	--	--	100	12.5	100	10.2
11	--	--	--	--	100	12.5	100	10.2
12	--	--	--	--	100	12.5	100	10.1

3.2.1.4. Observations

Following observation were noted from the tests conducted on the four specimens of Stage-I:

- No specific trend for voltage increase or decrease between rebar and SS mesh was observed.
- The time required for cracking of specimens and corrosion initiation was found to depend upon the anodic current.
- With the increase in anodic current, higher mass losses were observed.
- Damage to concrete in all the cases was severe (Fig. 3.7)

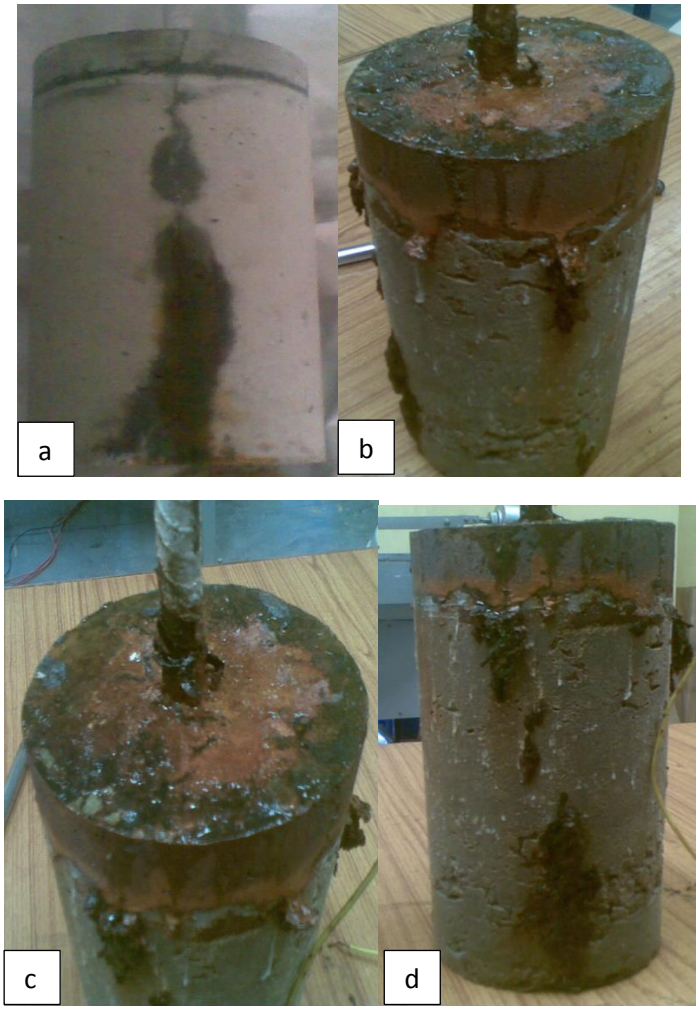

Fig. 3.7. Specimens after Testing (a) Specimen 1, (b) Specimen 2, (c) Specimen 3 and (d) Specimen 4

From the above observations, it was concluded that the higher current resulted in higher damage to concrete and higher mass loss. However, if the current density is reduced, the time required to reach the severe corrosion stage will increase. Therefore, in order to reduce the current density and to achieve the desired corrosion level in a reasonable period of time, it was decided to reduce the dimensions of test specimens. The testing was again repeated at different corrosion levels i.e. low, moderate and severe.

3.2.2. Stage-II

For stage-II, the dimensions of concrete specimens were reduced to 100 mm diameter and 200 mm height cylinders as shown in Fig. 3.8. The steps for preparation of steel rebar were the same as described in the previous section in Stage-I.

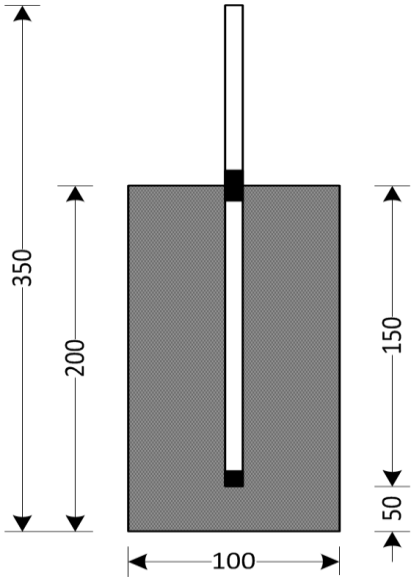

Fig. 3.8. Specimen details for Stage-II with Reduced Dimension

3.2.2.1. Specimen Preparation

The same materials as described in Stage-I were used for casting of these specimens. As the specimen dimensions were reduced, PVC pipe cut into the required dimensions were used as cylindrical molds which can be split into two halves for the sake of easy demolding. For casting of specimens, a special moulding system (Fig. 3.9) was used so as to accurately maintain the position and straightness of the bar with respect to that of the cylinder. To maintain the bottom cover and concentric position of rebar, the specimens were cast in inverted position with the help of this system.

Fig. 3.9. Special molding system used for casting in Stage-II

With the prepared rebar maintained at the center, three specimens were cast at a time with this moulding system. After casting, the specimens were cured for a period of seven days at the temperature of 27 ±2 ºC and relative humidity of 100%. After curing of 7 days, the specimens were subjected to accelerated corrosion using impressed current technique as described in section 3.2.1.3.

Anode to cathode voltage corresponding to constant current was monitored daily for all specimens. The testing was terminated when specimens showed large amount of oozing of corrosion products. All the specimens were then broken, the steel rebar was extracted and cleaned with wire brush to calculate the mass loss. Table 3.8 gives the details of corrosion monitoring and mass loss for these specimens. Fig. 3.10 shows the condition of specimens after testing.

Table 3.8. Corrosion Exposure Details (Stage-II)

Test Specimen	NaCl Concentration (%)	Induced Anodic Current (mA)	Duration of exposure (Days)	Wt. of bar before corrosion (g)	Wt. of bar after corrosion (g)	%Mass Loss
Specimen 1	5	300	8	476.0	435.0	8.61
Specimen 2	3.5	300	8	476.0	444.0	6.72
Specimen 3	3.5	100	8	479.0	465.5	2.82

3.2.2.2. Observations

From the tests conducted on three specimens in Stage II, following observations were made:

- No specific trend for voltage increase or decrease between rebar and SS mesh was observed.
- As the cracking of specimens was observed on 2nd day of current exposure, it was difficult to decide the level of corrosion. Hence, to decide low, moderate and severe corrosion levels, the induced anodic current were required to be reduced.
- Higher loss in diameter of reinforcing steel was observed near the steel-concrete interface where Teflon tape was used as bond breaker, which resulted into intense localized corrosion.
- Higher NaCl concentration of 5% did not show noticeable mass loss as compared to NaCl concentration of 3.5%.
- Higher induced anodic current showed higher mass loss indicating more corrosion for the same exposure duration along with more damage to concrete.

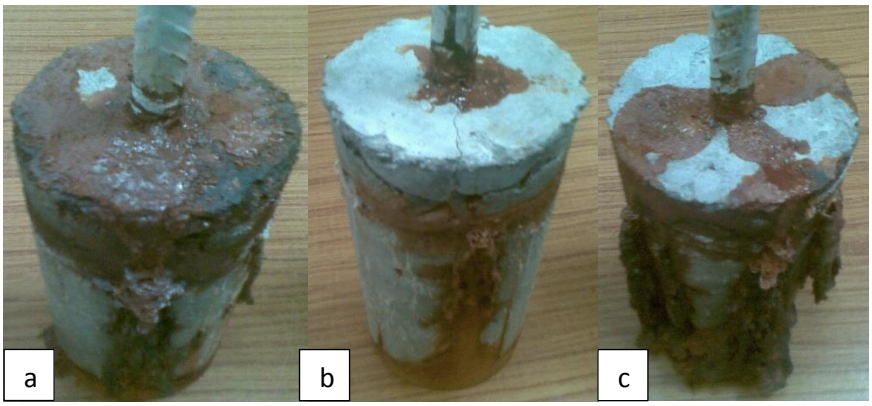

Fig. 3.10. Condition of Specimens of Stage-II at the conclusion of Testing (a) Specimen 1, (b) Specimen 2, (c) Specimen 3

3.2.3. Stage-III

Based on the observations from Stage-II, it was found that by keeping constant current, consistent results were not obtained. Hence, it was decided to choose constant voltage procedure of impressed current method to induce rebar corrosion. It was decided that the voltage levels will be kept low so that the corrosion process will be relatively slow. Use of Teflon tape at specific location had shown more concentration of current and hence more damage to steel due to corrosion at those specific locations was observed. Hence, it was decided to apply epoxy coating at these two locations as well as at protruded part of rebar to avoid corrosion. The specimen dimensions were further reduced so as to reduce the transverse cover to rebar and to complete the testing within lesser time period.

Thus, based on the observations from Stage-I and Stage-II tests, following variables were finalized:

1. Final dimensions of concrete specimen as well as steel rebar:
    - Diameter of concrete cylinder = 60 mm
    - Height of concrete cylinder = 100 mm
    - Total length of steel rebar = 105 mm
    - Length of steel exposed to corrosion = 40 mm
2. NaCl concentration = 5.0%
3. Method of inducing current = Constant voltage method.
4. Input value of voltage = 3V

Along with the change in dimensions and exposure parameters, the specimens of Stage-III were used for preliminary studies of AE technique. The material system, sample preparation and corrosion inducing system were common in all the subsequent long term test phases.

3.2.3.1. Material System

As the dimensions of specimens were reduced, it was required to redesign the concrete mix with smaller size of coarse aggregate. The cement and fine aggregates used in this test programme was the same as the ones taken for earlier stages. However, crushed stone of nominal size 10 mm was used as coarse aggregates, instead of 20 mm size used earlier. For all the specimens, M20 grade of concrete was prepared using the mix proportion of cement: sand: coarse aggregate as 1: 2.76: 2.66 with water-cement ratio of 0.5 as per *IS: 10262 - 2009*. The results of sieve analysis for 10 mm aggregate is shown in Table 3.9. The specific gravity and water absorption for coarse aggregate were 2.70 and 0% respectively. Average 7-days and 28-days compressive strength obtained for all specimens was 20 MPa and 32 MPa respectively as per *IS: 516 - 1959*.

Table 3.9. Results of sieve analysis for coarse aggregates (10 mm)

Sr. No.	I.S. Sieve size.	Weight retained on each sieve	Cumulative weight Retained	Cumulative percentage weight retained (%)	Cumulative percentage weight passing (%)
01.	12.5mm	158	158	7.90	92.10
02.	10mm	822	980	49.00	51.00
03.	4.75mm	1016	1996	99.80	0.20
04.	2.36mm	4	2000	100.00	0.00
	Total	**2000 g**			

3.2.3.2. Specimen Preparation

Cylindrical specimens with concentric steel rebar of length 105 mm were cast (Fig. 3.11). The steel bar was drilled and threaded at one end to accommodate the threaded copper screw for electrical connections, before casting. The bar was then cleaned with wire brush to remove any surface scale. To protect top and bottom portion of the rebar from corrosion, epoxy resin (Dobeckot 505C epoxy resin with

Hardener EH 411) was applied. The length on which epoxy resin was applied was 55 mm from top and 10 mm from bottom. The remaining middle portion of 40 mm was subjected to accelerated corrosion (Fig. 3.12). After allowing the epoxy to harden for 24 hours, the weight of reinforcing bar was recorded to an accuracy of 0.1g.

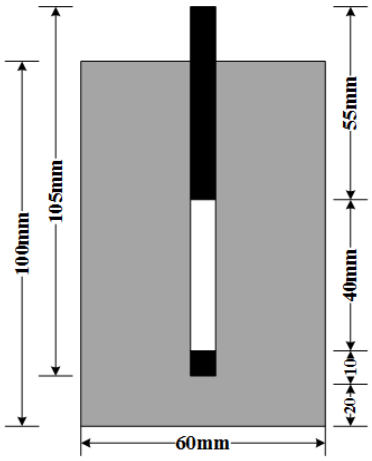

Fig. 3.11. Cylindrical reinforced concrete specimen for Stage-III

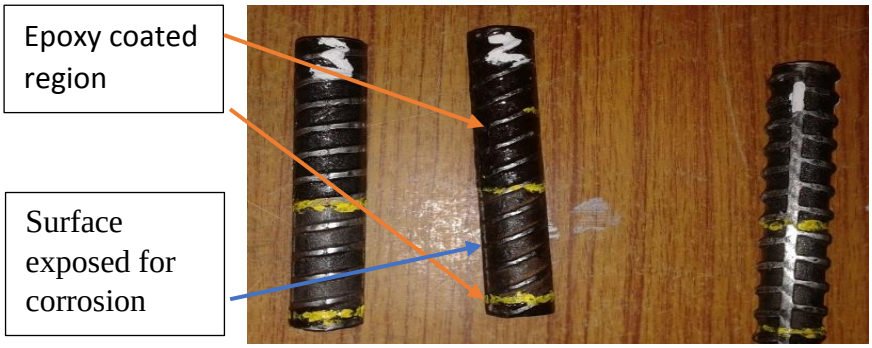

Fig. 3.12. Epoxy coated steel bars used in Stage-III

A new special moulding system (Fig. 3.13) was fabricated for casting of these specimens so as to accurately maintain the position and straightness of the bar with respect to that of the cylinder. To maintain the bottom cover and concentric position of rebar, the specimens were cast in inverted position with the help of this system.

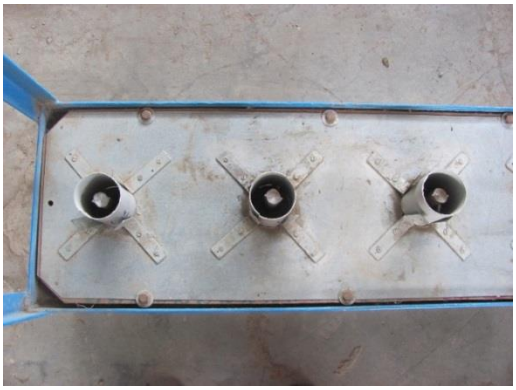

Fig. 3.13. New Special Molding System for casting of speciemns in Stage-III

Fig. 3.14 shows the specimens after casting. After casting, all specimens were kept immersed is water at the temperature of 27 ±2 ºC and relative humidity of 100% for curing for 7 days. The specimens were then kept immersed in 5% NaCl solution on 8th day for 24 hours to ensure full saturation and on 9th day, the specimens were subjected to accelerated corrosion using impressed current technique.

Figure 3.14. Specimens after casting

3.2.3.3. Accelerated corrosion test set-up

A new accelerated corrosion set-up was developed using DC power supply for impressed current technique as described in Stage-I. The set-up was so developed that all the three specimens of one set could be subjected to accelerated corrosion simultaneously using impressed current technique. Each specimen was connected to a

separate ammeter in parallel connection to monitor the variation of current corresponding to induced constant voltage individually. Fig. 3.15 represents the schematic diagram of accelerated corrosion system. The cathode and the specimen were placed in 5% NaCl solution. The level of NaCl solution was kept 30 mm below the top surface of the specimen to alleviate corrosion at the steel-concrete interface and to accommodate the AE sensor. High salinity and impressed current were both used to create aggressive environment by providing an abundance of chloride ions and by stimulating an increased flow of electrons, respectively. A constant voltage of 3V was applied between steel rebar and SS mesh. Anode to cathode current corresponding to constant applied voltage was monitored daily.

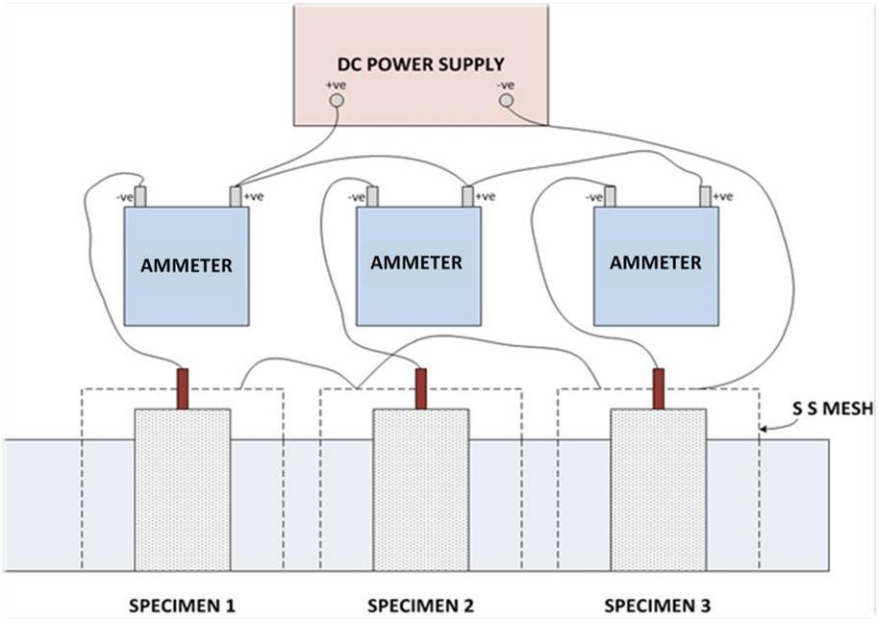

Fig. 3.15. Schematic Representation of Impressed current technique for Accelerated Corrosion

The specimens prepared in Stage-III were further utilized to perform trial test for corrosion monitoring using AE technique and electrochemical techniques simultaneously. Thus, a laboratory based experimental set-up was developed for corrosion monitoring of steel embedded in concrete using AE technique and

electrochemical techniques under accelerated corrosion. The test procedure for the same is described subsequently.

3.3. TEST PROCEDURE

Once the reinforced concrete specimens were prepared, the further test procedure consisted of following four steps:

- Inducing corrosion in steel embedded in concrete.
- Monitoring corrosion using AE technique continuously.
- Monitoring corrosion using electrochemical techniques periodically.
- Determination of mass loss in reinforcing bar after corrosion.

The procedure for each step is described in detail in the following sections:

3.3.1. Inducing corrosion in steel embedded in concrete

The procedure of inducing corrosion in steel embedded in concrete has already been explained in Section 3.2.3.3.

3.3.2. Corrosion monitoring using AE Technique

All the specimens were monitored continuously for AE activity due to corrosion till the end of testing. An instrumentation of AE used in the present research work consists of a transducer, a preamplifier and an acquisition device (MISTRAS from Physical Acoustic Corp.). It consists of single channel USB AE node, AE win-Light software including waveform option with license for USB based system. The sensors consists of R3A, 30 kHz resonant sensor having operating range of 25- 530 kHz. Single AE sensor was attached to each specimen at the top periphery of the concrete surface with the help of a highly viscous coupling agent and electric tape. After attaching the sensors, specimens were kept immersed in NaCl solution for 24 hours to ensure full saturation of specimens. During this saturation period, the specimens were

monitored using AE prior to the application of potential, to ensure that emission due to liquid absorption was not present and to obtain a typical background level of AE for a specimen to decide the threshold. Based on this, the threshold applied for all AE measurements was decided as 40 dB. After 24 hours, the constant potential was applied and specimens were continuously monitored for AE activity. Fig. 3.16 shows the schematic diagram of AE measurement system whereas Fig. 3.17 shows the actual laboratory set-up.

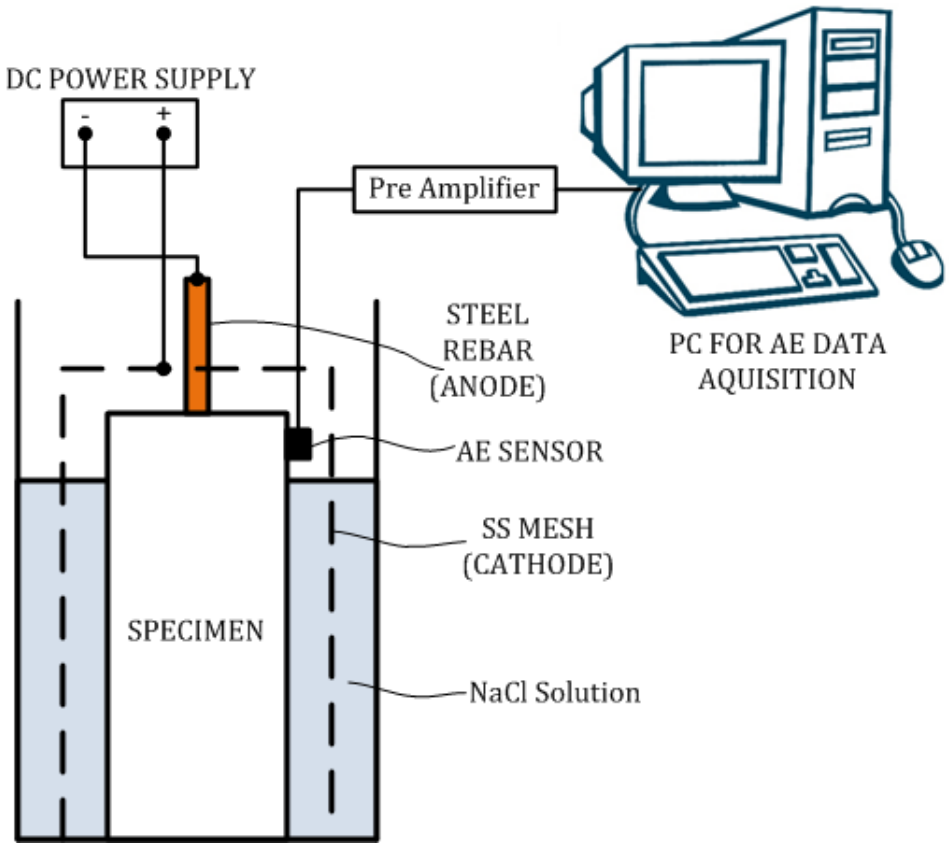

Fig. 3.16. Schematic representation of AE measurement system

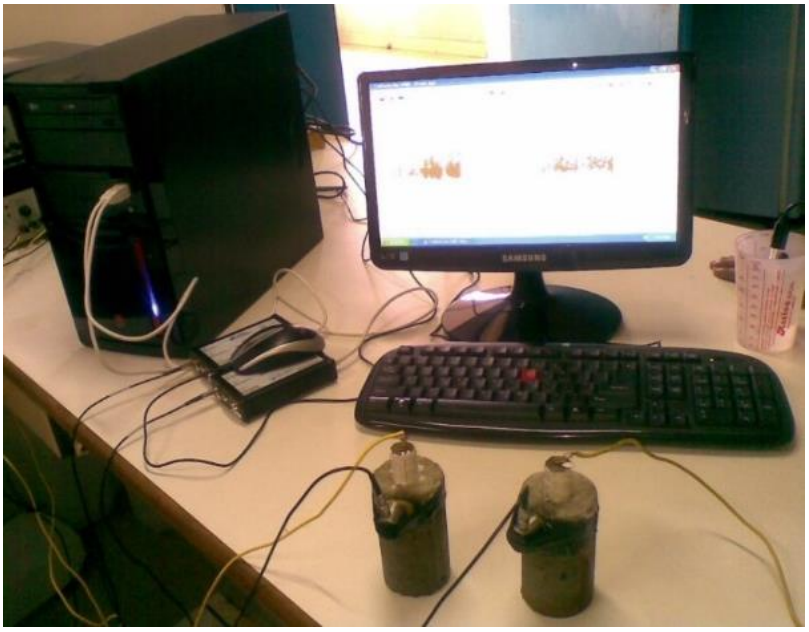

Fig. 3.17. Actual laboratory Set up for AE Testing

Fig. 3.18 and 3.19 reports the graphs as obtained from AE software during trial testing showing variation of hits and amplitude with time respectively. For trial tests the threshold was set to 30dB. Many researchers have used these basic parameters of AE for damage assessment. Fig. 3.20 represents the cumulative variation of various AE parameters i.e. rise time, amplitude, energy, counts and duration with time obtained from AE software for the specimen under active corrosion. The variation of energy and amplitude were found overlapping each other. Observing the graph it was found that variation of all the parameters with time have a specific trend showing sudden rise in activity after specific time. This variation in AE activity with time can be associated with damage due to corrosion. The comparison of such AE activities with well-established electrochemical techniques and visual inspection can enlighten the corrosion phenomenon, which is described in detail in Chapter 4.

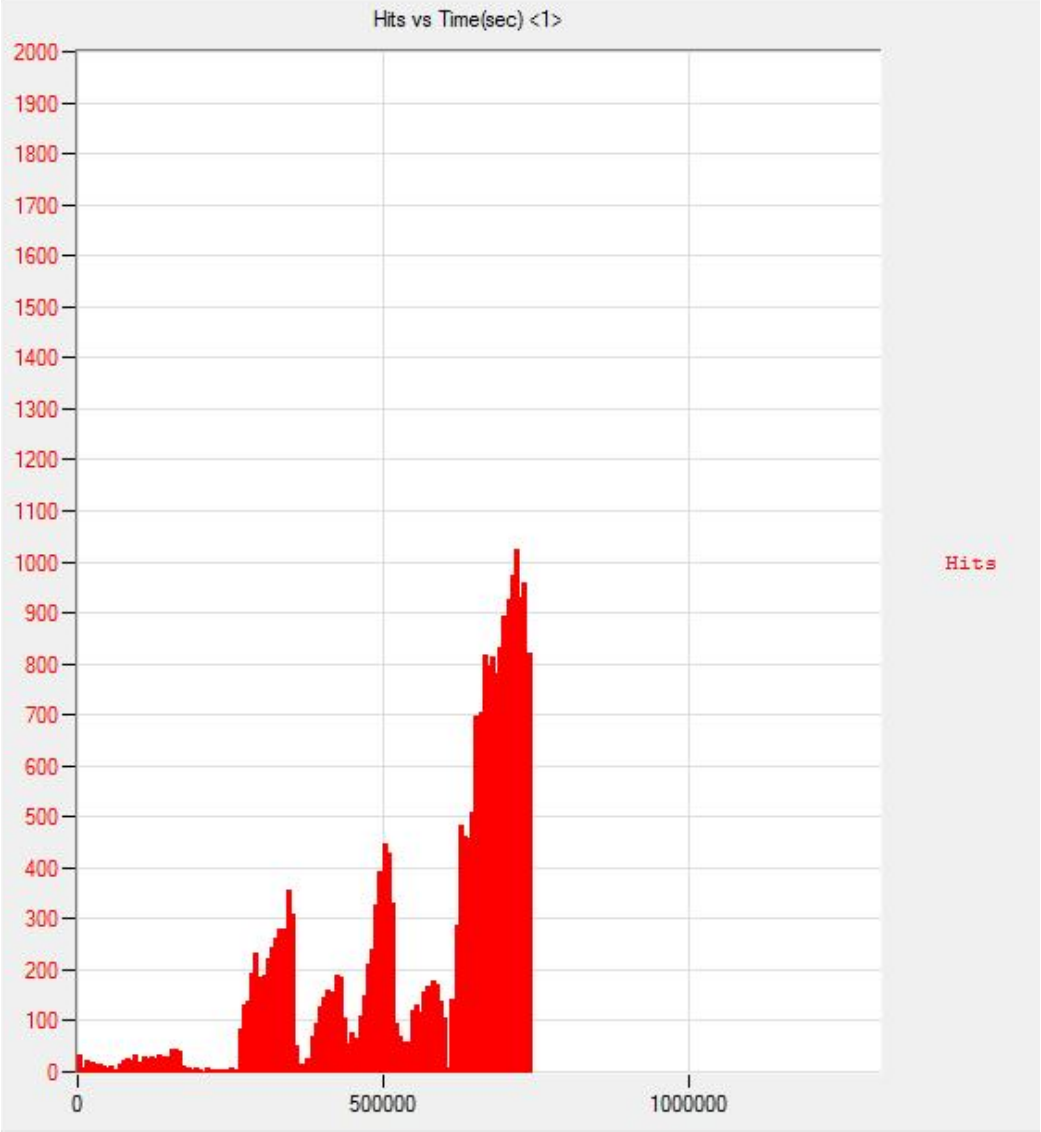

Fig. 3.18. A typical plot of Hits vs Time obtained by AE software

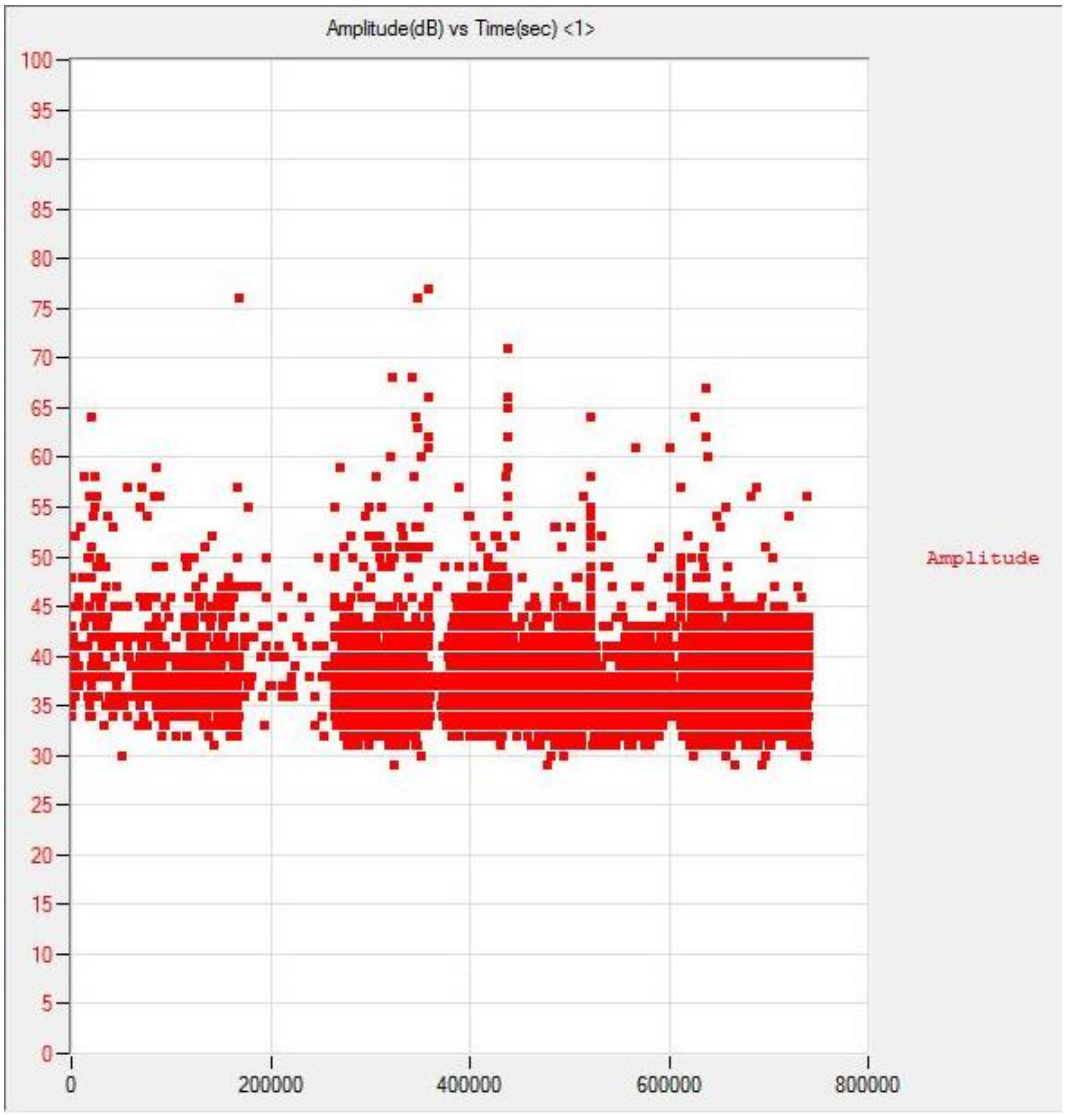

Fig. 3.19. A typical plot of Amplitude vs Time obtained by AE software

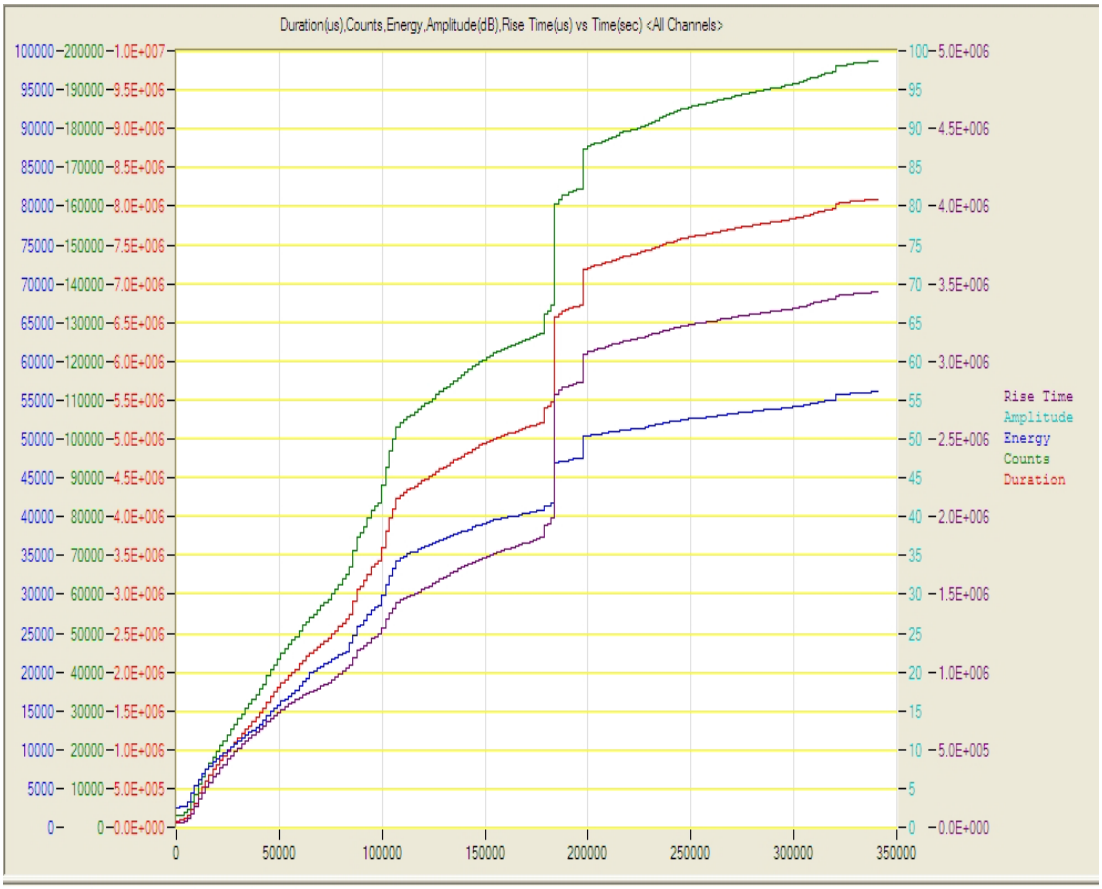

Fig. 3.20. Variation of various AE parameters with time

3.3.3. Corrosion monitoring using Electrochemical Techniques

The corrosion activity was monitored periodically using electrochemical techniques till the end of the test. Various electrochemical techniques employed were measurement of half-cell potential and corrosion current density. Prior to the electrochemical measurements, DC supply was interrupted for a period of half-an-hour. Electrochemical readings using both the techniques were taken whenever the change in colour of NaCl solution was observed which indicated corrosion activity. All the measurements were taken using fresh NaCl solution every time. The electrochemical readings were also obtained before imposing the potential to the specimens which indicated the initial corrosion status of steel rebar. During the

electrochemical measurements, AE monitoring was paused for approximately one hour in order to avoid acquisition of noise induced due to handling of specimen.

3.3.3.1. Half-cell Potential measurements

The half-cell potential measurements were carried out using "Saturated Calomel Electrode" (SCE). Fig. 3.21 indicates the set-up for measurement of half-cell potentials.

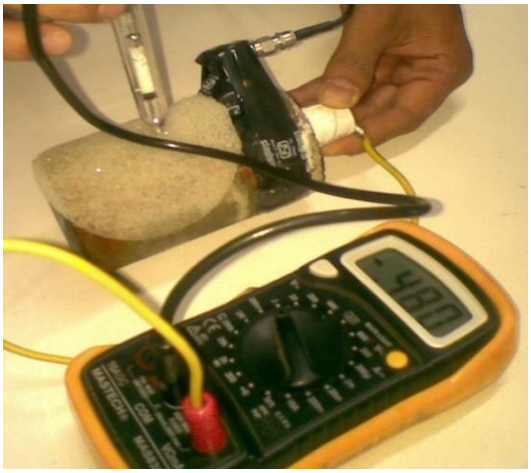

Fig. 3.21. Half-cell potential measurement

The measured half-cell potential values for each specimen were plotted against time to study the variation of half-cell potential with the progress of corrosion.

3.3.3.2. Current Density measurements

Immediately after measurement of half-cell potential, the potentiostatic electrochemical polarization scans were obtained for all the specimens. In the present investigation, Potentiostat model 1.0 (Crest Technology) was used to obtain Tafel plots. The scans were carried out at the rate of 0.5 mV/s between the potential range of -1.0 V and +1.0 V using the reinforcing bar as a working electrode, stainless steel mesh as a counter electrode and SCE as a reference electrode. From the potentiostatic plots, the corrosion current were determined using Tafel extrapolation technique as

described in Section 1.3.2 of Chapter 2. For extrapolating the linear regions of Tafel curves and for finding the corrosion current at the intersection of the two extrapolated lines, an excel program was developed which could provide these values directly on the graphs (Fig. 3.22). The corrosion current thus obtained were used to calculate the corrosion current density, from which the corrosion rates for all specimens were calculated based on Faraday's law using Eq. 2.1.

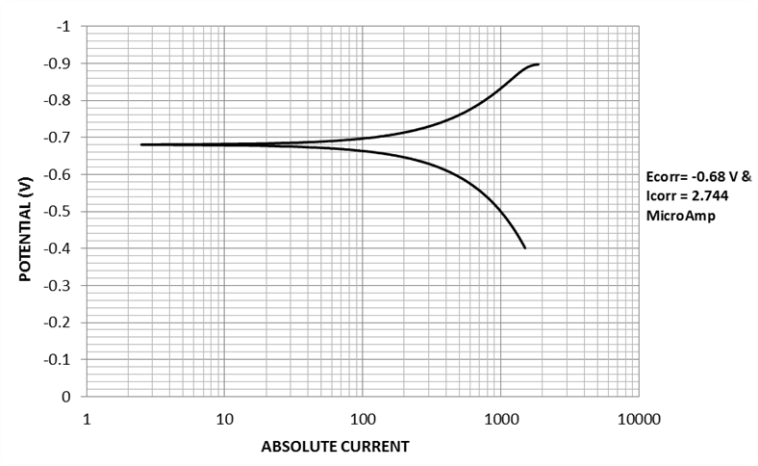

Fig. 3.22. Tafel plot obtained from potentiostat and Corrosion current value obtained from excel program

The measured corrosion current density values for each specimen were plotted against time to study the progress of corrosion.

3.3.4. Determination of mass loss

After completion of the tests, each sample was visually examined for cracks and then concrete cover to the rebar was carefully removed. After removing the concrete cover, the epoxy coating applied to steel rebar was observed to be intact. Corrosion products from steel surface were gently removed with a wire brush as per *ASTM: G1-03 - 2003*. The bars were then weighed with the epoxy coating to determine the mass loss to a precision of 0.1g. It is important to be mentioned here that although weighing scale with more precision was available, however, the weight of the rebars was the

constraint for the use of scale with the least count of 0.1 g only. Table 3.10 reports the corrosion exposure details of Stage-III testing.

Table 3.10. Corrosion Exposure Details (Stage-III)

Test Specimen	NaCl Concentration	Induced anodic Potential	Current Duration (Days)	Wt. of bar before corrosion (g)	Wt. of bar after corrosion (g)	% Mass Loss
Specimen 1	5%	3 V	12	255.19	249.47	2.24 %
Specimen 2	5%	3 V	12	253.31	251.97	0.528%
Specimen 3	5%	3 V	12	255.86	249.07	2.65%

3.4. CLOSING REMARKS

This chapter deals with the preliminary experimental investigations to decide the variables to accelerate corrosion of steel embedded in concrete. One of the challenges in the corrosion experiment is how to accelerate corrosion that simulates the failure in field conditions accurately. It has been found that application of a constant anodic potential through a steel embedded in concrete which is submerged in saline water is a very fast and effective method. The following observations were made in the preliminary experimentation, which helped in finalizing the test set-up for the study:

1. It has been found that the cell current maintaining a constant anodic potential is a better metric for corrosion monitoring than the cell voltage maintaining a constant anodic current.
2. The application of epoxy is more effective to serve as bond breaker and for protection of specific portion of steel rebar from corrosion as compared to use of Teflon tape which results in more concentration of current and hence more localized damage due corrosion at those specific locations.

3. Application of higher cell voltages and use of smaller dimensions of concrete specimen result in accelerated corrosion process of steel embedded in concrete.

Based on preliminary experimental investigations, a laboratory based experimental set-up was developed for corrosion monitoring of steel embedded in concrete using AE technique and electrochemical techniques (namely measurement of half-cell potential and corrosion current density) simultaneously under accelerated corrosion as described in Section 3.3. The test procedure so developed is utilized for further experimental investigations to explore the efficacy of AE technique for corrosion monitoring of steel rebar in concrete as explained in Chapter 4.

CHAPTER 4

CORROSION ASSESSMENT USING ACOUSTIC EMISSION VIS-À-VIS ELECTROCHEMICAL TECHNIQUES

4.1. INTRODUCTION

Corrosion of rebar in concrete is an electrochemical process and it can be studied using various electrochemical methods. As explained in Chapter 2, the most common method for corrosion monitoring is by measuring half-cell potential which indicates the probability of corrosion in reinforced concrete structures. The quantitative techniques for corrosion assessment mainly involve determination of corrosion rate which is an important parameter for predicting the service life of reinforced concrete structures. Tafel extrapolation technique is one of the widely used electrochemical techniques for this purpose. The corrosion process of rebar can also be studied using AE technique. AE is not an electrochemical method, but by utilising the sensitivity of the technique to the initiation and growth of micro-cracks, AE technique can identify corrosion by detecting micro-cracking induced to concrete as a consequence of the corrosion reaction *(Ing et al. 2005).*

The fundamental difference between the application of these two techniques is while electrochemical measurements require direct contact with steel rebar for measuring any parameter, AE measurements are taken on concrete surface and effect of corrosion is obtained through the response of concrete to corrosion. As such, the results obtained by these techniques differ from each other. Hence proper interpretation of the results obtained using AE in comparison with electrochemical techniques is necessary. Therefore, the first objective of the present study is to

investigate whether AE can offer direct information about damage due to corrosion in comparison with the results obtained using electrochemical techniques.

4.2. EXPERIMENTAL PROGRAMME

In order to get useful results within the realistic time period, the corrosion process was accelerated. Three procedures were used for acceleration of corrosion; viz. impressed current, alternate drying-wetting process and internal chloride exposure. Based on the acceleration procedures adopted, the experimental programme was divided into two sets. The details of two sets are as under:

1. "Set–I": In this set, the corrosion process was accelerated using impressed current technique. The level of impressed current and the amount of NaCl used was finalized on the basis of preliminary testing carried out on the specimens. The details of preliminary testing are described in Chapter 3.

   The results obtained from Set–I were used to explore the efficacy of AE technique for corrosion monitoring of steel rebar in concrete. The same results were also used to study the effect of material properties on corrosion as well as on AE measurements and to develop a mathematical model.
2. "Set–II": In this set, the corrosion process was accelerated by two techniques that take longer time for corrosion process as compared to impressed current technique. The two exposure techniques adopted in this set are:

   (a) Alternate drying-wetting process and

   (b) Internal chloride exposure.

The results of Set–II (a) were used to validate the effectiveness of impressed current technique and the results of Set-II (b) were used to validate the developed mathematical model.

The test layout for Set–I of the experimental programme is presented in Fig. 4.1 and the test results are discussed in subsequent sections whereas the details of Set-II of the experimental programme are discussed in Chapter 6.

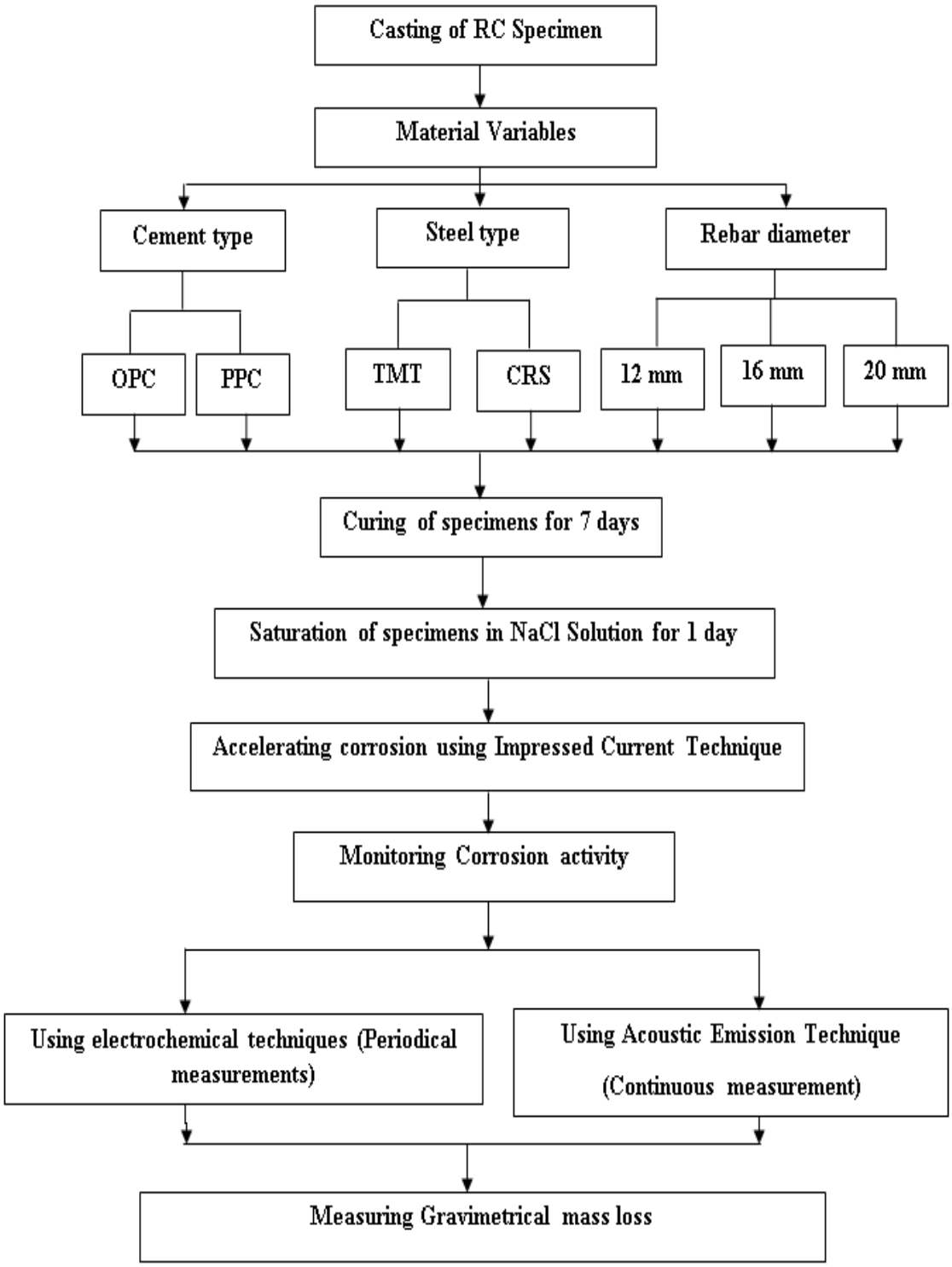

Fig. 4.1. Test Layout for Set–I of the experimental programme

4.3. MATERIAL SYSTEM

The major test variables for the Set-I of the experimental programme include cement type, steel type and rebar diameter. The basic properties of each test variable are described in the following sections:

4.3.1. Cement

In Indian scenario, the most commonly used cement types in practice are:

1) Ordinary Portland cement (OPC) of 53 grade confirming to Indian standards *IS: 12269-1999*
2) Portland pozzolana cement (PPC) having 15-35% pozzolana (fly ash) content, confirming to Indian standards *IS: 1489 (Part I) – 1991*.

Hence, the present investigation studies the influence of these two types of cement on the rebar corrosion. The physical properties of OPC and PPC as obtained from the manufacture are presented in Table 4.1. The chemical compositions of the two types of cement as obtained from the manufacture are presented in Table 4.2.

Table 4.1. Physical of cement Properties

Physical properties	**OPC**	**PPC**
Fineness		
Specific Surface	306 m^2/kg	365 m^2/kg
Soundness		
By Le – Chatelier Method	0.8 mm	0.5 mm
Setting Time		
Initial Setting Time	140 minutes	170 minutes
Final Setting Time	190 minutes	230 minutes
Compressive Strength		
i) 3 days	38.2 MPa	34.4 MPa
ii) 7 days	48.3 MPa	44.8 MPa
iii) 28 days	66.4 MPa	63.6 MPa
Temperature during Testing	27^0C	27^0C
Standard Consistency	29 %	31 %

Table 4.2. Chemical composition of cement

Compound	OPC (%)	PPC (%)
CaO	63.2	48.2
SiO_2	21.4	28.8
Al_2O_3	5.0	9.2
Fe_2O_3	3.6	4.4
MgO	0.8	1.5
SO_3	2.2	2.0
*LOI	1.5	2.2

*Loss on Ignition

4.3.2. Steel

For evaluation of the comparative performance of different types of steel reinforcement, following two types of steel bars were used for the experimental investigation.

1. TMT: Thermo-mechanically treated steel bars
2. CRS: Corrosion resistant steel bars

The TMT steel is the most commonly used steel type in Indian scenario. The yield strength of these two types of steel satisfies Fe 500 grade steel *(IS: 1786 - 1990)*. Table 4.3 reports the chemical composition of TMT and CRS steel as obtained from the manufacturer.

Table 4.3 Chemical composition of steel

Element	Tiscon TMT (%)	Tiscon CRS (%)
C	0.25	0.15
Mn	0.90	1.00
S	0.035	0.04
P	0.035	0.10
Si	0.45	0.45
*CRE	---	0.50

*Corrosion resistant element

Three different diameters of 12 mm, 16 mm and 20 mm of these steel types were used in the experimental investigation.

4.3.3. Aggregates

Crushed stone of nominal size 10 mm was used as coarse aggregates and natural river sand conforming to zone I as per *IS: 383-2002* was used as fine aggregates. The specific gravities of coarse and fine aggregates were found to be 2.7 and 2.75 respectively. Table 3.3 and 3.9 reports the result of sieve analysis for fine and coarse aggregates respectively.

From Table 3.3, it is seen that for fine aggregates, the percentage passing from 600 micron sieve is 28.34% which lies between 15 to 34% confirming to Zone-I of fine aggregates. The combined grading of coarse and fine aggregates in the proportion of 1:1 is presented in Table 4.4.

Table 4.4. Gradation of all in aggregates

Sieve Size	**Desired Limits *IS: 383-2002***	**All in Aggregate % Passing**		**Proportion**		**Combined grading**
		CA	**FA**	**CA**	**FA**	
				50 %	**50 %**	
12.5 mm	95 – 100	92.1	100	46.05	50	96.05
10 mm	75 – 90	51	99.68	25.5	49.84	75.34
4.75 mm	30 – 50	0.2	86.64	0.1	43.32	43.42
600 micron	10 – 35	0	28.34	0	14.17	14.17

4.3.4. Water

Potable tap water was used for casting of specimens in the experiment.

4.4. CONCRETE MIX PROPORTION

To achieve a sufficient degree of corrosion within the limited time period of experimentation, the concrete mix of grade M20 corresponding to mild exposure

condition was designed for all specimens with a water-cement ratio of 0.5 as per *IS: 10262 - 2009*. All the concrete mixes have been designed for similar workability with slump of 60-80 mm. To have similar workability, number of trial tests was conducted with different water contents and finally the water content was kept constant to 175 kg/m^3 for the desired slump in all the mixes with a water-cement ratio of 0.5. No admixture was used in the preparation of concrete. The w/c ratio, cement content, fine aggregate content and coarse aggregate content of the concrete mixes made with two types of cement are presented in Table 4.5.

Table 4.5. Concrete mix proportion

Cement type	**Water/cement Ratio**	**Cement content (Kg/m^3)**	**Fine aggregate Content (Kg/m^3)**	**Coarse aggregate Content (Kg/m^3)**	**Mix-proportions**
OPC	0.5	350	966.85	932.85	1: 2.76: 2.66
PPC	0.5	350	966.85	932.85	1: 2.76: 2.66

The compressive strength of the mixes designed was checked at 7 days and 28 days by casting cubes of size 150 mm using both OPC and PPC cement. The specimens were cured at temperature of 27 ±2 ºC and relative humidity of 100%. The average compressive strength of both mixes are presented in Table 4.6.

Table 4.6 Compressive strengths

Cement type	**Specimen No.**	**7 days Compressive strength (MPa)**	**Average (MPa)**	**28 days Compressive strength (MPa)**	**Average (MPa)**
OPC	1	21.37	21.83	34.62	32.89
	2	22.88		32.08	
	3	21.24		31.97	
PPC	1	17.55	17	31.02	31.72
	2	16.33		31.40	
	3	17.12		32.75	

4.5. PREPARATION OF REINFORCED CONCRETE SPECIMENS

The dimensions of specimens used in the present experimentation were finalized through preliminary experimental investigation as explained in Chapter 3. Based on preliminary investigations, cylindrical concrete specimens of diameter 60 mm and height 100 mm were cast with a concentric steel rebar. The length of steel rebar was 105 mm, out of which 40 mm was subjected to corrosion. The procedure of reinforced concrete specimen preparation is explained in detail the section 3.2.3.2 of Chapter 3 and is briefly outlined hereunder.

A steel rebar of length 105 mm was taken. Before embedding the bar in concrete, it was drilled and threaded at one end to accommodate the threaded copper screw for electrical connections. The bar was then cleaned with a wire brush to remove any surface scales. To protect top and bottom portion of the rebar from corrosion, epoxy resin (Dobeckot 505C epoxy resin with Hardener EH 411) was applied. The length on which epoxy resin was applied was 55 mm from top and 10 mm from bottom. The remaining middle portion of 40 mm was subjected to accelerated corrosion. After allowing the epoxy to harden for 24 hours, the weight of reinforcing bar was recorded to an accuracy of 0.1g. The reinforced concrete cylinders were then cast using the special moulding assembly.

4.6. TEST PROCEDURE

After casting the specimens, the same test procedure as described in section 3.3 of Chapter 3 was followed. The test procedure consisted of following four phases:

- Inducing corrosion in steel embedded in concrete.
- Monitoring corrosion using AE technique continuously.
- Monitoring corrosion using electrochemical techniques periodically.

- Determination of mass loss of reinforcing bar after corrosion.

4.6.1. Inducing corrosion in steel embedded in concrete

The motive of inducing corrosion in steel embedded in concrete and the procedure followed is the same as that explained in section 3.2.3.3 of Chapter 3. For inducing corrosion, the cathode (SS mesh) and the specimen were placed in 5% NaCl solution. The level of NaCl solution was kept 30 mm below the top surface of the specimen to alleviate corrosion at the steel-concrete interface and to accommodate the AE sensor. All the specimens were then exposed to constant voltage for accelerating the corrosion process. The specimens with 12 mm rebar were exposed to 4V voltage whereas for the remaining specimens 3V voltage is used as the concrete cover is more for specimen with 12 mm rebar as compared to other two rebar diameter specimens.

In the present experimental investigation, total 15 reinforced concrete cylindrical specimens were cast with three diameters of steel rebar viz. 12 mm, 16 mm and 20 mm, two types of cement viz. OPC and PPC and two types of steel viz. TMT and CRS which are widely used in practice. The typical test matrix adopted is summarized in Table 4.7. For all the specimens, the testing was stopped when the crack due to corrosion appeared and became distinct on the surface of concrete.

Table 4.7. Test Matrix

Set No.	Corrosion acceleration procedure	Cement type	Steel type	Rebar diameter (mm)	Test duration (days)	Nomenclature	Repetitions
Set I	Impressed current	OPC	TMT	12	20	OT-12 SP-1	3
						OT-12 SP-2	
						OT-12 SP-3	
		OPC	TMT	16	12	OT-16 SP-1	3
						OT-16 SP-2	
						OT-16 SP-3	
		OPC	TMT	20	20	OT-20 SP-1	3
						OT-20 SP-2	
						OT-20 SP-3	
		PPC	TMT	20	35	PT-20 SP-1	3
						PT-20 SP-2	
						PT-20 SP-3	
		OPC	CRS	20	20	OC-20 SP-1	3
						OC-20 SP-2	
						OC-20 SP-3	

4.6.2. Corrosion monitoring using AE Technique

The procedure followed for corrosion monitoring of reinforced concrete cylinders using AE technique was as described in section 3.3.2 of Chapter 3. All the specimens were monitored continuously for AE activity due to corrosion till the end of testing. A single AE sensor was attached to each specimen at the top periphery of the concrete surface with the help of a highly viscous coupling agent and electric tape and was used for recording AE activity.

There are a number of parameters of AE technique that can be used to extract information about AE activity. AE signal strength is one such parameter which is defined as the measured area of the rectified AE signal, with units proportional to volt-seconds. The signal strength is often referred to as relative energy which is a measure of the amount of energy released by specimen *(ASTM: E1316 - 2010)*. The research shows that when cumulative signal strength (CSS) is plotted versus time, the

CSS will generally increase sharply at a certain time which can be correlated to damage and corrosion *(Noorsuhada et al. 2011, Di Benedetti et al. 2013)*. Similar pattern for variation of other different parameters were shown in Fig. 3.20 and discussed in section 3.3.2 of chapter 3. As signal strength is referred to a measure of the amount of energy released by specimen during damage process, it can identify and evaluate the corrosion process. Hence, in the present study, CSS parameter of AE is used to identify the extent of damage to concrete due to corrosion and it is compared with electrochemical results.

All the specimens of Set–I were monitored continuously for AE activity due to corrosion. Typical variation of CSS with time for OT-12 SP-1 is shown in Fig. 4.2.

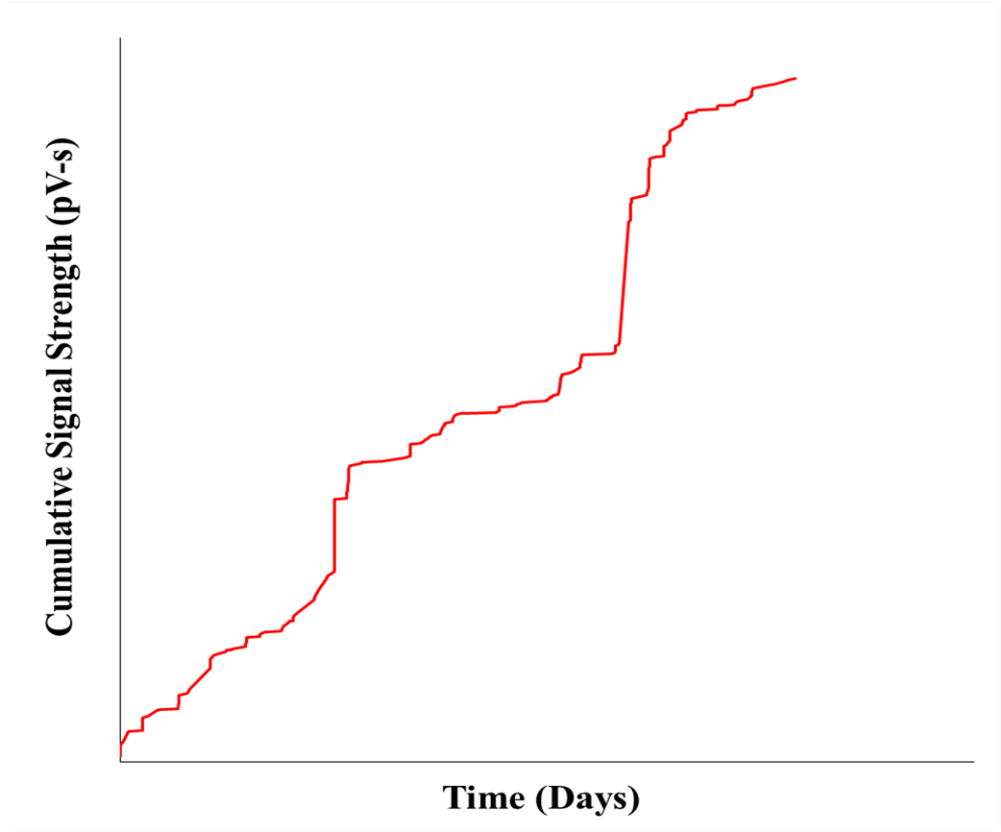

Fig. 4.2. Typical variation of cumulative signal strength with time for reinforced concrete specimen under accelerated corrosion

The corrosion monitoring of specimens was started on the ninth day of casting and it is known that the cement hydration process is not complete by that time. Therefore, it was necessary to discriminate between the AE signals associated with corrosion and the signals due to cement hydration which is an ongoing process as concrete cures. To tackle this issue, concrete cylinder having the same dimensions but without steel reinforcement were cast and continuously monitored for AE activity. The typical variation of CSS with time for such specimens is presented in Fig. 4.3. The CSS curve in Fig. 4.3 clearly distinguishes the AE activity recorded for concrete specimen during curing period from the specimen under active corrosion shown in Fig. 4.2.

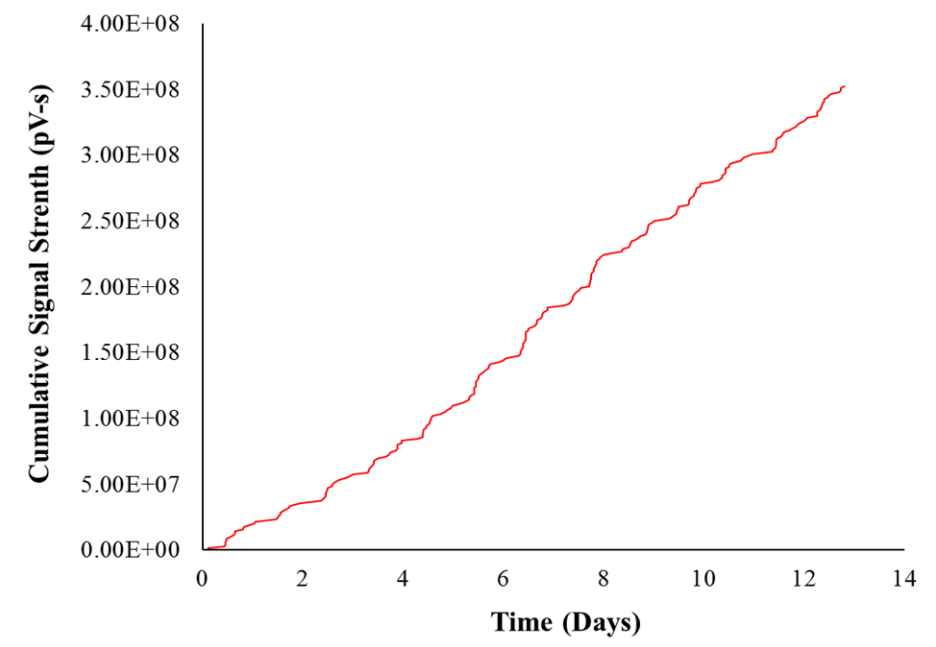

Fig. 4.3. Typical variation of Cumulative signal strength with time for concrete specimen under curing

4.6.3. Corrosion monitoring using Electrochemical Techniques

The corrosion activity was monitored periodically by the electrochemical techniques. Various electrochemical techniques employed were measurement of half-

cell potential and corrosion current density. The procedure followed for corrosion monitoring of reinforced concrete specimens using electrochemical techniques was as described in section 3.3.3 of Chapter 3. During the electrochemical measurements, AE monitoring was paused in order to avoid acquisition of noise induced due to handling of specimens.

4.6.3.1 Half-cell Potential measurements

The procedure followed for corrosion monitoring of reinforced concrete specimens using half-cell potential has been described in detail in section 3.3.3.1 of Chapter 3. For half-cell potential measurements, Saturated Calomel Electrode (SCE) was used as reference electrode. Half-cell potential measurements were carried out whenever the change in colour of NaCl solution was observed which indicated corrosion activity. All the measurements were taken using fresh NaCl solution every time. Prior to the measurement of half-cell potential, DC supply was interrupted for half an hour. The half-cell potential readings were also obtained before imposing the potential to the specimens. The measured half-cell potential values for each specimen were plotted against time to study the variation of half-cell potential with the progress of corrosion. Typical variation of half-cell potential with time for three replicates of OT-12 specimens is shown in Fig. 4.4 which shows that the pattern of variation for three replicates is perfectly in agreement with each other.

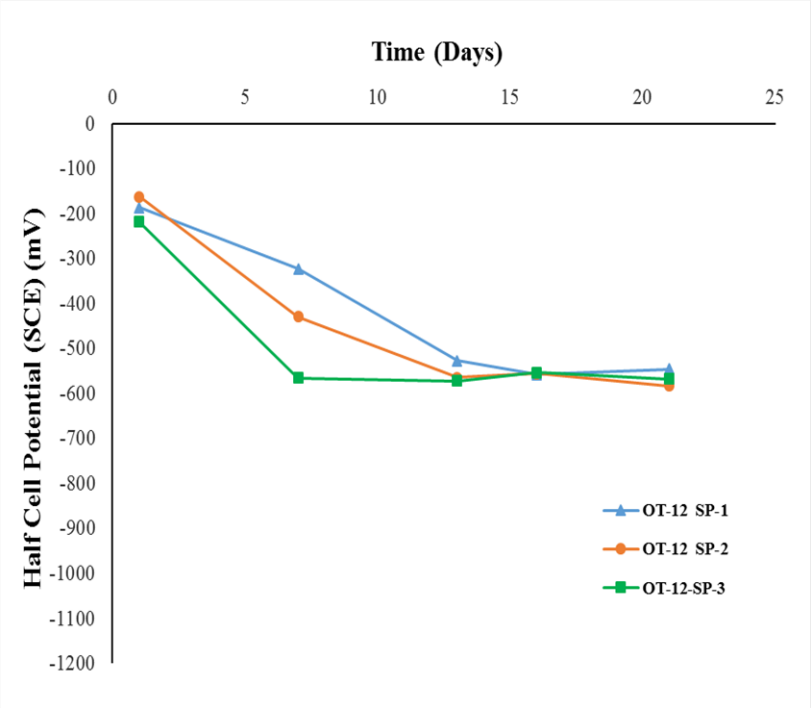

Fig. 4.4. Typical variation of half-cell potential with time for three replicates of OT-12 specimen

4.6.3.2 Current Density measurements

Although half-cell potential is a good indicator of initiation of corrosion, it may not be effective in monitoring its progress in terms of level of corrosion as low, moderate or severe. Hence to monitor the progress of corrosion process, potentiostatic electrochemical polarization scans were obtained for all specimens immediately after measurement of half-cell potential every time. The procedure adopted to obtain the potentiostatic polarization scans has been described in section 3.3.3.2 of Chapter 3. Briefly, the scans were carried out at the rate of 0.5 mV/s between the potential range of -1.0 V and +1.0 V using the reinforcing bar as a working electrode, stainless steel mesh as a counter electrode and SCE as a reference electrode. From the potentiostatic plots, the corrosion current were determined using Tafel extrapolation technique. The measured corrosion current density values for each specimen were plotted against time to study the progress of corrosion. Typical variation of corrosion current density

(i_{corr}) with respect to time for three replicates of OT-12 specimens is presented in Fig. 4.5 which shows that the variation for three replicates is perfectly in agreement with each other.

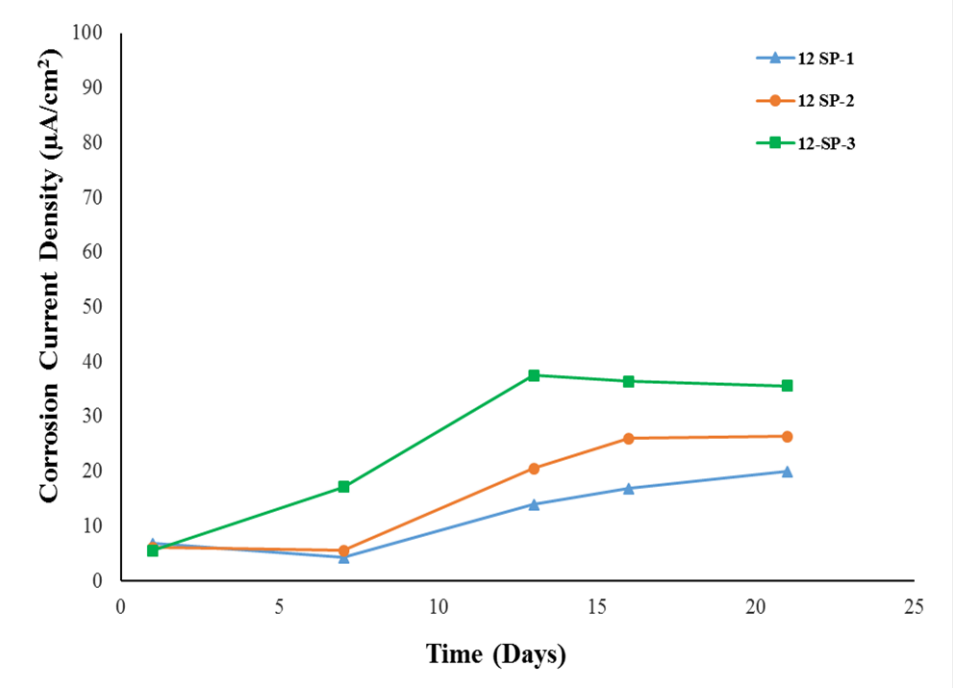

Fig. 4.5. Variation of Corrosion current density with time for three replicates of OT-12 specimens

4.6.4. Determination of mass loss

After completion of tests (i.e. after appearance of distinctly visible crack on the concrete surface), the specimens were broken so to remove the concrete cover and get the steel rebar. After removing the concrete cover, the epoxy coating applied to steel rebar was observed to be intact. Corrosion products from steel surface were gently removed with a wire brush as per *ASTM: G1-03* - 2003. The bars were then weighed with the epoxy coating to determine the mass loss to a precision of 0.01g. Table 4.8 reports gravimetric mass loss values along with results of AE (cumulative signal

strength) and electrochemical technique (corrosion current density) for all specimens at the end of testing.

Table 4.8 Gravimetric mass loss, Corrosion Current Density and Cumulative Signal Strength values

Specimen	Gravimetric mass loss (g)	Final i_{corr} ($\mu A/cm^2$)	max CSS (pV-sec)
OT-12 SP-1	2.61	19.88	8.04×10^6
OT-12 SP-2	3.53	26.27	7.49×10^7
OT-12 SP-3	5.68	38.95	3.48×10^7
OT-16 SP-1	6.50*	24.48*	$9.51 \times 10^{9*}$
OT-16 SP-2	3.18	31.98	1.82×10^7
OT-16 SP-3	3.63	36.80	1.39×10^7
OT-20 SP-1	12.38	27.72	1.18×10^{10}
OT-20 SP-2	11.78	47.64	1.37×10^{10}
OT-20 SP-3	14.98	39.44	3.90×10^9
PT-20 SP-1	4.78	24.21	1.29×10^7
PT-20 SP-2	8.62	25.47	2.73×10^7
PT-20 SP-3	7.59	23.98	1.17×10^8
OC-20 SP-1	5.52	37.23	2.64×10^7
OC-20 SP-2	5.91	34.3	2.70×10^7
OC-20 SP-3	4.29	32.65	6.00×10^6

*erroneous data hence not considered in further analysis.

4.7. RESULTS AND DISCUSSIONS

The CSS curve shown in Fig. 4.2 was compared with the phenomenological model of corrosion of steel embedded in concrete in marine environments represented in Fig. 4.6. It can be observed that the trend of CSS curve obtained is similar to the curve corresponding to the phenomenological model of corrosion, which divided corrosion into four phases. Similar to that trend, the CSS curve can also be divided into 4 phases. There is only one exception in the CSS curve, i.e. the curve shows two sudden rises, first at the end of phase 1 and second at the end of phase 2 as shown in

Fig. 4.7. If these sudden rises are excluded from the curve, the curve shown with dotted line will be obtained which, if connected with smooth line, will be exactly in agreement with curve shown in Fig. 4.6. The presence of sudden rises in CSS curve may indicate damage to concrete due to expansion of corrosion products, which was further verified with electrochemical results.

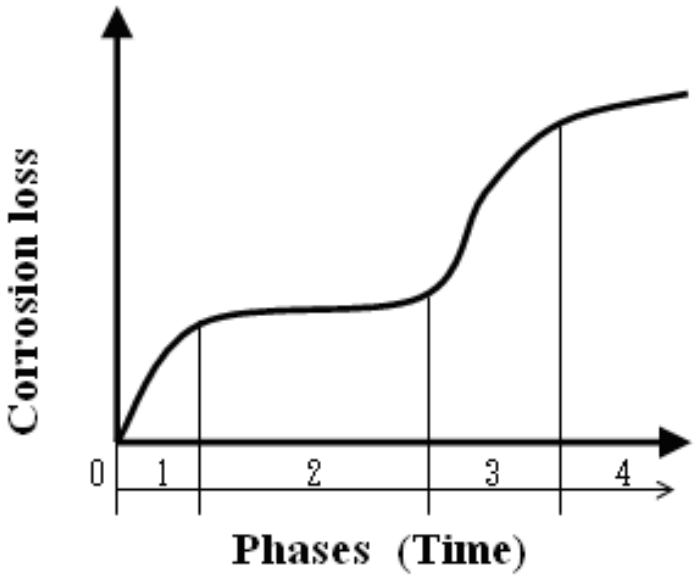

Fig. 4.6. Typical corrosion loss for steel in seawater immersion

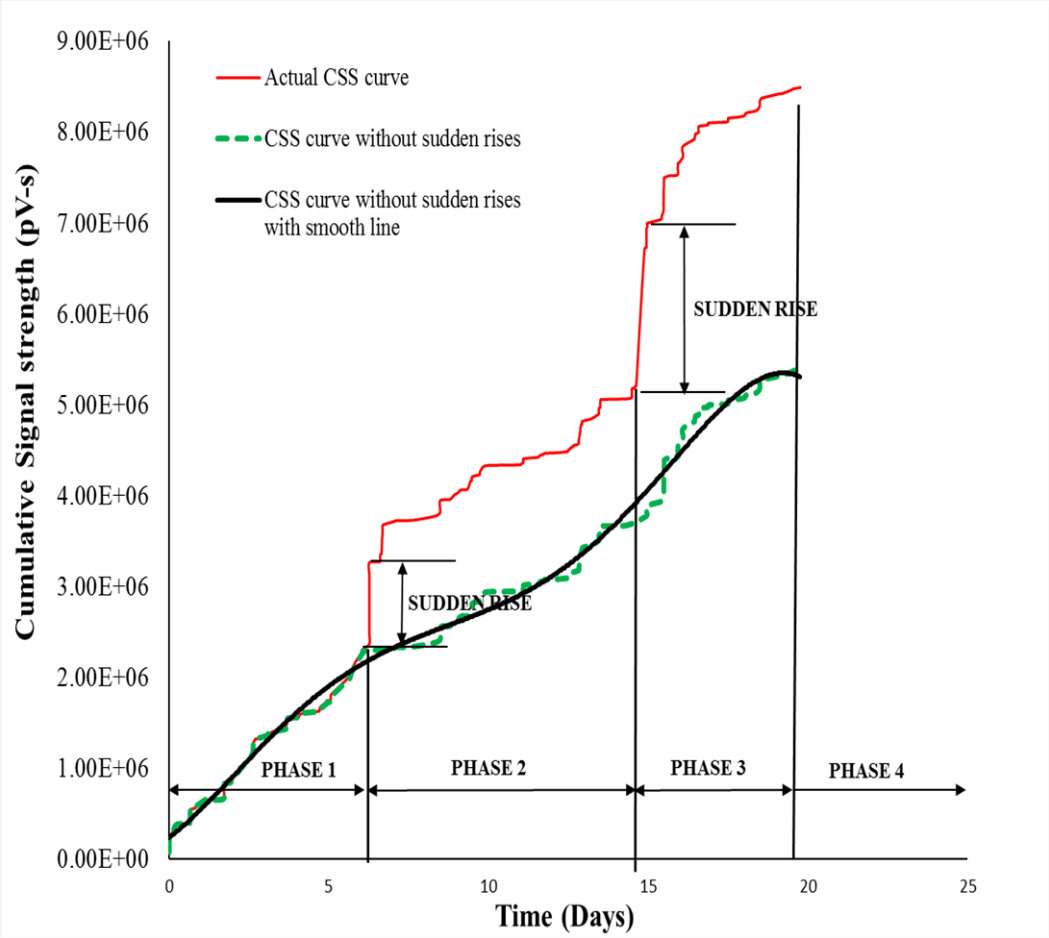

Fig. 4.7. Phases in CSS curve for actively corroding specimen

From Fig. 4.4 it was observed that for all replicates of OT-12 specimens, initial potentials indicated very low probability of corrosion (half-cell potential w.r.t. SCE > -126 mV i.e. passive condition). However, the potentials quickly dropped indicating high probability of active corrosion condition (half-cell potential w.r.t. SCE < -276 mV), roughly at the same time. The general trend of drop in potential readings indicates increasing probability of active corrosion. Later on, the potentials started increasing indicating increase in concrete resistance and finally stabilized in high probability active corrosion condition. The increase in concrete resistance could be due to migration of chloride ions, through concrete under the influence of an electrical field of impressed current. These migrating ions get accumulated in pore solutions and change the electrical resistance of concrete, which may first decrease and then

increase with time. Similar observations were made by Care and Raharinaivo (2007). The corrosion products oozing out from concrete also get accumulated in concrete pores changing the concrete resistance. Fig. 4.8 shows the variation of current imposed from anode to cathode for three replicates of OT-12 specimens with time which also confirmed this phenomenon.

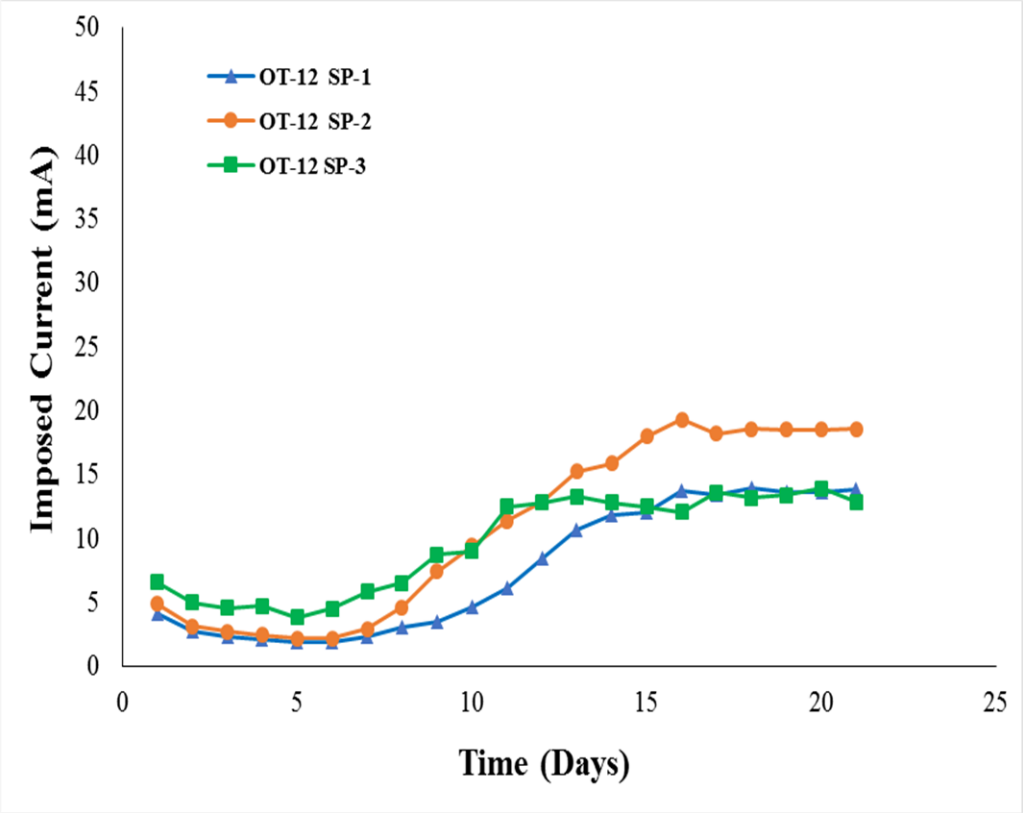

Fig. 4.8. Variation of imposed current with time for three replicates of OT-12 specimens

Similar pattern of variation of half-cell potential with time for three replicates of OT-16, OT-20, OC-20 and PT-20 specimens are shown in Fig. 4.9 to 4.12 whereas variation of imposed current with time for these specimens are shown in Fig. 4.13 to 4.16 respectively.

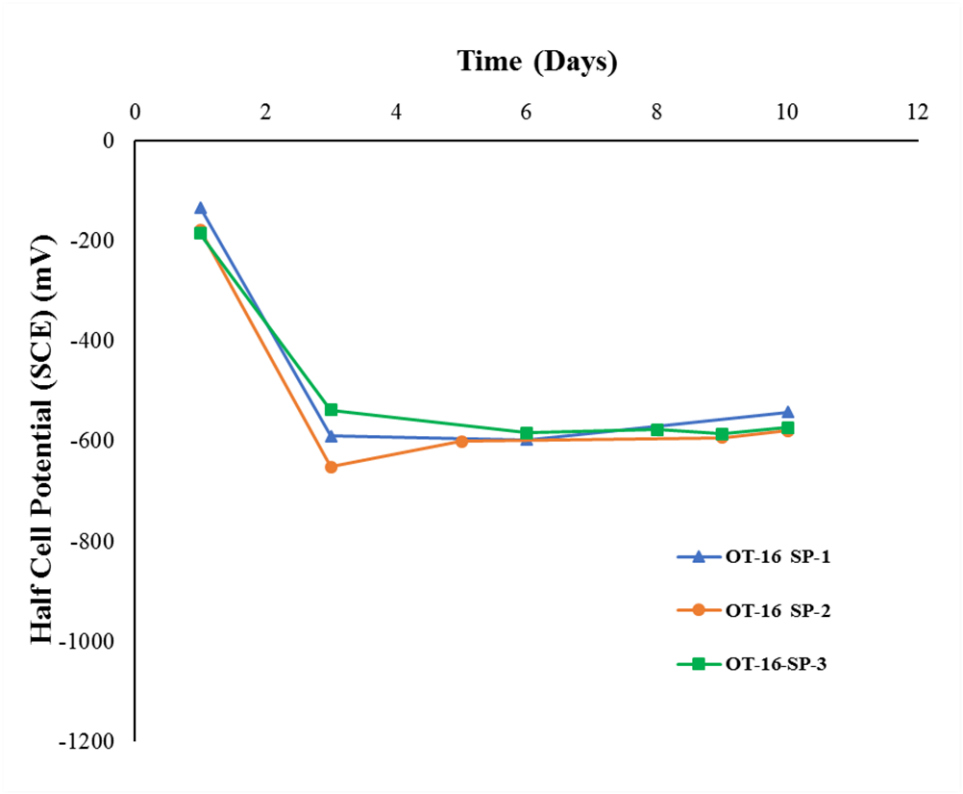

Fig. 4.9. Variation of half-cell potential with time for three replicates of OT-16 specimens

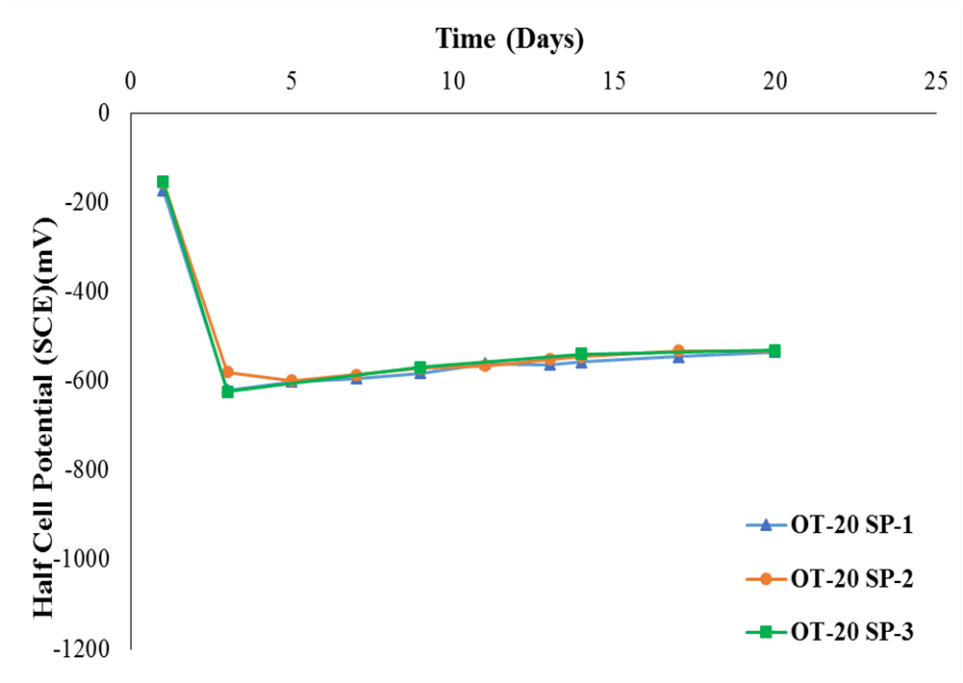

Fig. 4.10. Variation of half-cell potential with time for three replicates of OT-20 specimens

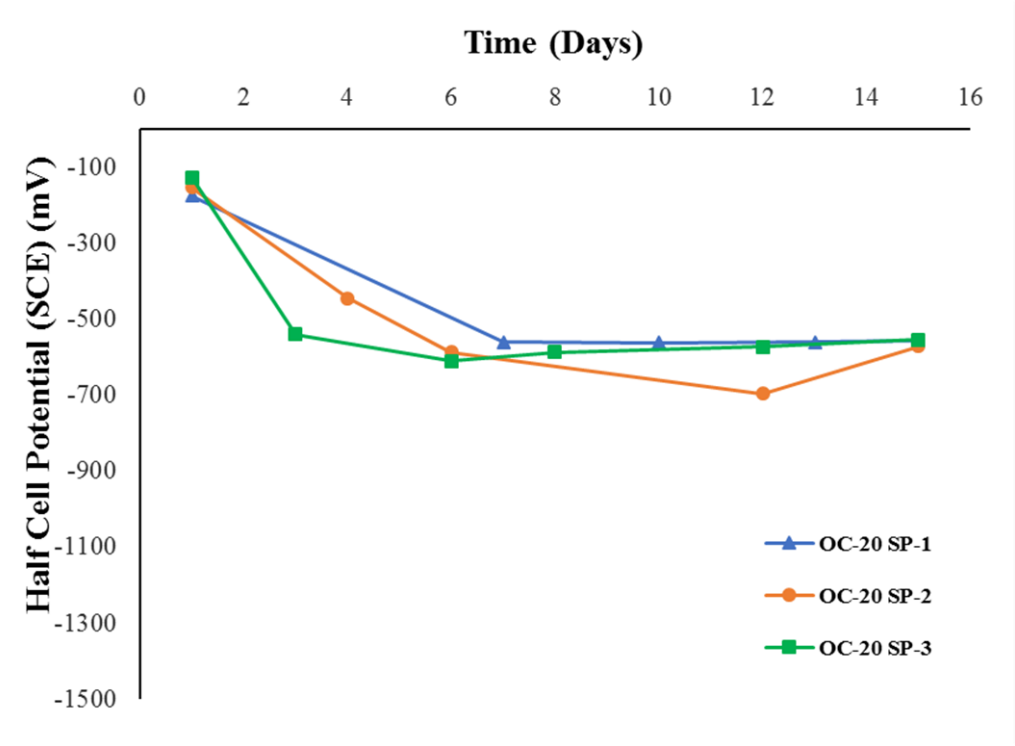

Fig. 4.11. Variation of half-cell potential with time for three replicates of OC-20 specimens

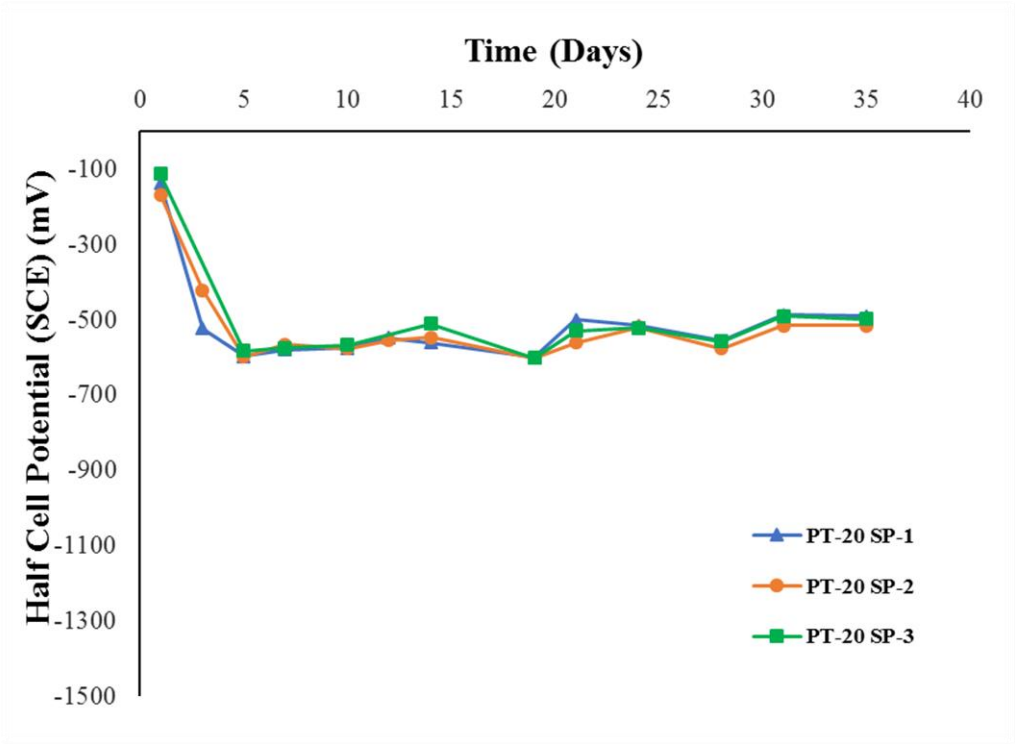

Fig. 4.12. Variation of half-cell potential with time for three replicates of PT-20 specimens

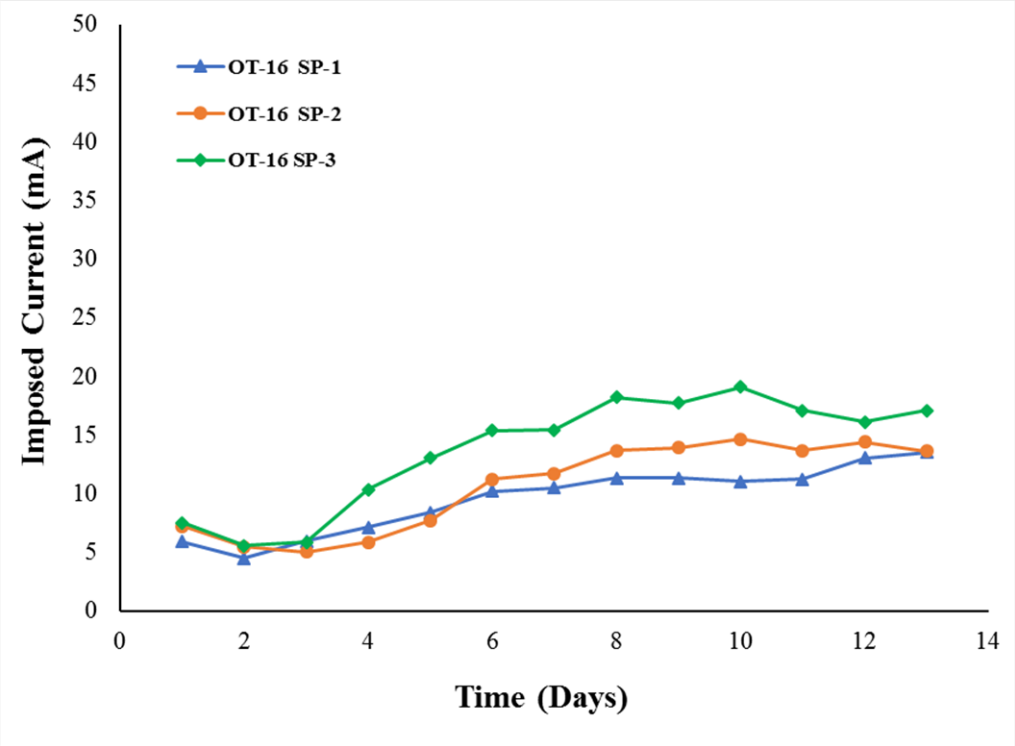

Fig. 4.13. Variation of imposed current with time for three replicates of OT-16 specimens

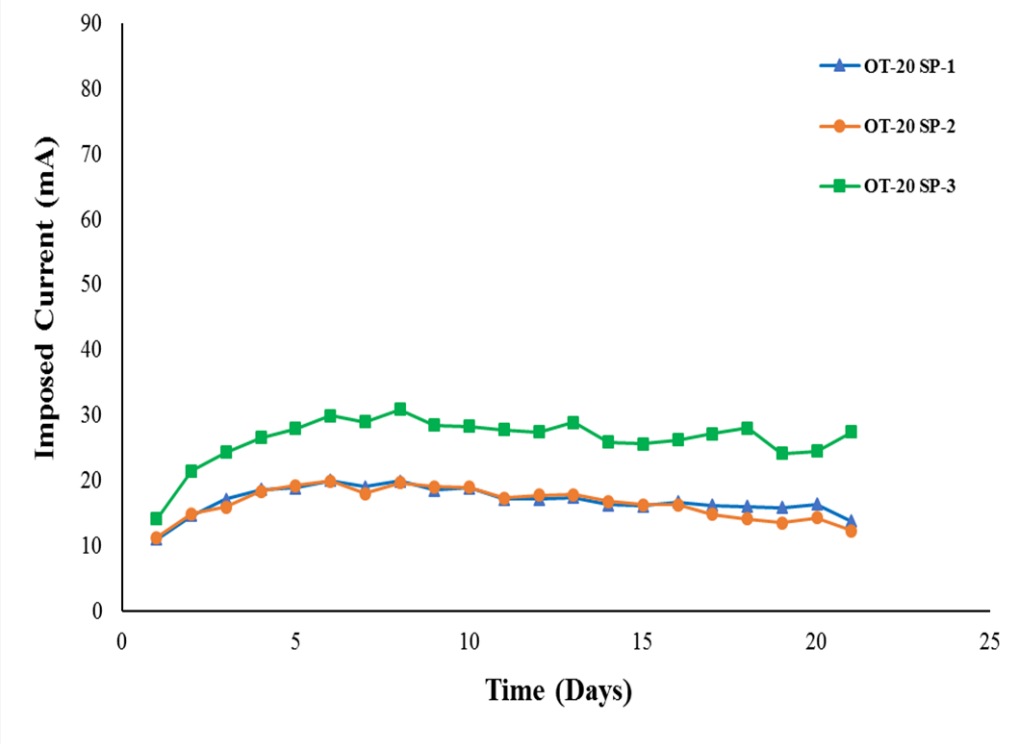

Fig. 4.14. Variation of imposed current with time for three replicates of OT-20 specimens

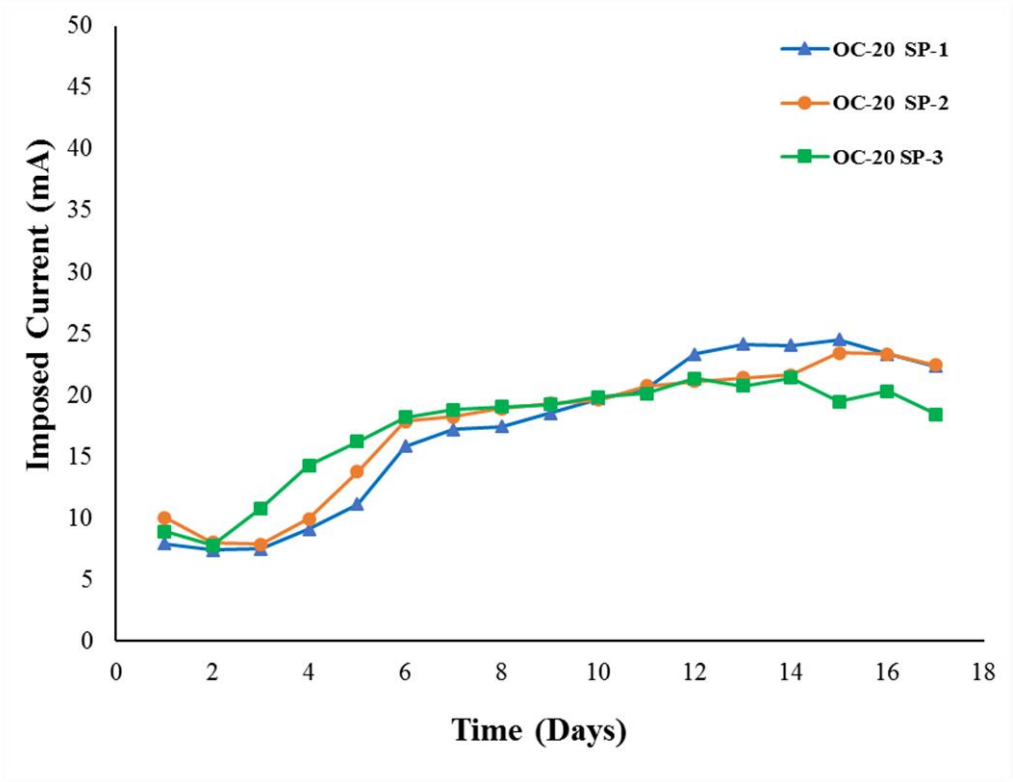

Fig. 4.15. Variation of imposed current with time for three replicates of OC-20 specimens

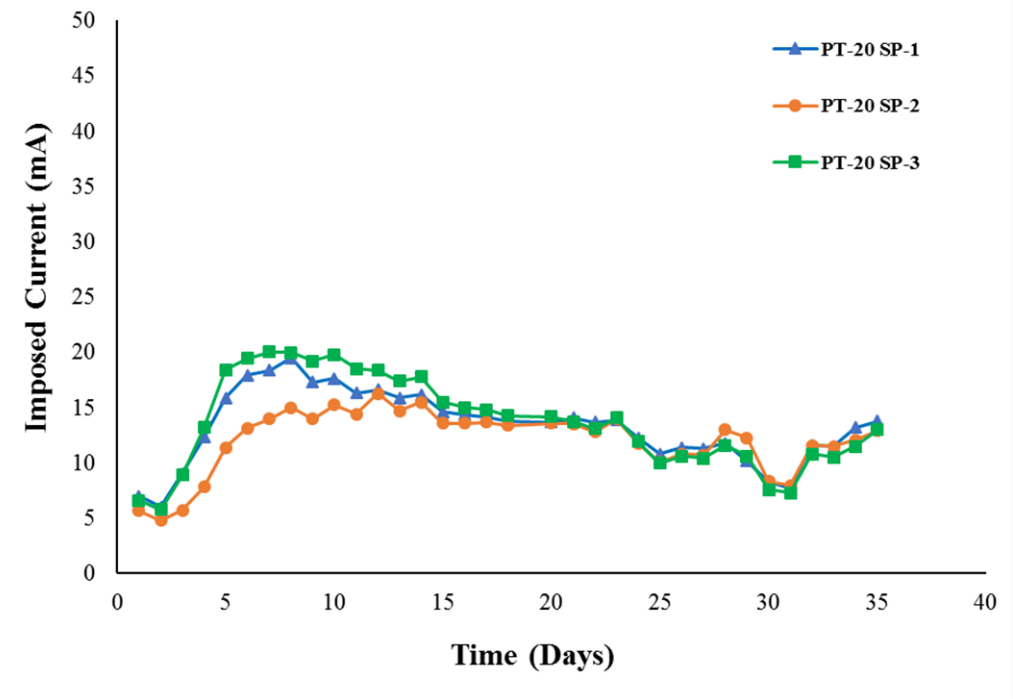

Fig. 4.16. Variation of imposed current with time for three replicates of PT-20 specimens

From Fig. 4.5 it was observed that initially for about 6 days, the i_{corr} values for all replicates of OT-12 specimens decreased and then started increasing. This could be either due to accumulation of ions in concrete pore solution under the influence of an electrical field or accumulation of corrosion products in concrete pores resulting into reduction of corrosion rate. Similar observations were made by Care and Raharinaivo (2007). The oozing out of corrosion products were observed on around 7th day of current exposure for all specimens which confirmed this phenomenon. The variation of i_{corr} values with time for three replicates of OT-16, OT-20, OC-20 and PT-20 specimens are shown in Fig. 4.17 to 4.20. Variation of i_{corr} values with time for these specimens slightly differed from that of OT-12 specimens as shown in Fig.4.5. The difference in variation was observed during initial period of corrosion in which the rapid increase in i_{corr} values were observed. This was may be because of the rapid drop in half-cell potential values for these specimens (can be seen from Fig. 4.9 to 4.12) which indicated rapid increase in corrosion activity. As a result, the i_{corr} values for these specimens also increased rapidly without showing decrease in its value during initial period.

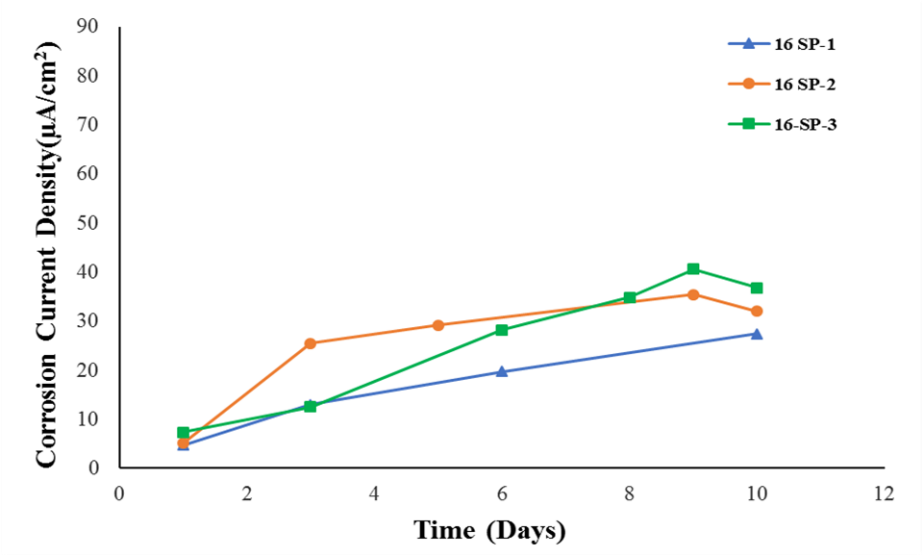

Fig. 4.17. Variation of Corrosion current density with time for three replicates of OT-16 specimens

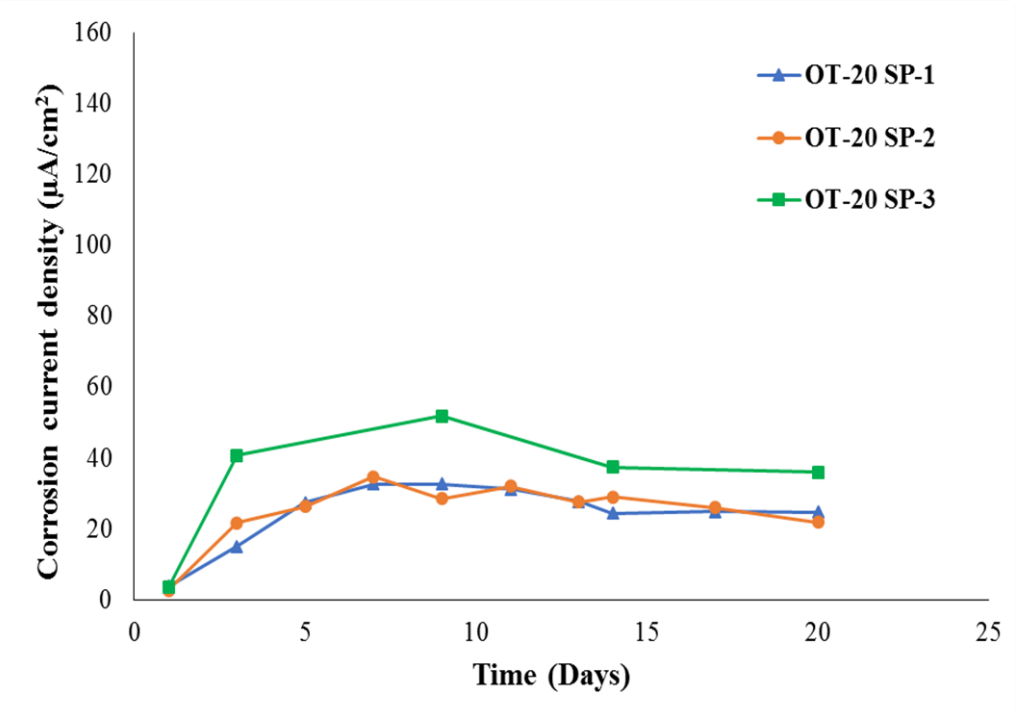

Fig. 4.18. Variation of Corrosion current density with time for three replicates of OT-20 specimens

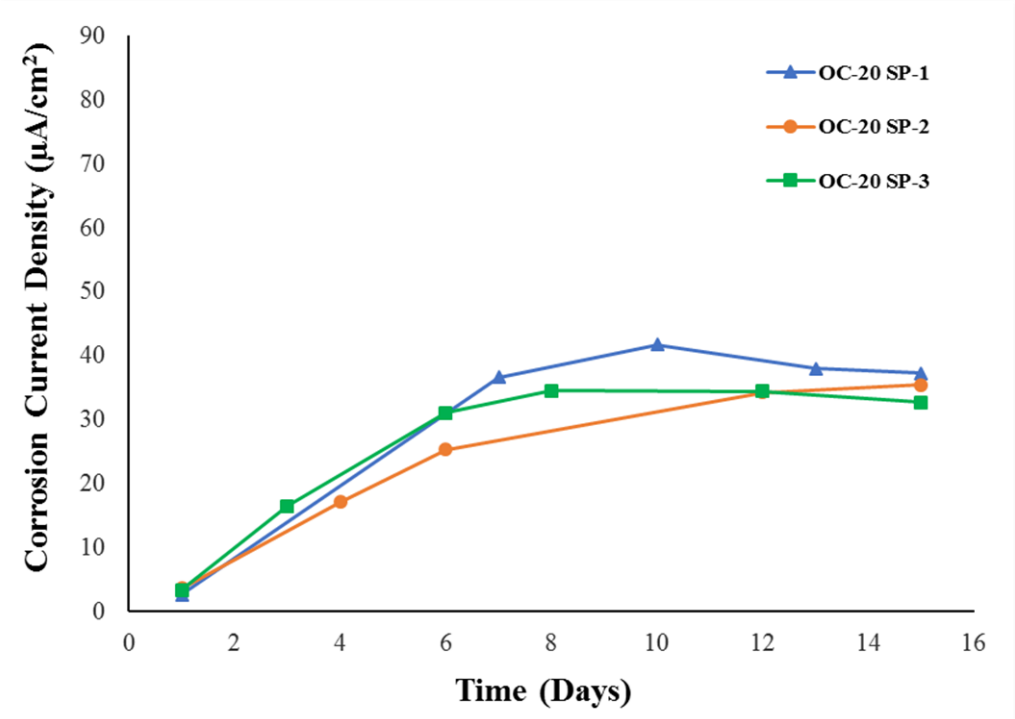

Fig. 4.19. Variation of Corrosion current density with time for three replicates of OC-20 specimens

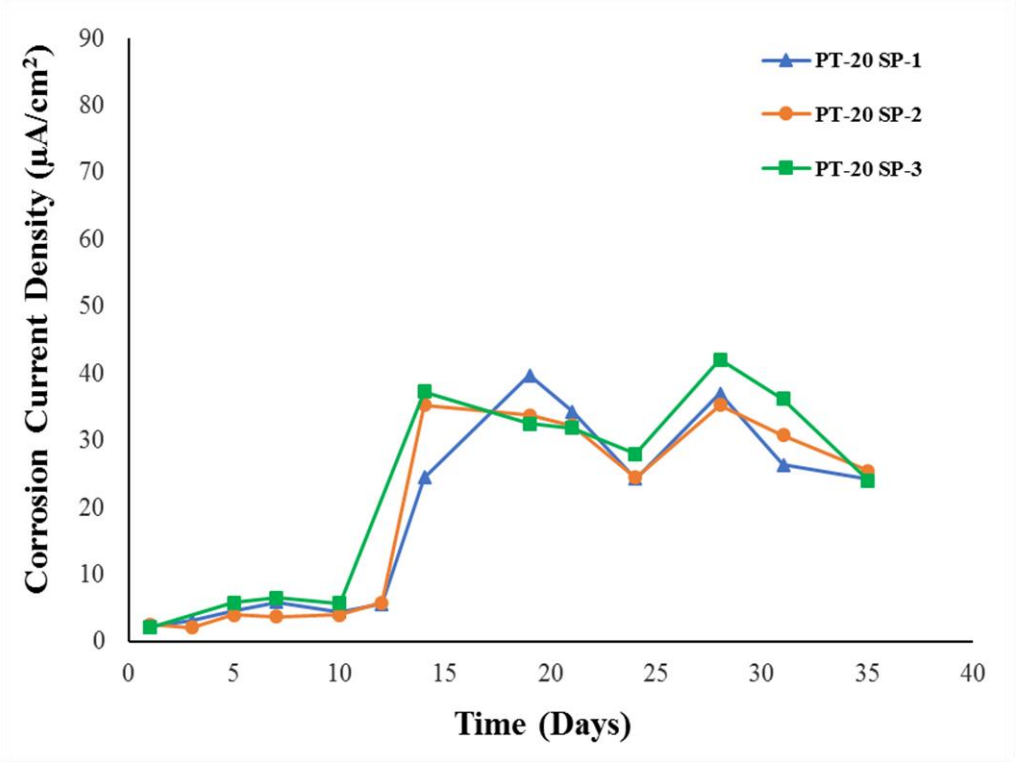

Fig. 4.20. Variation of Corrosion current density with time for three replicates of PT-20 specimens

In order to compare the results of AE technique and electrochemical techniques for study of corrosion process in reinforced concrete element, a graph of half-cell potential and CSS vs time as well as a graph of i_{corr} and CSS vs time are plotted for all specimens. Fig. 4.21 and 4.22 show these graphs for specimen OT-12 SP-1 respectively.

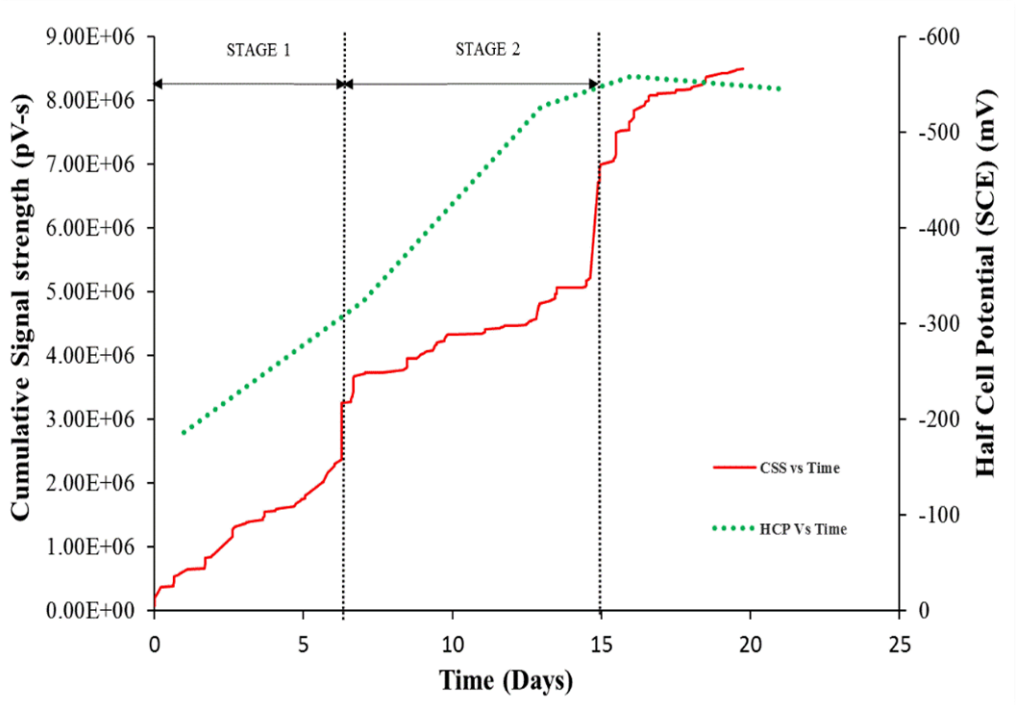

Fig. 4.21. Simultaneous evolution of half-cell potential and CSS for actively corroding OT-12 SP-1 specimen

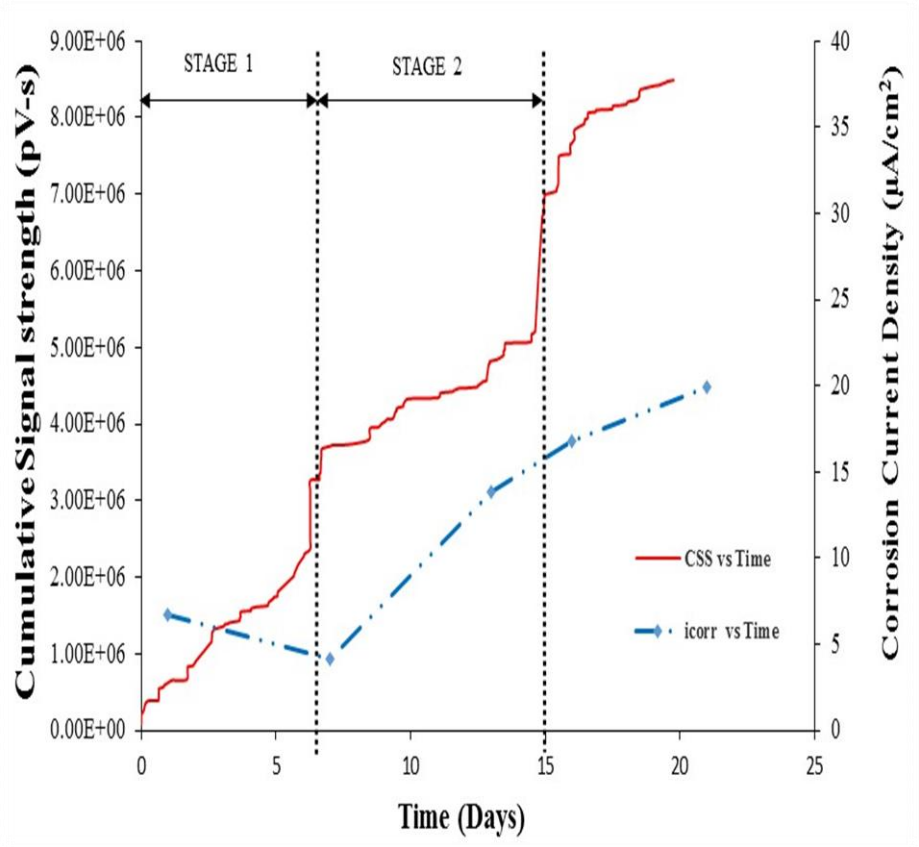

Fig. 4.22. Simultaneous evolution of i_{corr} and CSS for actively corroding OT-12 SP-1 specimen

The shape of these curves can be divided into two major stages and repetition of second stage thereafter:

(a) **'Stage 1'** is characterized by low current density, low but slowly dropping half-cell potential values and gradually increasing CSS values. In this stage modification of concrete medium takes place due to diffusion and accumulation of chloride ions in the concrete pores and results in increase in resistance of concrete. Similar observations were made by Care and Raharinaivo (2007). As a consequence during this stage i_{corr} values decrease from 6.75 $\mu A/cm^2$ to 4.17 $\mu A/cm^2$ whereas half-cell potential values gradually drop from a range of no corrosion to active corrosion (SCE less than -0.276 V) indicating greater than 90 % probability of active corrosion. This indicates onset of corrosion. The CSS values increase slowly in this stage indicating depassivation of layer surrounding steel and onset of corrosion. Near the end of 'Stage 1', CSS values increase suddenly at around 7^{th} day of testing which may indicate initiation of micro-cracks as a result of corrosion activity. Oozing of corrosion products was observed on the same day which confirms the initiation of micro-cracks on the surface of specimen.

(b) **'Stage 2'** consists of gradual increase in current density, further drop in half-cell potential values and rise in CSS values. This indicates active corrosion. This stage is also accompanied by the friction of corrosion products against the walls of concrete pores and micro-cracks developed in 'Stage 1'. The rise in CSS value with time indicates corrosion accompanied by this activity. The sudden rise in CSS value around 14^{th} day of testing seems to be due to propagation of micro-cracks leading to development of visual crack on the surface of concrete specimen. This entire stage is representative of several

events such as active corrosion, friction of corrosion products against the inner side of the pores, penetration of electrolytic solution in the reinforced concrete and subsequent cracking of concrete. The concrete being cracked, the penetration of the electrolyte in the concrete pores results in increasing current density and drop in half-cell potential values. High amount of oozing of corrosion products from different cracks around the periphery of concrete and appearance of a distinct crack confirms this stage (Fig. 4.23).

(c) Further stages are repetition of the 'Stage 2' mentioned above as further corrosion and further deterioration of concrete continues in the same manner.

From the above discussion it can be noted that the corrosion process of steel reinforcement embedded in concrete can be well monitored using electrochemical techniques but, these techniques do not provide any information about deterioration of concrete as a consequence of corrosion. AE technique can be used effectively to monitor corrosion process of steel reinforcement embedded in concrete and can also give information about deterioration of concrete due to corrosion.

Similar representative graphs of half-cell potential and CSS vs time as well as i_{corr} and CSS vs time for all remaining specimens are included in Annexure A.

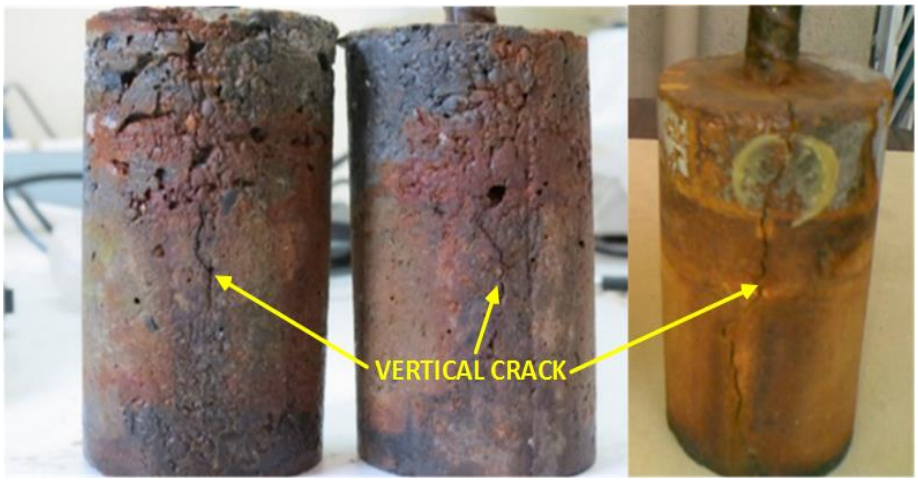

Fig. 4.23. Specimens after testing OT-12 SP-1, OT-12 SP-2 and OT-12 SP-3 respecively

4.8. CLOSING REMARKS

It can be concluded that CSS parameter of AE technique is a promising parameter for corrosion monitoring studies as it has a specific trend indicating active corrosion which is similar to the curve of typical phenomenological corrosion loss of steel due to seawater immersion. From the comparative study of AE technique and electrochemical techniques for corrosion monitoring, it can be concluded that chloride induced corrosion of steel embedded in concrete may be classified in two different stages. 'Stage 1' consists of depassivation of concrete surrounding the rebar and indicates onset of active corrosion leading to initiation of micro-cracks in concrete specimen. 'Stage 2' is indicative of further increase in corrosion activity and accumulation of corrosion products in concrete pores resulting in development of major cracks in concrete. Both these stages are well identified by electrochemical techniques as far as corrosion process of steel embedded in concrete is concerned, whereas AE technique can identify the corrosion process of steel reinforcement as well as damage to concrete due to subsequent cracking.

In the next chapter, effect of material variables on corrosion process (in terms of electrochemical and AE measurements) are investigated. Further, the mathematical model for corrosion assessment using AE technique is developed considering different variables.

CHAPTER 5

EFFECT OF MATERIAL VARIABLES ON AE MEASUREMENTS AND DEVELOPMENT OF MATHEMATICAL MODEL

5.1. INTRODUCTION

The corrosion of steel embedded in concrete and subsequent cracking of concrete depend on the material properties of constituents of reinforced concrete. The electrochemical process during corrosion of reinforcing bar in concrete involves the transfer of electrically charged ions between two surface areas of a reinforcing bar with different potentials (anode and cathode) through the pore fluid of the concrete, which serves as an electrolyte. The corrosion rate of reinforcing bar in concrete depends on the ease of flow of the ions which participate in the electrochemical process. Various factors such as electrical resistivity of concrete, electrochemical potential of reinforcing bar, availability of oxygen and moisture at the cathodic area and ratio of cathodic to anodic area control the flow of electrically charged ions in concrete (*El-Gelany, 2001)*. Thus, corrosion of steel embedded in concrete largely depends on the material properties. Concrete surrounding the steel provides chemical and physical protection to the embedded steel reinforcement. The formation of thin layer of oxides surrounding the steel surface due to high alkalinity of concrete pore solution serves as chemical protective layer whereas the retarding access of oxygen, moisture and various aggressive species to the steel/concrete interface provides physical protection. Thus, initiation and progress of corrosion both depend on the chemical composition of steel as well as protection provided by the concrete cover.

When information regarding the performance of reinforced concrete structures against rebar corrosion has to be obtained within a restricted time, the application of

various non-destructive techniques becomes important. As the corrosion process depends on material properties, it is also necessary to identify the effect of material variables on results of various non-destructive techniques used for the purpose of corrosion measurement. Further, the corrosion activity monitored by non-destructive techniques is required to be compared with the destructive i.e. gravimetric (mass loss) measurements in order to verify the extent of damage due to corrosion.

AE technique detects transient acoustic waves generated due to release of energy as a consequence of development of flaws inside the material. Therefore the magnitude of energy released is a function of damage inside the material *(Ing et al. 2005)*. Thus, if the level of damage and material properties are known, the technique may have a capacity to quantitatively assess the damage to a given material. Reinforced concrete is a composite material made up of steel and concrete. The corrosion of steel embedded in concrete results into development of cracks inside the concrete. The energy released during cracking of concrete can be captured using AE technique, where the data recorded may be used to quantify the corrosion. Therefore, any relationship between metal loss and AE should be investigated by understanding the influence of structure-specific parameters. The technique, thus, can be developed further for field application based on laboratory investigations.

In this chapter, the results of an experimental investigation are presented by considering rebar diameter, cement type and steel type as material variables. The performance of material variables under accelerated corrosion condition is evaluated based on gravimetric measurements. To evaluate the effect of the said variables on non-destructive measurements, the performance of these materials, as identified by electrochemical as well as AE measurements, were compared with that of gravimetric

(mass loss) measurement. For the purpose of identifying the factors those affect the non-destructive measurements significantly; analysis of variance (ANOVA) was carried out. Further, to develop AE technique for quantitative assessment of corrosion, the relation between gravimetric mass loss and AE measurement was established by considering variation in material properties. For development of mathematical model, regression analysis was performed.

5.2. EXPERIMENTAL PROGRAMME

To examine the influence of material properties on various measurements, the testing programme varied the cement type, steel type and rebar diameter keeping two variables constant. Test matrix Set-I of the experimental programme was designed keeping this aspect in mind. Therefore, the experimental test results of Set-I are used to study the effect of material variables on the non-destructive measurements. Also, an attempt is made to establish a generic relation between mass loss and AE measurement. For example, two cement types were investigated, whilst keeping the steel type and rebar diameter constant. Different combinations of cement type, steel type and rebar diameter were not considered as the focus of the study was to find the effect of specific variable on corrosion and hence on non-destructive measurements, while keeping other variables the same.

5.3. EFFECT OF MATERIAL VARIABLES ON NON-DESTRUCTIVE MEASUREMENTS

The various non-destructive measurements taken in the study are cumulative strength signal parameter obtained by acoustic emission, electrochemical parameters like half-cell potential and corrosion current density. The effect of material variables on both AE measurements and electrochemical measurements are investigated and are

presented in the subsequent sections. It is to be noted here that among the electrochemical parameters studied, only corrosion current density is considered because half-cell potential describes the onset of corrosion, while the propagation of corrosion and its severity level is understood by corrosion current values.

5.3.1. Variation of mass loss, corrosion current density and cumulative signal strength

From literature it was found that the mode of failure of concrete cover resulting from the accumulation of corrosion products is a function of cover to rebar diameter (C/D) ratio *(Ing et al. 2005)*. This factor is considered the most influential in cracking initiation, where it has been shown that a linear trend exists between the C/D ratios versus attack penetration *(Alonso et al. 1998)*. To study the effect of rebar diameter on corrosion and non-destructive measurements, the rebar diameter was varied which resulted in variation of concrete cover also as diameter of concrete cylindrical specimen was kept constant. This variation in concrete cover was very small ranging from 24 mm, 22 mm and 20 mm for rebar diameters 12 mm, 16 mm and 20 mm respectively. As per *IS: 456 - 2000*, for mild exposure conditions minimum concrete cover specified is 20 mm and the deviation in concrete cover should not be more than 0 to +10 mm. As the deviation in concrete cover was very small, the effect of variation in cover was neglected in the analysis.

The literature also suggest that in blended cements, the formation of additional C–S–H gel results in the formation of finer pore structure and thereby a denser microstructure in the hardened concrete. This increases the resistivity of concrete resulting in reduction of corrosion rate. Through experimental work, the researchers concluded that the blended cements, like PPC and Portland slag cement (PSC),

performed better as compared to OPC against chloride induced rebar corrosion in concrete *(Pradhan and Bhattacharjee, 2009)*. In the present investigation, to study the effect of cement type on corrosion and non-destructive measurements, the cement type was varied by keeping steel type and rebar diameter constant.

The corrosion performance of steel embedded in concrete exposed to chlorides is a function of both concrete and steel characteristics. Corrosion propagation rates are influenced by surface characteristics, steel composition, and steel microstructure *(Trejo and Monteiro, 2005)*. The corrosion resistance of reinforced concrete structures is many times enhanced by using coating on rebars. Such coatings have ranged from cement slurries to epoxies and zinc *(Chowdhury P.C., 2004)*. However, these coatings suffer from the major disadvantage that they may get physically damaged or can be electrochemically penetrated resulting in the base steel vulnerable to pitting corrosion. Debonding of rebar and concrete is another major problem in case of coated rebars. All these issues resulted into use of low-alloy steels or corrosion resistant steel (CRS) containing elements like phosphorus, copper, chromium and nickel which improve the corrosion resistance *(Chowdhury P.C., 2004)*. In the present study, to study the effect of steel type on corrosion and non-destructive measurements, the steel type was varied by keeping cement type and rebar diameter constant.

As discussed in section 4.6.2 and 4.6.3, the corrosion was monitored using AE technique and electrochemical technique. After completion of tests, mass loss for all specimens was determined by gravimetric method as explained in section 4.6.4 of chapter 4. Table 5.1 shows average values of gravimetrical mass loss, corrosion current densities (i_{corr}) and maximum CSS values for specimen with different variables. It is to mention here that the objective of the present work was to quantify

rebar corrosion by AE technique, therefore the results of technique were compared with only corrosion current density values and not with half-cell potential values which is a qualitative measure.

Table 5.1. Average Gravimetric mass loss, Corrosion Current Density and Cumulative Signal Strength

Variables	Materials			Nomen-clature	Average mass loss (g)	Average i_{corr} ($\mu A/cm^2$)	Average max CSS (pV-sec)
	Cement	Steel	Rebar diameter				
Cement type	OPC	TMT	20	OT-20	13.04	35.68	5.53×10^9
	PPC	TMT	20	PT-20	6.99	24.55	5.29×10^7
Steel type	OPC	TMT	20	OT-20	13.04	38.26	5.53×10^9
	OPC	CRS	20	OC-20	5.24	34.73	1.98×10^7
Rebar diameter	OPC	TMT	12	OT-12	3.94	28.37	3.92×10^7
	OPC	TMT	16	OT-16	4.43	31.09	3.18×10^9
	OPC	TMT	20	OT-20	13.04	35.68	5.53×10^9

From Table 5.1, it was observed that the average mass loss values for specimens cast with OPC (OT-20) was higher than that of specimens cast with PPC (PT-20). Similar results were obtained in variation of average i_{corr} values and average max CSS values. This indicated that the specimen cast with PPC performed better as compared to that of OPC against chloride induced corrosion of rebar in concrete. Similar results were obtained by *Pradhan and Bhattacharjee (2007)*. Through experimental investigation, *Pradhan and Bhattacharjee (2007)* reported the corrosion performance of different types of steel and cement in different concrete mixtures contaminated with admixed chloride. From the study, it was concluded that PSC performed best in increasing the corrosion initiation period while PPC performed best in extending the propagation period among over OPC.

While studying the performance of steel type, it was observed that the average mass loss values for specimens cast with TMT steel (OT-20) were higher than that of

CRS steel (OC-20). Similar results were obtained in variation of average i_{corr} values and average max CSS values. Thus, the variation in mass loss, i_{corr} and max CSS values indicated better performance of CRS steel as compared to that of TMT steel against chloride induced rebar corrosion in concrete.

Similarly, while studying the performance of rebar diameters, it was observed that the average mass loss for specimens cast with 20 mm rebar diameter (OT-20) showed highest mass loss followed by specimens cast with 16 mm rebar diameter (OT-16) and then specimens cast with 12 mm rebar diameter (OT-12). Similar results were observed in the variation of average i_{corr} values and average max CSS values. This indicated that 12 mm rebar diameter performed better amongst all followed by 16 mm rebar diameter and finally 20 mm rebar diameter against chloride induced rebar corrosion in concrete. Similar results were obtained by *Ing et al. (2005).* In the research work, *Ing et al. (2005)* identified the influential cover zone factors that affect the magnitude of the AE measurements per gram of steel loss. Prisms with various concrete strength, cover thickness, aggregate and rebar diameters were studied to ascertain the important variables likely to be encountered on reinforced structures. The results indicated that by increasing the rebar diameter and keeping strength and cover depth constant, there was an increase in the absolute energy per gram of steel loss.

Though from Table 5.1 the variation in gravimetric mass loss, corrosion current density and cumulative signal strength is clearly understood, these values are average values of three replicates and there is a variation in values within the replicates, the inference drawn by considering only average values may become erroneous. Therefore ANOVA is needed to be perform.

5.3.2. Analysis of variance for corrosion current density and cumulative signal strength parameters

The analysis of variance (ANOVA) is a very effective technique to evaluate the effect of independent variables on dependent variable. Sometimes it may be difficult to analyse the effect of different independent variables on variation of dependent variable. In such cases, ANOVA results help to find out the significance of different independent variables on dependent variable. In the present work, ANOVA calculations were carried out for i_{corr} values and max CSS values of all the specimens of Set-I of the experimental programme. The material variables in this set, as already described, are three types of rebar diameter, two types of cement and two types of steel.

5.3.2.1. ANOVA for corrosion current density

Following step by step procedure was followed while performing ANOVA:

1. The i_{corr} values for all variables were arranged in a tabular form.
2. The total sum of squares were calculated, which was partitioned into sum of squares between factors and sum of squares (SS*) within factors.
3. The mean squares (MS) of the factors were then calculated by dividing their corresponding SS by the associated degrees of freedom.
4. The effect of individual factor was evaluated by testing the hypothesis of equality of variances, which is the significance test at a particular probability level.
5. For this, the F-statistic is calculated as the ratio of MS between factors to MS within factors.
6. This value was then compared to the tabulated F-values related to Fisher distribution. The F-values related to Fisher distribution depend upon the degrees of freedom (df) corresponding to between factors and within factor variance and

the probability level, which are available in tabular form in relevant texts *(Kothari C. R., 2004 and Spiegel et al. 2010).*

The details of ANOVA technique are discussed in Annexure B.

The results of ANOVA for i_{corr} for three variables under study are shown in Table 5.2.

Table 5.2. ANOVA results for i_{corr}

Source	Level	df	SS*	MS	F - ratio	'F' from Fisher's distribution (99% probability)	P-value
Cement type	2	1	185.81	185.81	3.32	21.19	0.14
Steel type	2	1	18.79	18.79	0.35	21.19	0.58
Rebar diameter	3	2	82.06	41.03	0.50	10.92	0.62

5.3.2.2. ANOVA for maximum cumulative signal strength

The max CSS values for all variables were arranged in a tabular form and ANOVA was performed as explained earlier in section 5.3.2.1. The results of ANOVA for max CSS values for three variables under study are shown in table 5.3.

Table 5.3. ANOVA results for max CSS

Source	Level	df	SS*	MS	F - ratio	'F' from Fisher's distribution (99% Probability)	P - value
Cement type	2	1	4.50×10^{19}	4.50×10^{19}	2.79	21.19	0.17
Steel type	2	1	4.55×10^{19}	4.55×10^{19}	2.82	21.19	0.16
Rebar diameter	3	2	4.55×10^{19}	2.27×10^{19}	1.09	10.92	0.39

5.3.3. Discussion

The test results presented in previous sections reveal that with increase in rebar diameter, the average CSS values measured using AE technique increased. As blended cements show reduced corrosion activity, for similar conditions, specimens cast with PPC cement indicated more time for initiation and propagation of cracks in concrete as compared to that of OPC cement. This resulted in lesser extent of formation of micro-cracks in concrete with PPC cement indicating lesser magnitudes of CSS. From Table 5.1, it is also clear that CRS rebars performed better as compared to TMT rebars by showing lesser magnitudes of CSS which indicated that specimens cast with CRS rebars have shown better resistance to corrosion and hence lesser extent of micro-cracking. Similar variation of gravimetrical mass loss and i_{corr} for these variables confirmed the results of variation of CSS magnitudes obtained using AE technique.

From Table 5.2 and 5.3 it was observed that the calculated F-values are lower than the corresponding tabulated F-values at 99% confidence level for all the variables with P-value greater than 0.01. This clearly indicated that there is not enough evidence to reject the null hypothesis that all the data are drawn from populations with the same mean. Thus, from the results of ANOVA it can be inferred that all the variables under study i.e. rebar diameter, cement type and steel type are statistically insignificant and the difference in magnitudes of CSS is just a matter of chance. Similar results of ANOVA obtained for magnitudes of i_{corr} confirmed the ANOVA results obtained for AE measurements. Thus, it can be again concluded that the results obtained by AE technique are satisfactorily validated with that of well-established electrochemical technique.

Based on these results, it can be concluded that, as the effect of material properties on AE measurements are not significant when statistical tool is used, the mathematical relation can be developed using the experimental data with all these variables.

5.4. MATHEMATICAL MODELING

The major objective of the present research is to establish a quantitative analysis of rebar corrosion by using AE measurements. For this, the relation between AE and mass loss is established and discussed in the subsequent sections.

5.4.1. Relation between mass loss and AE measurement

Based on the discussion given in section 5.3.3, it was found that all the material variables under study are statistically insignificant. Hence it was thought that a generic relation may be established between mass loss and CSS values. Therefore, a graph of max CSS vs. gravimetrical mass loss was plotted for all specimens considered in Set-I of the experimental programme to establish a generic relation between mass loss and AE measurement by curve fitting method as shown in Fig. 5.1. The max CSS and gravimetric mass loss values considered for the analysis are given in Table 4.10 of Chapter 4.

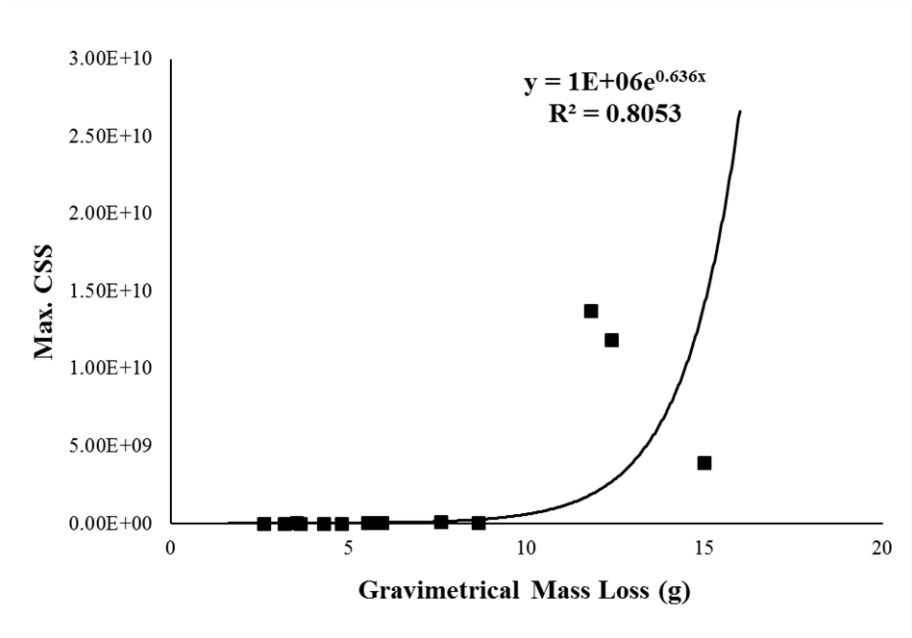

Fig. 5.1. Relation between max CSS value and gravimetric mass loss

From the Fig. 5.1 it was observed that a non-linear relation exists between max CSS value and gravimetric mass loss with coefficient of determination R^2 of 0.8053 (greater than 0.7). The relation obtained was,

$$y = 10^6 e^{0.636x} \tag{5.1}$$

It was observed that Eq. (5.1) is analogous to the natural exponential growth model which is given as,

$$y(t) = Ae^{bt} \tag{5.2}$$

Where, A is the initial value and b is the growth rate with b>0.

To validate the coefficients of equation and to check the goodness of fit, regression analysis was performed. To fit the non-linear functions, the SOLVER function of Microsoft Excel was used. The SOLVER function of Microsoft Excel is ideally suited for fitting data with non-linear functions through an iterative process. The details of SOLVER are described in subsequent section.

5.4.2. Refinement of the developed model by SOLVER

SOLVER uses a method suitable to fit a non-linear function to the data called as iterative nonlinear least squares fitting which minimizes the value of the squared sum of the difference between data and fit via an iterative or cyclical process. For this, it is required to make an initial estimate of the parameter values. The initial parameter estimates should be based on prior experience of the data or a sensible guess based on knowledge of the function used to fit the data. The first iteration involves computing the sum of squares based on the initial parameter values. The second iteration involves changing the parameter values by a small amount and recalculating the sum of squares. This process is repeated many times to ensure that changes in the parameter values result in the smallest possible value of sum of squares. The iteration protocol used in SOLVER is based on the robust and reliable generalized reduced gradient method. Thus, while using SOLVER function, the initial parameter values of constants 'A' and 'b' (Eq. (5.2)) entered were 10^6 and 0.636 respectively, as these were obtained through curve fitting. After operating SOLVER function, the programme processed iterative cycles through the fitting routine, changing the parameter values of 'A' and 'b' until the largest value of R^2 was calculated. Thus, the optimal values of 'A' and 'b' obtained are 1.05 x 10^6 and 0.711 respectively for R^2 = 1. Thus, the refined mathematical model developed using SOLVER for quantification of corrosion is given as,

$$y = 1.05 * 10^6 e^{0.711x} \quad (5.3)$$

5.4.3. Final mathematical model

Eq. (5.3) presents the developed mathematical model. By taking natural log on both sides and rearranging the terms we get,

$$X = \frac{\ln y - 13.86}{0.711} \quad (5.4)$$

Putting X = Gravimetric mass loss and Y = CSS and simplifying we get,

$$\text{Gravimetric mass loss} = (1.407 * \ln\text{CSS}) - 19.49 \quad (5.5)$$

Thus, if max CSS values are obtained using AE technique for the elements under active corrosion condition, the mass loss of steel embedded inside the concrete can be predicted using Eq. (5.5). According to *ASTM: G1-03 - 2003* the corrosion rate is calculated as,

$$\text{Corrosion Rate (mm/year)} = \frac{\text{K X W}}{\text{A X T X D}} \quad (5.6)$$

Where, K = a constant equal to 8.76 x 10^4,

W = mass loss in grams,

A = exposed surface area of steel bar in cm^2,

T = time of exposure in hours,

D = density of steel, i.e. 7.85 g/cm^3.

Thus, once the mass loss is obtained, using Eq. (5.6) corrosion rate can be calculated.

The comparative plots of average corrosion rates calculated using gravimetrical mass loss (actual mass loss of steel), theoretical mass loss obtained using Faraday's law and mass loss calculated from developed mathematical model using AE technique for all specimens under accelerated corrosion using impressed current technique is shown in Fig. 5.2. From Fig. 5.2 it is clear that the corrosion rates calculated using all three techniques are fairly in agreement with each other.

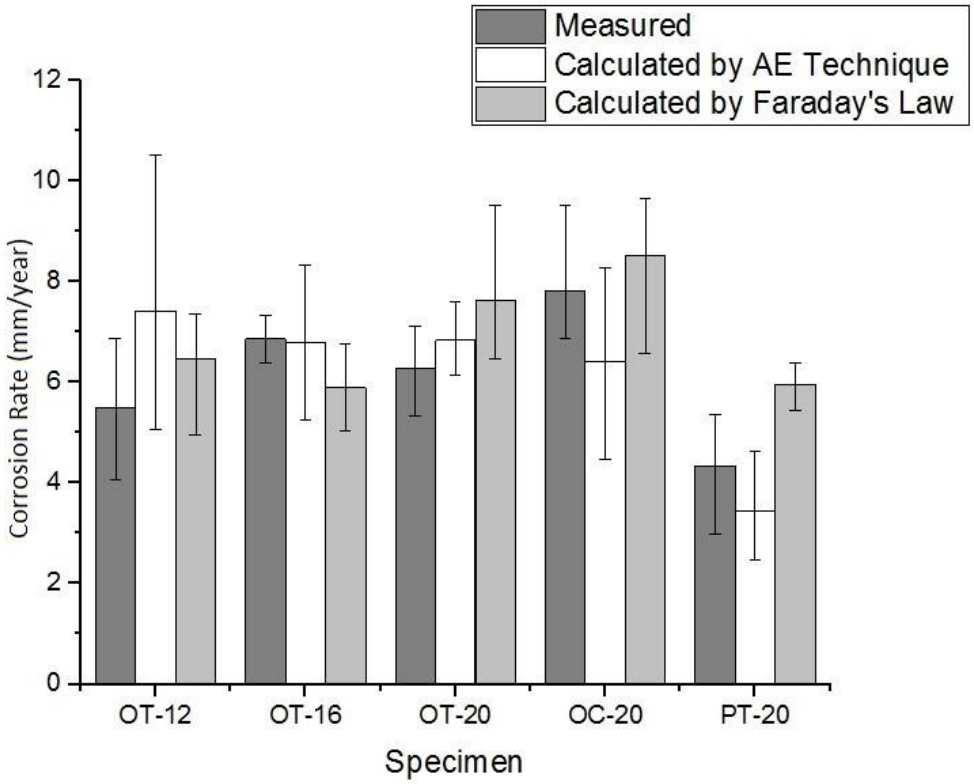

Fig. 5.2. Comparative plot of Corrosion rate from gravimetrical method, Faraday's law and AE technique for accelerated corrosion exposure

5.5. CLOSING REMARKS

From the discussion presented in this chapter, It can be concluded that the observed variation in magnitudes of max CSS for different material properties is just due to chance, as results of ANOVA indicates that the variables under study i.e. rebar diameter, cement type and steel type are statistically insignificant. These results obtained by AE technique are satisfactorily validated with that of well-established electrochemical technique. Thus, it is possible to carry out field investigation to assess extent of damage due to corrosion using CSS parameter of AE, irrespective of the material characteristics of the specimen.

From the results of SOLVER it is concluded that a significant non-linear relation exists between max CSS value and gravimetrical mass loss which is

analogous to natural exponential growth function. The fair agreement between corrosion rates calculated using developed mathematical model, gravimetric method and Faraday's law indicates that the developed mathematical model can predict the mass loss and corrosion rate conservatively under accelerated corrosion using the impressed current technique. Thus, AE technique is a powerful non-destructive technique for corrosion assessment and can be successfully used for quantification corrosion of steel embedded in concrete without having physical contact with the steel.

To check the applicability of the developed mathematical model for natural corrosion exposure conditions, the faithful simulation of corrosion by subjecting the specimens for relatively long duration was required. The next chapter explores validation of developed mathematical model as well as the impressed current technique for realistic prolonged corrosion exposure condition.

CHAPTER 6

VALIDATION OF IMPRESSED CURRENT TECHNIQUE AND MATHEMATICAL MODEL

6.1. INTRODUCTION

In the Set-I of the experimental programme of the present research work, the corrosion process was accelerated by using impressed current technique. The objective of Set-I was to develop a mathematical model that relates AE parameter with the corrosion related distress. For the proposed model to be valid for the natural exposure conditions, two things are to be validated. Firstly, the technique that is used to generate experimental results for the corrosion process (i.e. impressed current technique) is to be authenticated. Secondly, the proposed mathematical model is to be endorsed for prolonged exposure conditions.

Previous studies *(Yoon et al. 2000; Idrissi and Limam, 2003; Caré and Raharinaivo, 2007 and Gadve et al. 2009)* confirmed that impressed current technique is a valid method to study the corrosion process of steel in concrete and showed similarities to natural corrosion pattern when electrolyte contains chlorides. On the other hand, *Poursaee and Hansson (2009)* stated that because of the perceived need to produce the experimental data very rapidly, the results may not be representative of the actual behaviour of the rebar. It has also been reported that varying the current density level to get different degrees of corrosion may have other effects, which may mislead the interpretation of test results *(Maaddawy and Soudki, 2003)*. Hence, it is necessary to validate the results obtained using impressed current technique, having a particular rate of exposure by predefining the applied voltage.

As the mathematical model for prediction of mass loss of steel embedded in concrete using AE technique was also developed under accelerated corrosion using impressed current technique, its validation is also necessary.

The present Chapter describes the procedure adopted for validation of impressed current technique as well as developed mathematical model using AE technique in subsequent sections.

6.2. EXPERIMENTAL PROGRAMME

As explained in section 4.2 of Chapter 4, the experimental programme was divided into two sets: "Set–I" includes monitoring of accelerated corrosion using impressed current technique whilst "Set–II" includes monitoring of induced corrosion using,

(a) Alternate drying-wetting process and

(b) Internal chloride exposure.

The details of Set–I of the experimental programme have already been explained in Chapter 4, whereas details of Set–II are explained in subsequent sections. Set–II of the experimental programme was divided into two parts as Set–II (a) and Set- II (b). The results of Set–II (a) were used to validate the effectiveness of impressed current technique and results of Set-II (b) were used to validate the developed mathematical model. The flow chart of the test layout for Set-II is presented in Fig. 6.1.

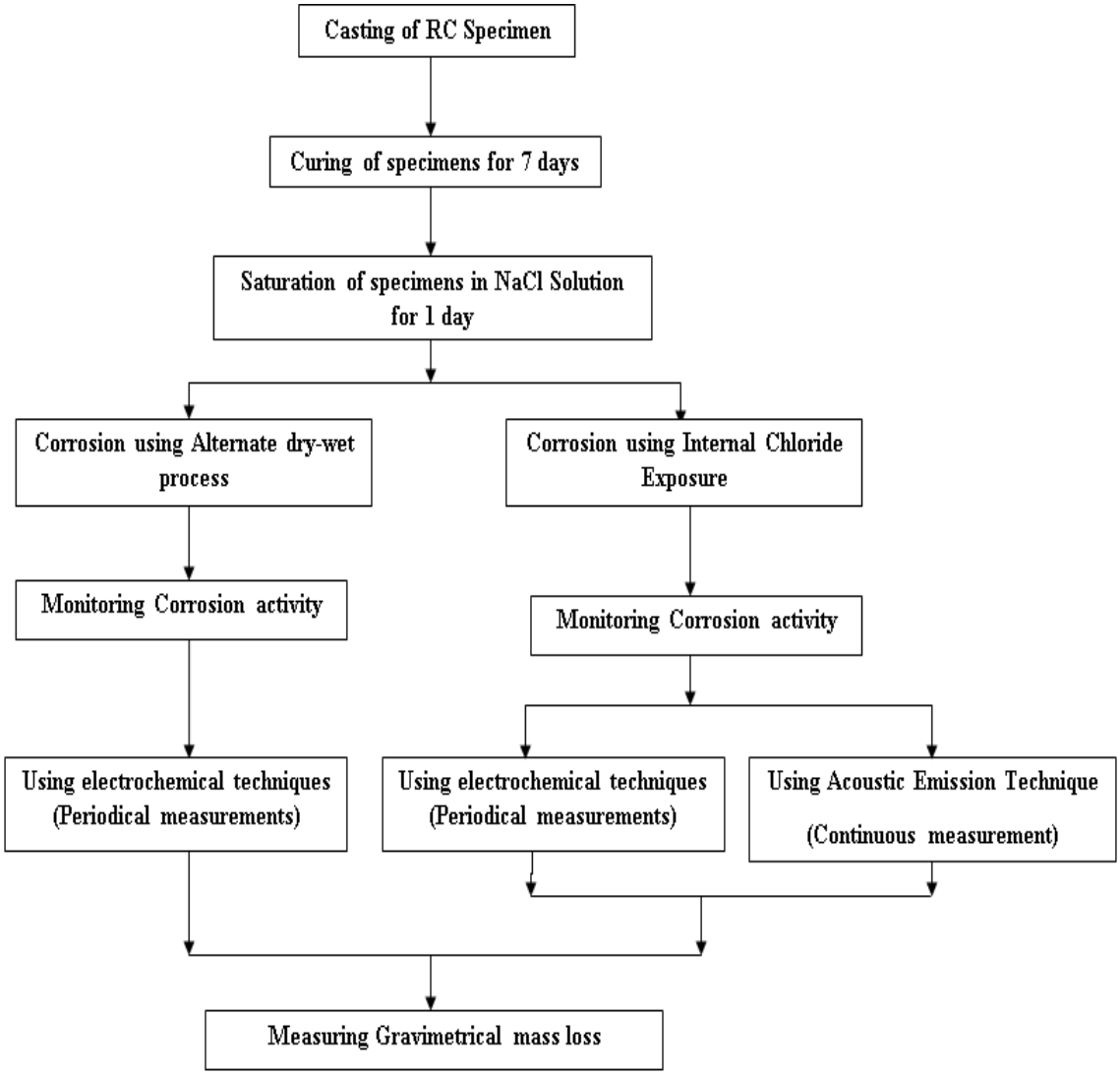

Fig. 6.1. Test Layout for Set – II of the experimental programme

As the test duration used for Set–II experimental programme was longer, lesser number of samples were cast. Therefore, the test variables were reduced. OPC being the most common cement type and TMT being the most common steel type, these variants of cement and steel were chosen along with three rebar diameters viz. 12 mm, 16 mm and 20 mm for Set–II of the experimental programme. The properties of these materials were the same as the ones explained in section 4.3. The concrete mix proportion used for preparation of reinforced concrete specimen for Set-II was also similar to Set–I as described in section 4.4.

The procedure for preparation of reinforced concrete specimens was also kept unaltered. Keeping all these aspects similar to Set-I ensured that the variability in test results will only be due to the change in the corrosion exposure procedure adopted.

6.3. TEST PROCEDURE

After casting of the specimens, the test procedure was divided into four phases and is in the following sections:

- Casting of specimens and inducing corrosion in steel rebar.
- Monitoring corrosion using AE technique continuously.
- Monitoring corrosion using electrochemical techniques periodically.
- Determination of mass loss of reinforcing bar at conclusion of test programme.

6.3.1. Casting of specimens and inducing corrosion in steel rebar

Set–II of the experimental programme was planned so as to have more realistic exposure for corrosion. The corrosion by these methods resembles the natural corrosion process and, to some extent, is representative of real world conditions. The details of the exposure conditions for two different processes involved in this set are as follows:

(a) Alternate drying and wetting process: The casting procedure of the specimens (60 mm diameter and 100 mm high cylindrical specimens with concentric steel rebar) was exactly similar to the one adopted for Set-I and is explained in detail in Section 4.5 of Chapter 4. After casting, the specimens were cured at for a period of seven days at the temperature of 27 ±2 ºC and relative humidity of 100%. Thereafter, the specimens were subjected to alternate dry/wet cycle of 7 days (3 days of wetting and 4 days of drying) each for a period of one year. The immersion procedure was kept same as that for Set-I as explained in section 4.6.1.

It is to be noted here that the data from this set of experimentation was used to validate the effectiveness of impressed current technique only. Hence, the specimens prepared in Set-II (a) were monitored periodically for corrosion activity using electrochemical techniques only. The AE monitoring during this process was not carried out as liquid absorption during wetting process and capillary action during drying process in concrete is likely to develop noise in AE data acquisition which was observed during trial test.

(a) **Internal chloride exposure:** For casting of the specimens (60 mm diameter and 100 mm high cylindrical specimens with concentric steel rebar), the mix proportions and materials were kept the same as those used for Set-I and Set-II (a). However, since the exposure condition demanded some level of internal chlorides in the specimens, 5% NaCl by weight of cement was introduced into the concrete during casting of specimens. These specimens were cured for a period of 7 days at the temperature of 27 ±2 ºC and relative humidity of 100% and were then immersed in 5% NaCl solution for a period of 142 days. The specimens were monitored continuously during this period using AE technique for corrosion activity. Periodic measurements were taken using electrochemical techniques. The results obtained from this process were used to validate the developed mathematical model.

For all the specimens, the testing was stopped when the corrosion products oozed out from steel-concrete interface. Typical test matrix adopted is summarized in Table 6.1.

Table 6.1. Test Matrix

Set No.	Corrosion acceleration procedure	Cement type	Steel type	Rebar diameter (mm)	Test duration (days)	Nomen-clature	Repetitions
Set-II (a)	Alternate dry-wetting process	OPC	TMT	12	324	OT-12A	1
		OPC	TMT	16	365	OT-16A	1
		OPC	TMT	20	298	OT-20A	1
Set-II (b)	Admixed chloride	OPC	TMT	12	142	OT-12N	1
		OPC	TMT	16	142	OT-16N	1
		OPC	TMT	20	142	OT-20N	1

6.3.2. Corrosion monitoring using AE Technique

The procedure followed for corrosion monitoring of reinforced concrete cylinders using AE technique was as described in section 4.3.2 of Chapter 4. As explained in section 6.3.1, only the specimens subjected to internal chloride exposure (Set-II (b)) were monitored using AE technique whereas the specimens under alternate dry/wet cycles (Set-II(a)) were not monitored using AE technique to avoid acquisition of noise in AE data due to successive liquid absorption and capillary action during wetting and drying of specimens respectively.

6.3.3. Corrosion monitoring using Electrochemical Techniques

The procedure followed for corrosion monitoring of reinforced concrete specimens using electrochemical techniques was as described in section 4.3.3 of Chapter 4. All the specimens of Set–II (both (a) and (b)) were monitored using electrochemical techniques periodically irrespective of method adopted for inducing corrosion.

6.3.4. Determination of mass loss

After completion of tests, the mass loss of steel rebar in concrete due to corrosion was determined as explained in section 4.3.4 of Chapter 4. Table 6.2 and 6.3 presents the mass loss values along with the results of AE and electrochemical technique for all specimens at the end of testing of Set-II (a) and (b) of the experimental programme. It can be noted here that the trend in the values of i_{corr} between Set II-(a) and Set-II (b) is opposite with steel bar diameter. This may be due to the difference in the exposure condition for both sets. Set-II (a) is an external exposure condition, where the specimens are subjected to chloride ions after casting. Since the diameter of specimen is kept constant, the concrete side cover to rebar will vary with the change in diameter of rebar. The maximum cover will be obtained for 12 mm rebar diameter, therefore more time will be taken for chloride ion migration to steel surface it this case, resulting in lesser value of $i_{corr.}$ In Set-II (b), chlorides are introduced in the specimen at the time of casting. Therefore, the effect of cover to rebar becomes immaterial in this case. Further, since NaCl is added to concrete by weight of cement, the absolute amount of NaCl will be slightly higher for 12 mm diameter rebar specimen. This can be probably the reason for higher i_{corr} for this specimen.

Table 6.2. Gravimetric mass loss, Corrosion Current Density and Cumulative Signal Strength values for Set II (a)

Set Number	Specimen nomenclature	Gravimetric mass loss (g)	i_{corr} ($\mu A/cm^2$)	max CSS (pV-sec)
Set-II (a)	OT-12A	0.17	5.03	---
	OT-16A	0.65	14.41	---
	OT-20A	0.95	19.80	---

Table 6.3. Gravimetric mass loss, Corrosion Current Density and Cumulative Signal Strength values for Set II (b)

Set Number	Specimen nomenclature	Gravimetric mass loss (g)	i_{corr} ($\mu A/cm^2$)	max CSS (pV-sec)
Set-II (b)	OT-12N	0.559	23.15	3.61×10^6
	OT-16N	0.065	11.85	2.24×10^6
	OT-20N	0.057	12.94	1.08×10^6

6.4. RESULTS AND DISCUSSIONS

6.4.1. Validation of Impressed current technique

The results obtained from specimens of Set-II (a), in which the specimens were subjected to alternate drying and wetting process, were used to validate the effectiveness of impressed current technique. The similarities in the test results for both cases helped in validating the exposure by impressed current technique. The similarities are discussed hereunder:

1. ***Half-cell potential results:*** In order to compare both the techniques, the half-cell potential data of Set-I and Set-II (a) was plotted simultaneously and the pattern of variation was analyzed. Figs. 6.2, 6.4 and 6.6 shows the comparative plots of half-cell potential with time for the corresponding specimens cast from the same batch of concrete in each set of the experimental programme. It was observed from the figures that the pattern of variation of half-cell potential values during both the tests was similar for all specimens. It was observed from the comparative plots that, using impressed current technique, the similar level of corrosion can be achieved approximately 10 times faster as compared to the level of corrosion achieved during alternate drying-wetting process for the present developed experimental set-up for all specimens.

2. ***Corrosion rate results:*** Figs. 6.3, 6.5 and 6.7 shows the comparative plots of corrosion rate with time for the corresponding specimens cast from the same batch of concrete in each set of the experimental programme. From the figures, it was observed that, the pattern of variation of corrosion rates during both the tests were also similar for all specimens. It was also observed that using impressed current technique, the similar rate of corrosion can be achieved approximately 10 times faster as compared to the rate of corrosion achieved during alternate drying-wetting process for the present developed experimental set-up for all specimens.
3. ***Analysis of rust formed in both the cases:*** In the present study, green rust was observed for a couple of minutes, which turned into ordinary red rust for specimens of both sets of experiment. Thus, the corrosion products formed in accelerated corrosion test using impressed current technique were the same as that for induced corrosion using alternate drying-wetting process. Similar to the case of induced corrosion using alternate drying-wetting cycles, in impressed current corrosion process, rust formed on steel expanded and concrete cover was cracked. Similar results were obtained by *Care and Raharinaivo (2007)*. The results obtained by *Care and Raharinaivo (2007)* provided information on corrosion kinetics of embedded steel when corrosion is accelerated by impressed current and showed the similarities to natural corrosion pattern when solutions contain chlorides. The study concluded that accelerated corrosion test by impressed current is a valid method to study the corrosion process of steel in mortar, and its effects on the damage of mortar cover.
4. ***Crack patterns on concrete surface and type of corrosion:*** The final pattern of concrete cracking observed in both the processes was parallel to the steel reinforcement. All the specimens under alternate dry-wet cycles and impressed

current had shown finally pitting corrosion showing extremely localized attack resulting in pot-holes in the metal. The steel rebar after alternate dry-wet cycles showed small isolated pot-holes on its surface whereas the steel rebar subjected to impressed current showed very close pits together looking like a rough surface. Fig. 6.8 presents the condition of 12 mm diameter rebar after dry-wet cycles while Fig. 6.9 shows the steel rebar surface (12 mm diameter) subjected to impressed current. Similar results were obtained for 16 mm and 20 mm diameter rebars as well. Thus, accelerated corrosion test using "Impressed Current Technique" proved to be a valid method to study the corrosion process of steel rebar.

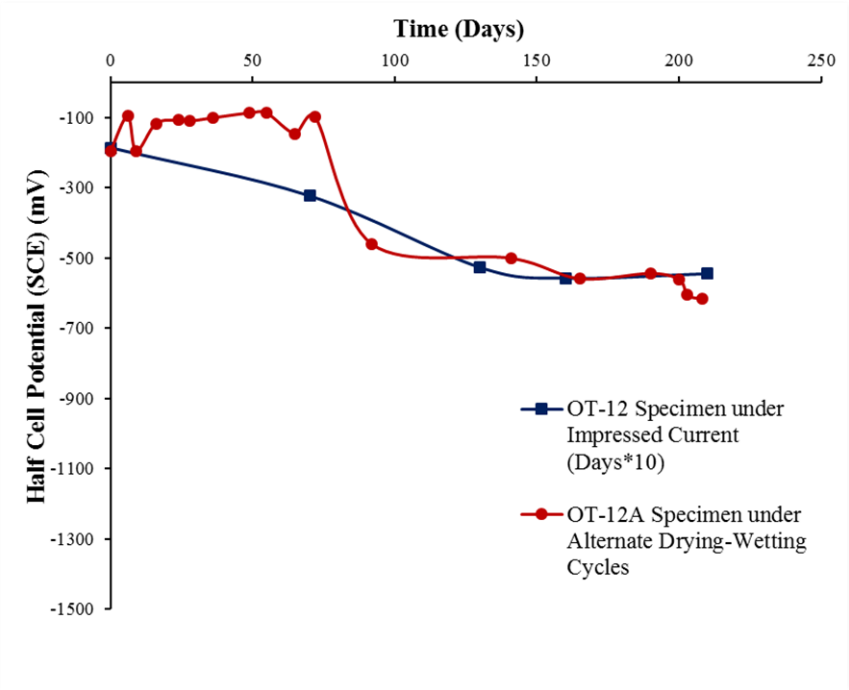

Fig. 6.2. Variation of half-cell potential with time for specimens under impressed current (OT-12) and alternate drying-wetting process (OT-12A)

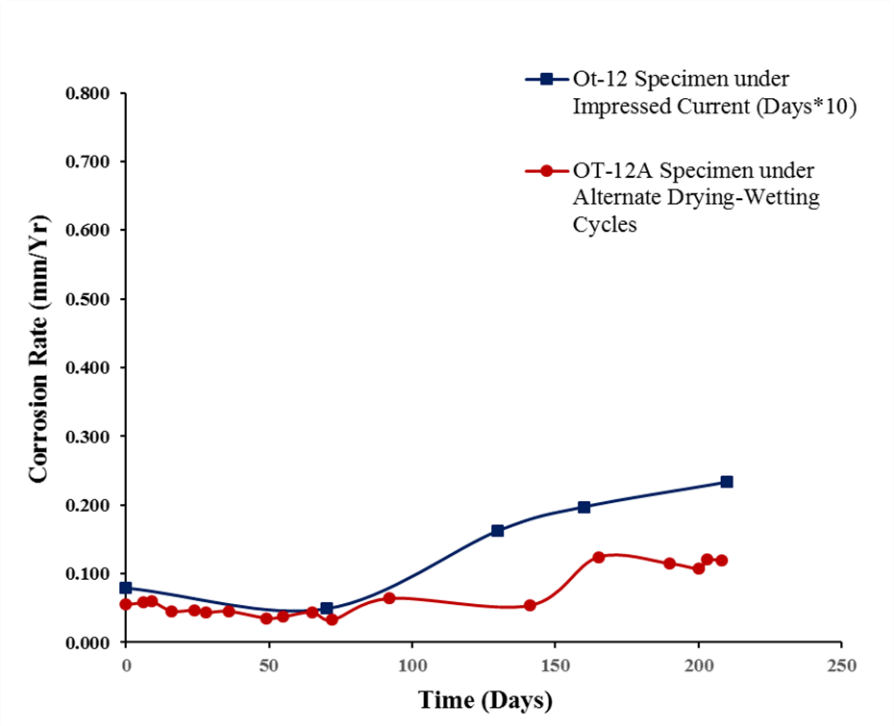

Fig. 6.3. Variation of corrosion rate with time for specimens under impressed current (OT-12) and alternate drying-wetting process (OT-12A)

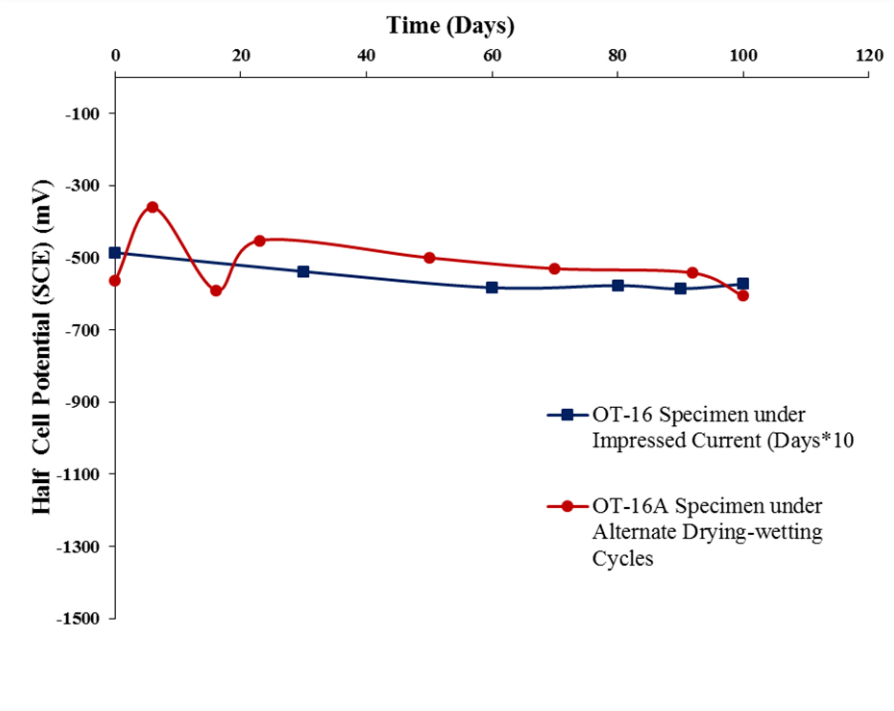

Fig. 6.4. Variation of half-cell potential with time for specimens under impressed current (OT-16) and alternate drying-wetting process (OT-16A)

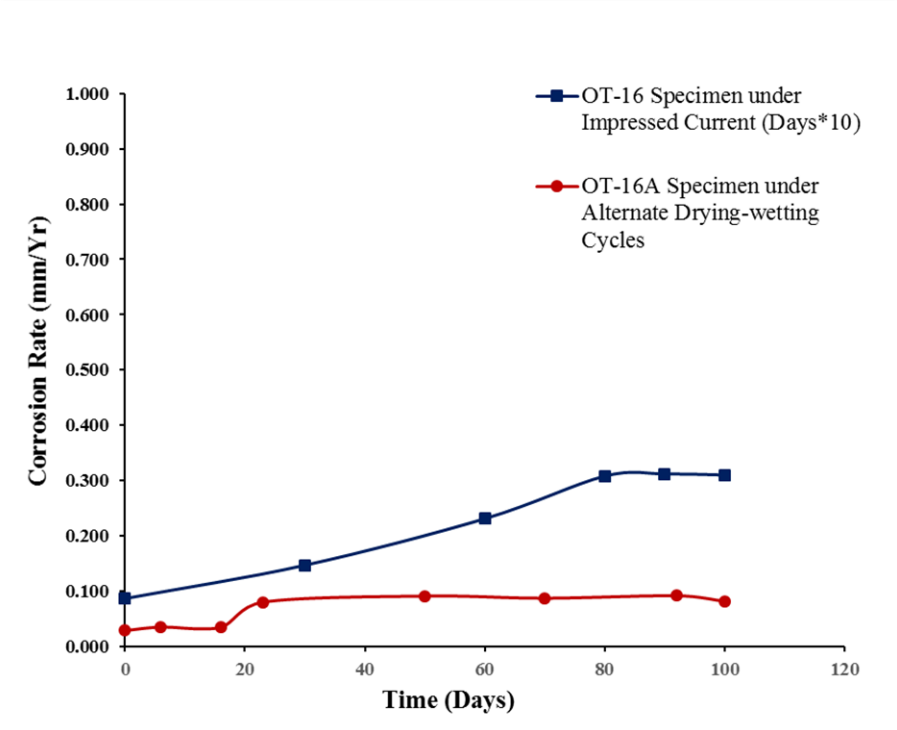

Fig. 6.5. Variation of corrosion rate with time for specimens under impressed current (OT-16) and alternate drying-wetting process (OT-16A)

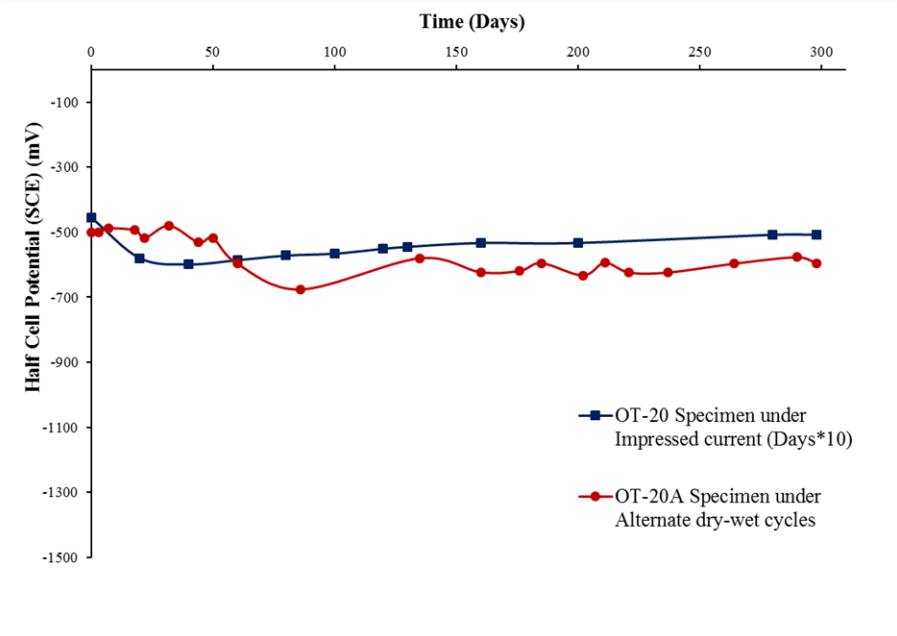

Fig. 6.6. Variation of half-cell potential with time for specimens under impressed current (OT-20) and alternate drying-wetting process (OT-20A)

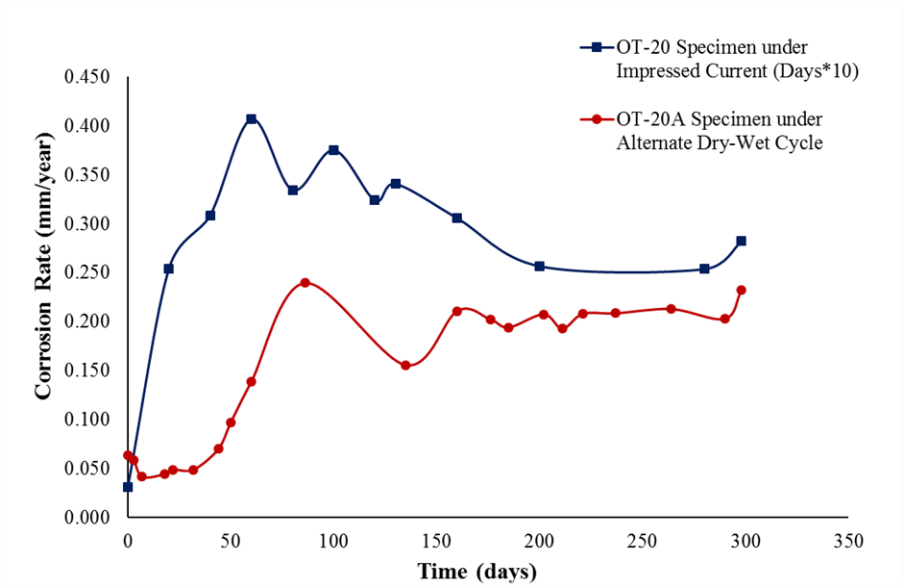

Fig. 6.7. Variation of corrosion rate with time for specimens under impressed current (OT-20) and alternate drying-wetting process (OT-20A)

Fig. 6.8. Condition of steel surface after testing using alternate drying-wetting cycles

Fig. 6.9. Condition of steel surface after testing using impressed current technique

6.4.2. Validation of developed mathematical model

The developed mathematical model was further used for calculation of mass loss of specimens under realistic prolonged corrosion exposure conditions of Set-II (b) as described in section 6.3.1. Fig. 6.10 show the comparative plot of mass losses calculated using gravimetrical method (actual mass loss of steel), using Faraday's law and from developed mathematical model using AE technique for all specimens under internal chloride exposure condition.

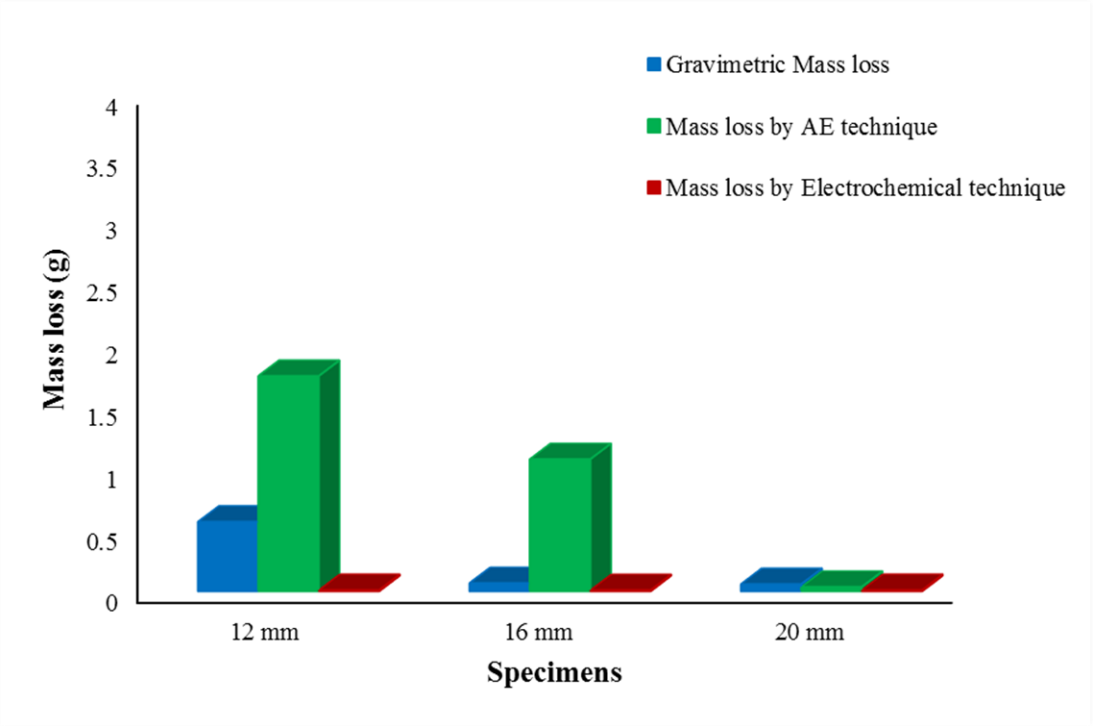

Fig. 6.10. Comparative plot of mass loss from gravimetrical method, Faraday's law and AE technique for internal chloride exposure

As the corrosion under internal chloride exposure is very slow, the specimens showed very little mass loss as seen in Fig. 6.10. From visual inspection of specimens, it was found that OT-12N specimen showed three cracks emerging at the bottom of concrete specimen in perpendicular direction to that of steel, OT-16N specimen showed one crack at the bottom whereas OT-20N specimen showed no crack on concrete surface (Fig. 6.11). Consequently, magnitude of max CSS observed for OT-12N specimen was highest among all specimens followed by OT-16N and OT-20N. As AE technique identifies corrosion by detecting micro-cracking in concrete as a consequence of the corrosion reaction, for the specimens showing more cracking, AE technique is likely to predict more mass loss.

Thus, from Fig. 6.10, it was observed that the mass loss predicted by the developed model using AE technique was comparable or on the conservative side of the actual mass loss. For first two specimens the mass losses predicted by AE

technique were higher than the actual mass loss values which is on the conservative side. In comparison to this, the mass losses calculated by electrochemical technique were much less than the actual mass loss values. For the third specimen, the actual mass loss was very low and is comparable to the value predicted by the developed model and by the electrochemical technique. This indicates that the prediction of mass loss by AE technique using developed mathematical model is acceptable. Thus, it can be concluded that it is possible to predict the mass loss using the developed mathematical model by AE technique for realistic prolonged corrosion exposure conditions.

The difference in predicted mass loss by electrochemical techniques and AE technique is due to fundamental difference in obtaining data. The predicted mass loss by AE technique is higher because chloride induced corrosion results in pitting type of corrosion. Therefore, the AE activity will be higher and sudden for such type of corrosion, giving rise to more CSS and hence higher predicted mass loss. On the other hand, mass loss predicted by electrochemical is based on Faraday's law which assumes uniform corrosion. The calculation of penetration or mass loss from electrochemical measurements, as described in *ASTM G 102-89 (Reapproved 2004)*, assumes that uniform corrosion is occurring. In cases where non-uniform corrosion processes are occurring, the use of these methods may result in a substantial underestimation of the true values.

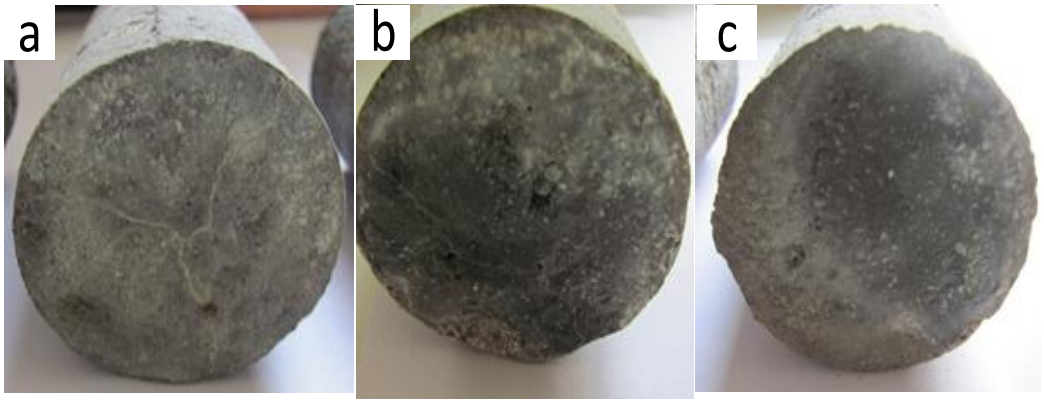

Fig. 6.11. Specimens of Set II (b) after testing: (a) OT-12N, (b) OT-16N and (c) OT-20N.

6.5. CLOSING REMARKS

The test results discussed in the present chapter reveal that the results of electrochemical measurements for specimens subjected to alternate drying-wetting cycles and impressed current were found to be similar. The similarities found in cracking pattern of concrete, corrosion products formed as well as condition of steel surface after completion of tests using two techniques confirm that impressed current technique is a valid method to study the corrosion process of steel rebar and its effect on damage to concrete. It is further observed that impressed current technique offered faster and easy means of simulation of corrosion to natural condition under low impressed voltage.

From the comparative study of corrosion rates calculated using gravimetric method, Faraday's law and developed mathematical model using AE technique, it can be concluded that, the developed mathematical model is well validated and it can also be used appropriately for realistic corrosion exposure conditions in the laboratory using internal chloride exposure.

CHAPTER 7

CONCLUSIONS AND SCOPE OF FUTURE WORK

7.1. INTRODUCTION

The aim of the experimental study was to assess the corrosion of steel embedded in concrete using AE technique quantitatively. The results obtained from AE technique were compared with the results of well-established electrochemical techniques. The study was carried out on small scale singly reinforced cylindrical RC specimens in laboratory. The corrosion was accelerated using impressed current technique. Further the effect of various material properties on corrosion and non-destructive measurements was studied. To quantify the corrosion using AE technique, a mathematical model was developed using non-linear regression analysis. The efficacy of impressed current technique and cogency of developed mathematical model was further verified by comparing the results through additional experiments on specimens subjected to more realistic corrosion conditions in laboratory, simulating natural corrosion conditions. The conclusions spread over the entire report are summarized in the following sections.

7.2. ACOUSTIC EMISSION VIS-À-VIS ELECTROCHEMICAL TECHNIQUES

1. Cumulative signal strength (CSS) parameter of AE technique is found to be a promising parameter for corrosion monitoring studies as the variation of CSS w.r.t. time has shown a specific trend indicating active corrosion which is similar to the curve of typical phenomenological corrosion loss of steel due to seawater immersion.

2. Chloride induced corrosion of steel embedded in concrete can be classified in two different stages. 'Stage 1' consists of depassivation of concrete surrounding the rebar and indicates onset of active corrosion leading to initiation of micro-cracks in concrete specimen. 'Stage 2' is indicative of further increase in corrosion activity and accumulation of corrosion products in concrete pores resulting in development of major cracks in concrete. Both these stages are well identified by electrochemical techniques as far as corrosion process of steel embedded in concrete is concerned, whereas AE technique can identify the corrosion process of steel reinforcement as well as damage to concrete due to subsequent cracking.

3. Variation of CSS values with time indicates two distinct characteristics namely, gradual increase in CSS value with time and sudden rise in CSS value with time. The gradual increase in CSS value represents active corrosion whereas sharp increase in CSS at a certain time indicates damage to concrete due to cracks developed because of corrosion. If the sudden rises are removed from the curve, the curve obtained by CSS resembles the phenomenological model of corrosion of steel embedded in concrete in marine environments.

7.3. EFFECT OF MATERIAL VARIABLES ON CORROSION AND AE MEASUREMENT

1. To study the effect of material variables such as cement type, steel type and rebar diameter on corrosion, ANOVA was performed using corrosion current density values for all material variables. From the ANOVA, it was observed that the calculated F- values are lower than the corresponding tabulated F-values at 99% confidence level for all the variables with P-value greater than

0.01. Thus, the results of ANOVA proved that there is not enough evidence to reject the null hypothesis indicating the difference in magnitudes of corrosion current density values for different variables is just a matter of chance.

2. Similarly, to study the effect of material variables such as cement type, steel type and rebar diameter on AE measurements, ANOVA was performed using CSS values for all material variables. The results of ANOVA proved that there is not enough evidence to reject the null hypothesis indicating the difference in magnitudes of CSS for different variables is just a matter of chance.
3. Similarity in the results of ANOVA obtained for magnitudes of corrosion current densities and CSS values satisfactorily validated the results of AE measurements.

7.4. DEVELOPMENT OF MATHEMATICAL MODEL

1. AE technique is a powerful non-destructive technique for corrosion assessment and can be successfully used for quantification of corrosion of steel embedded in concrete. The results of SOLVER confirmed that a non-linear relation exists between max. CSS value and gravimetric mass loss. The relation between the two parameters is analogous to natural exponential growth function.
2. Thus, AE technique proves to be a truly non-destructive technique for quantification of corrosion of steel rebar in concrete without having physical/electrical contact with the steel, which is required in electrochemical techniques.

7.5. VALIDATION OF IMPRESSED CURRENT TECHNIQUE AND MATHEMATICAL MODEL

1. The comparative results of electrochemical measurements obtained using impressed current technique and alternate drying-wetting process confirms that impressed current technique is a valid method to study the corrosion process of steel rebar and its effect on damage to concrete. It is further observed that, impressed current technique offers faster and easy means of simulation of corrosion to natural condition under low impressed voltage.
2. From the comparative study of corrosion rates calculated using gravimetric method, Faraday's law and developed mathematical model using AE technique, it can be concluded that the developed mathematical model can predict the mass loss and corrosion rate conservatively under accelerated corrosion using the impressed current technique.
3. The results of experimental work conducted using internal chloride exposure, indicated difference in predicted mass loss by electrochemical techniques and AE technique which is due to fundamental difference in obtaining data. The predicted mass loss by AE technique is higher because chloride induced corrosion results in pitting type of corrosion. Therefore, the AE activity will be higher and sudden for such type of corrosion, giving rise to more CSS and hence higher predicted mass loss. On the other hand, mass loss predicted by electrochemical is based on Faraday's law which assumes uniform corrosion.
4. Thus, from the results of experimental work conducted using internal chloride exposure, it is concluded that the developed mathematical model is

acceptable and can also be used appropriately for realistic corrosion exposure conditions in the laboratory.

7.6. SCOPE FOR FUTURE WORK

Under the conditions given in present experimental investigations, AE is observed to be a reliable laboratory method to evaluate the corrosion activity in a variety of concentrically reinforced cylindrical concrete specimens under accelerated corrosion. It is believed that interesting results have emerged in an area where very little research is published. The mathematical relation established between maximum CSS and gravimetrical mass loss in present investigation is obtained through laboratory experiments under specific conditions of accelerated corrosion by impressed current technique and for specific shape and size of concentrically reinforced cylindrical concrete specimens under no load condition. As the mathematical model was validated for the specimens with internal chloride exposure condition, the relation is applicable for the prescribed laboratory conditions only. The model was further validated for the real time damage assessment of RC structure. It is recommended to extend the research further to apply AE technique extensively structural health monitoring of real life structural elements. The developed mathematical model may be generalized and commercialized with regards to this. The developed model can further be refined by obtaining more data using various combination of material variables.

ANNEXURES

ANNEXURE – A

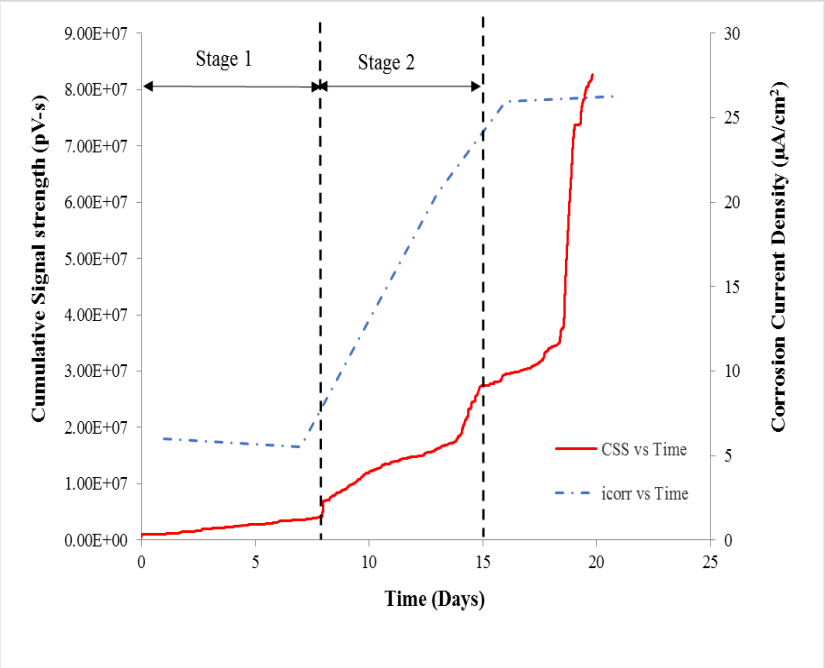

Fig. A-1. Simultaneous evolution of i_{corr} and CSS for actively corroding OT-12 SP-2 specimen

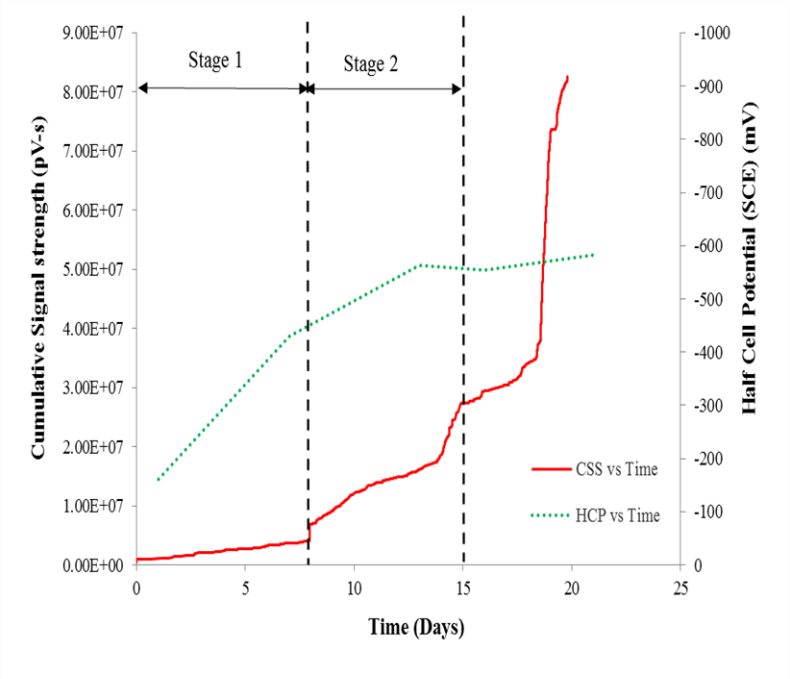

Fig. A-2. Simultaneous evolution of half-cell potential and CSS for actively corroding OT-12 SP-2 specimen

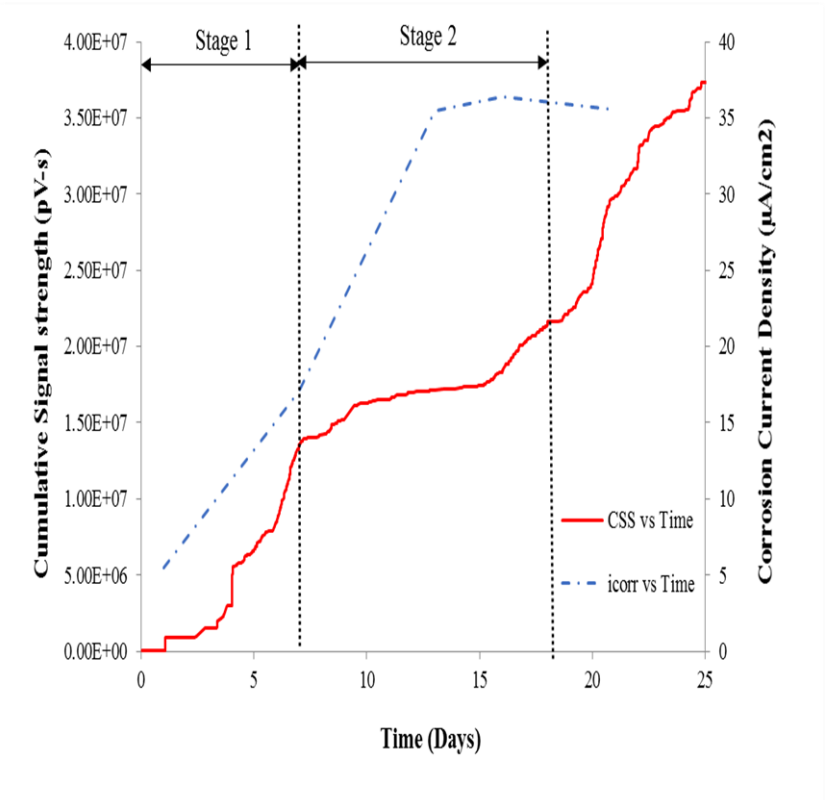

Fig. A-3. Simultaneous evolution of i_{corr} and CSS for actively corroding OT-12 SP-3 specimen

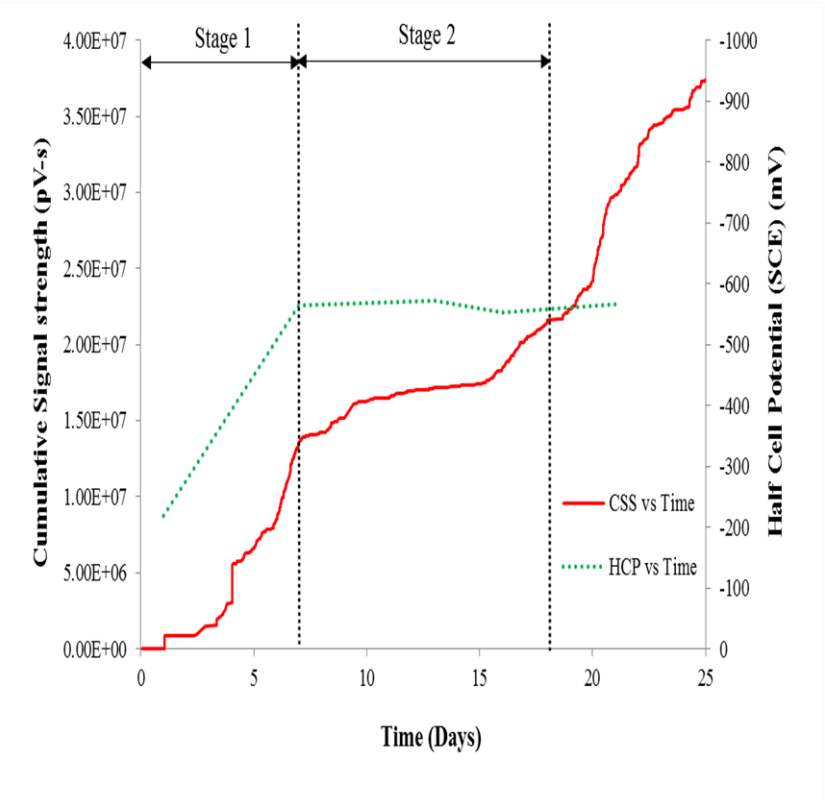

Fig. A-4. Simultaneous evolution of half-cell potential and CSS for actively corroding OT-12 SP-3 specimen

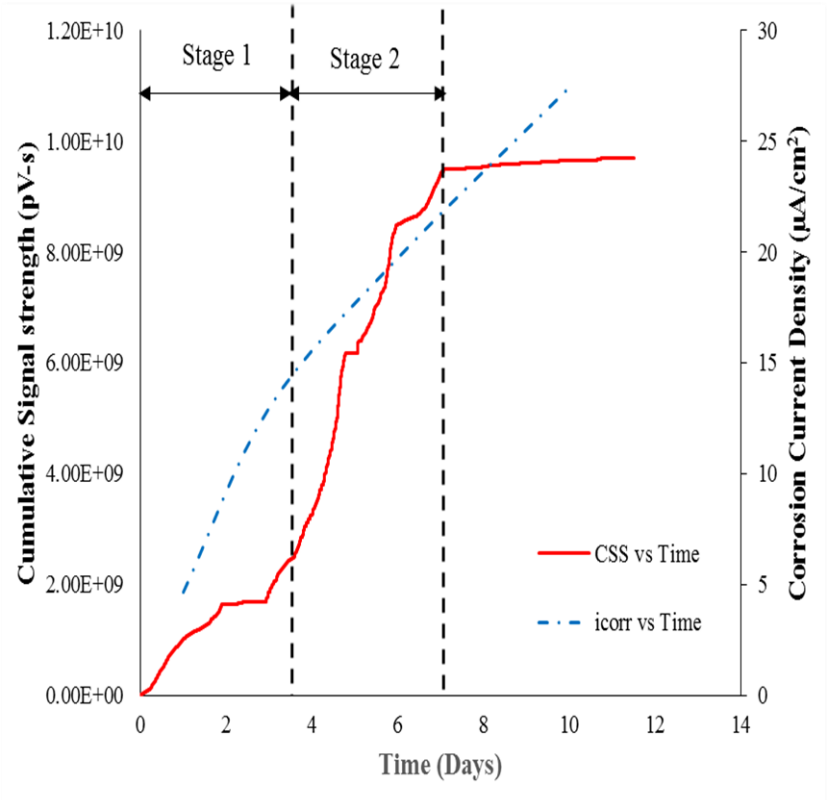

Fig. A-5. Simultaneous evolution of i_{corr} and CSS for actively corroding OT-16 SP-1 specimen

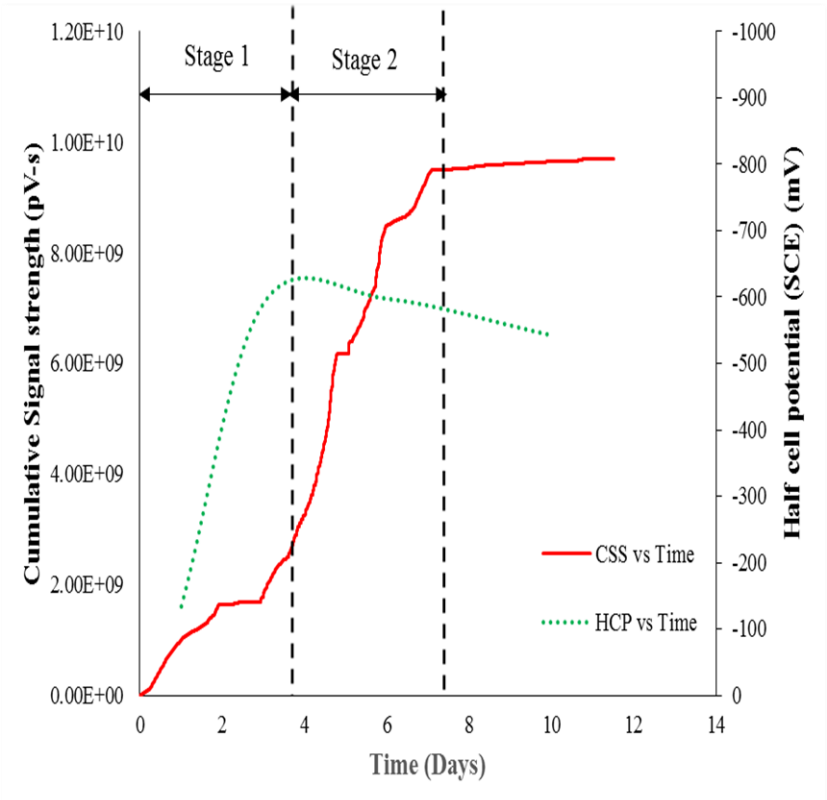

Fig. A-6. Simultaneous evolution of half-cell potential and CSS for actively corroding OT-16 SP-1 specimen

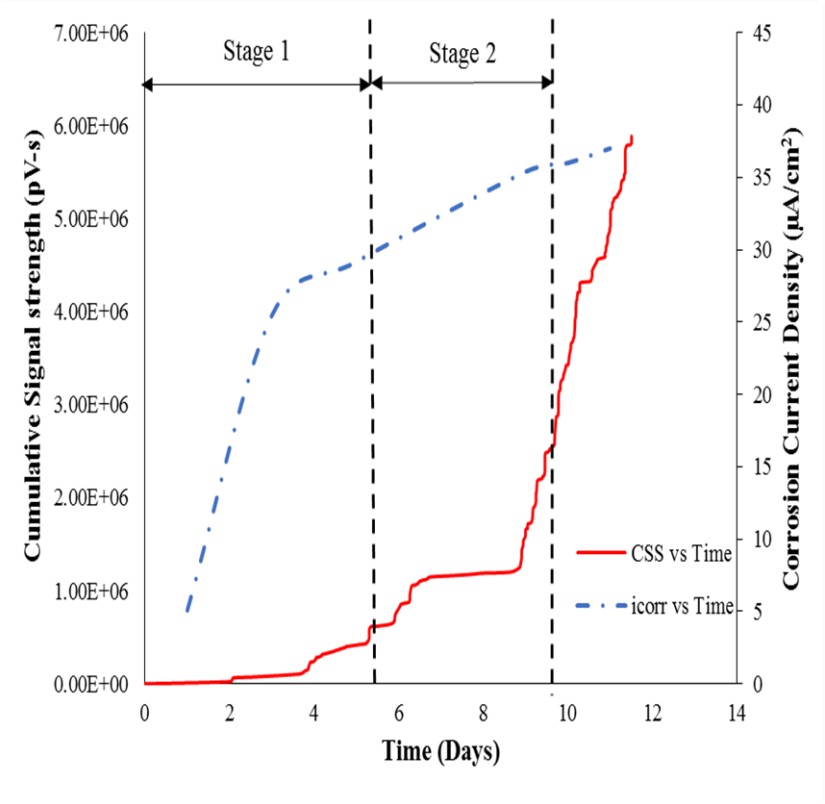

Fig. A-7. Simultaneous evolution of i_{corr} and CSS for actively corroding OT-16 SP-2 specimen

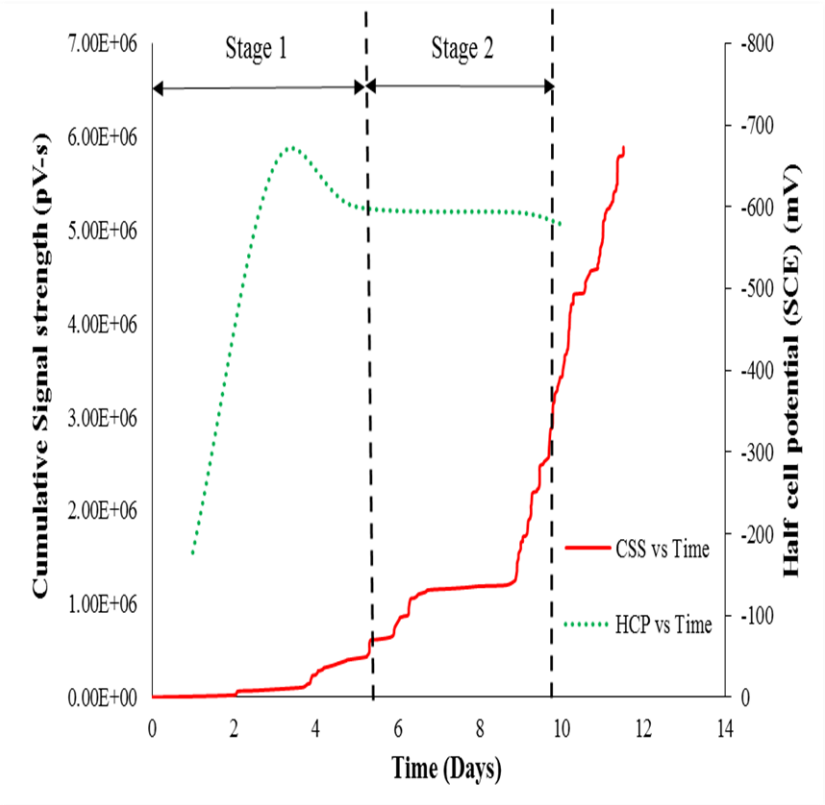

Fig. A-8. Simultaneous evolution of half-cell potential and CSS for actively corroding OT-16 SP-2 specimen

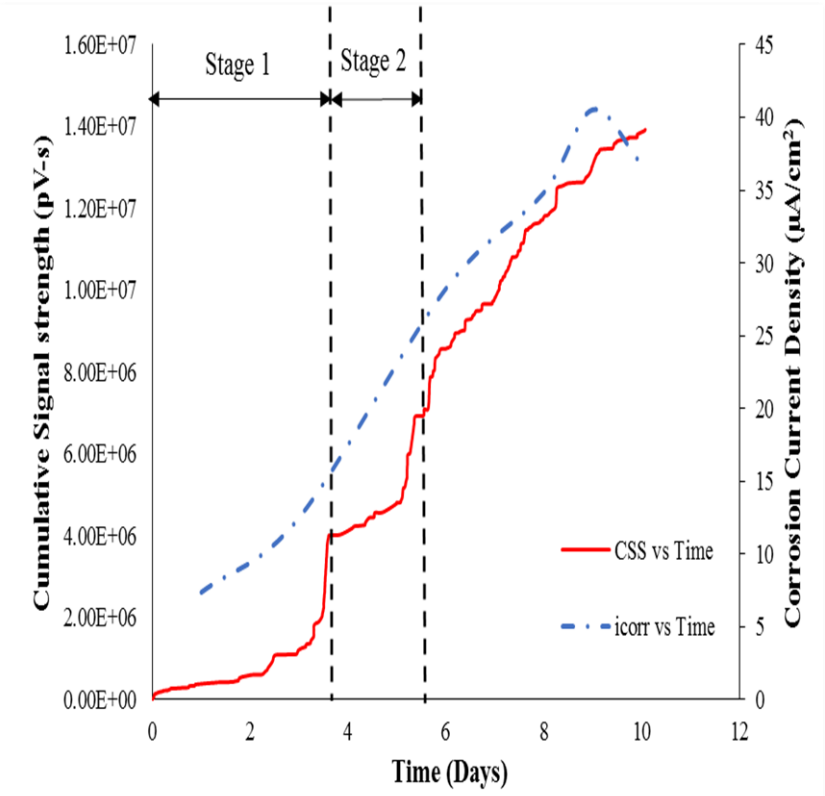

Fig. A-9. Simultaneous evolution of i_{corr} and CSS for actively corroding OT-16 SP-3 specimen

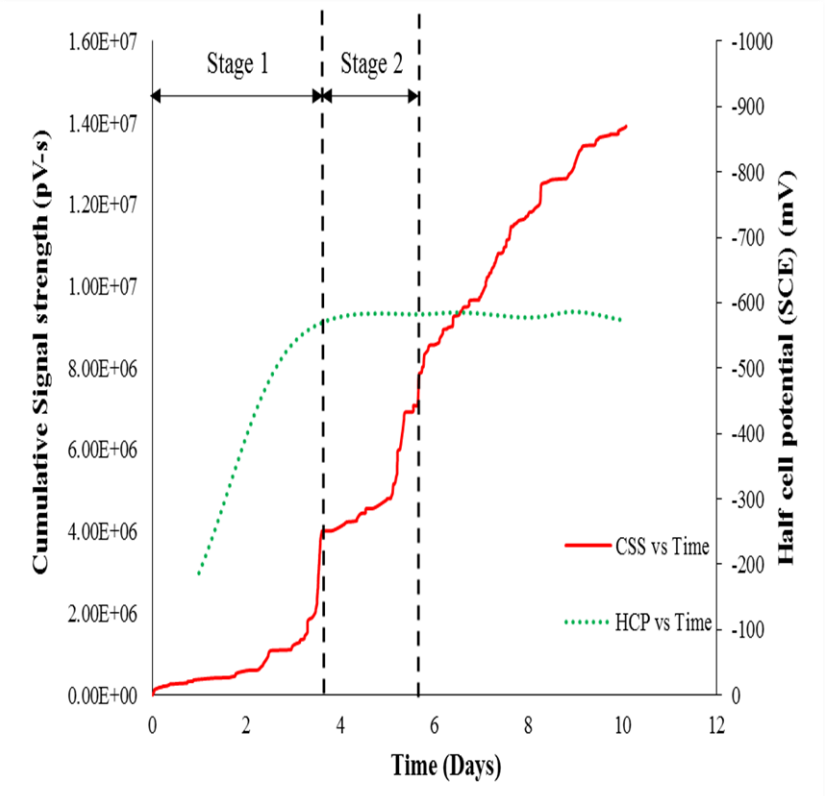

Fig. A-10. Simultaneous evolution of half-cell potential and CSS for actively corroding OT-16 SP-3 specimen

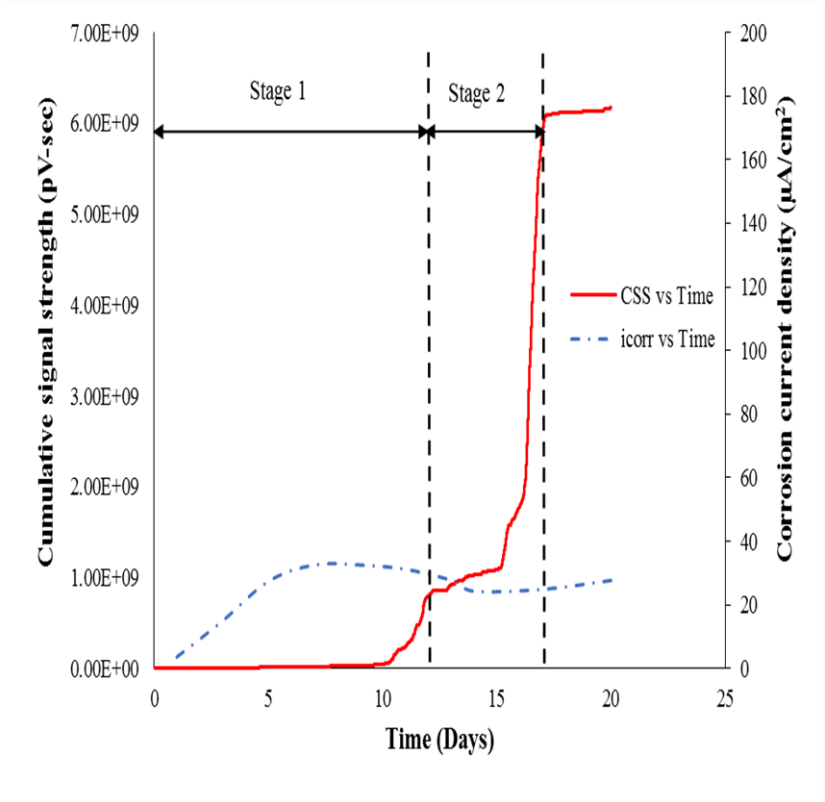

Fig. A-11. Simultaneous evolution of i_{corr} and CSS for actively corroding OT-20 SP-1 specimen

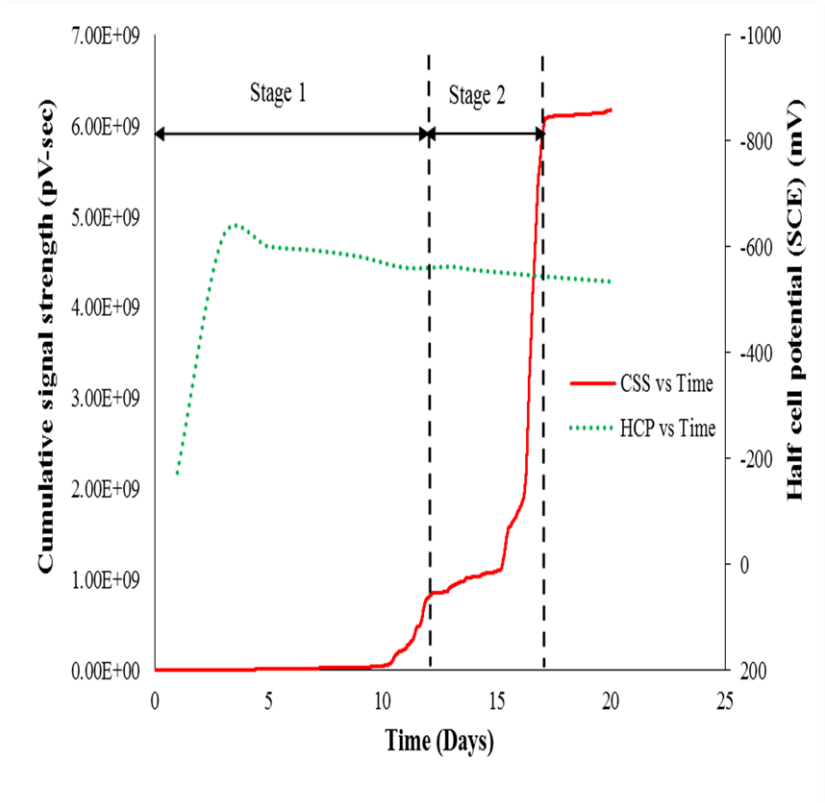

Fig. A-12. Simultaneous evolution of half-cell potential and CSS for actively corroding OT-20 SP-1 specimen

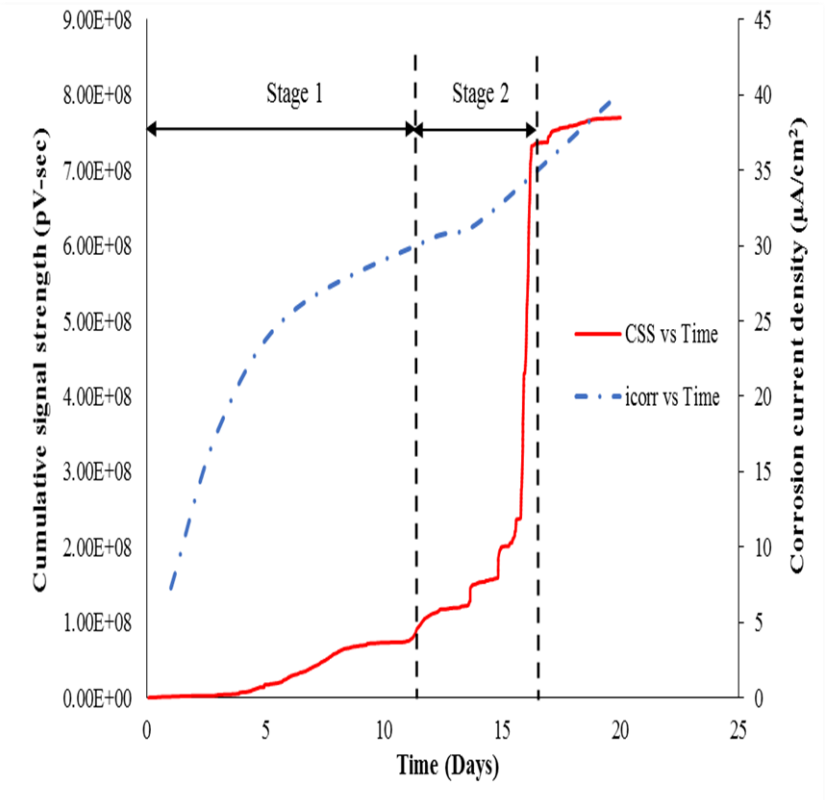

Fig. A-13. Simultaneous evolution of i_{corr} and CSS for actively corroding OT-20 SP-2 specimen

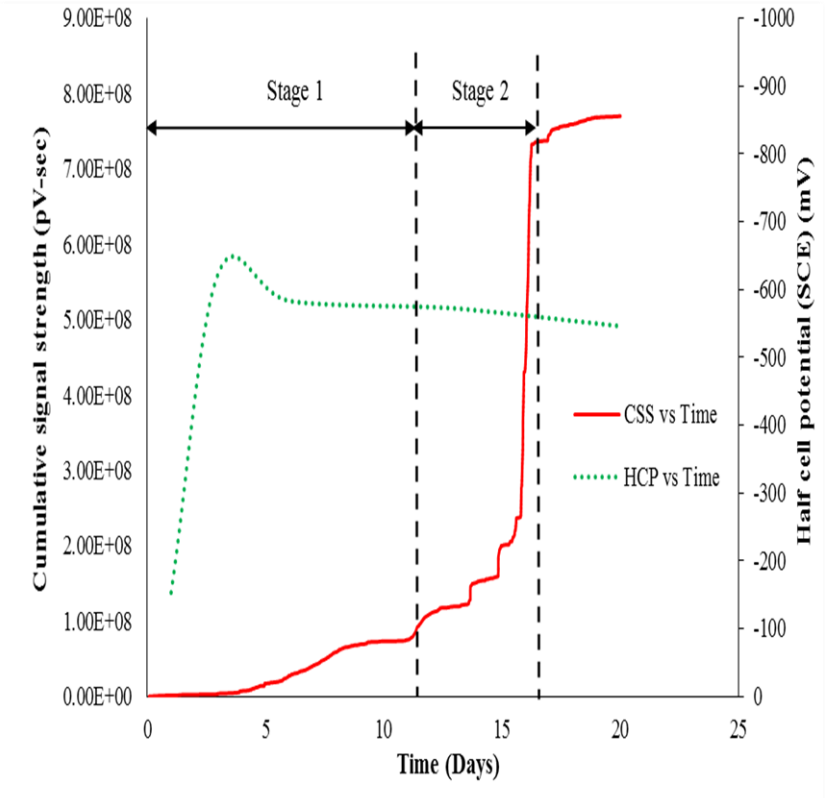

Fig. A-14. Simultaneous evolution of half-cell potential and CSS for actively corroding OT-20 SP-2 specimen

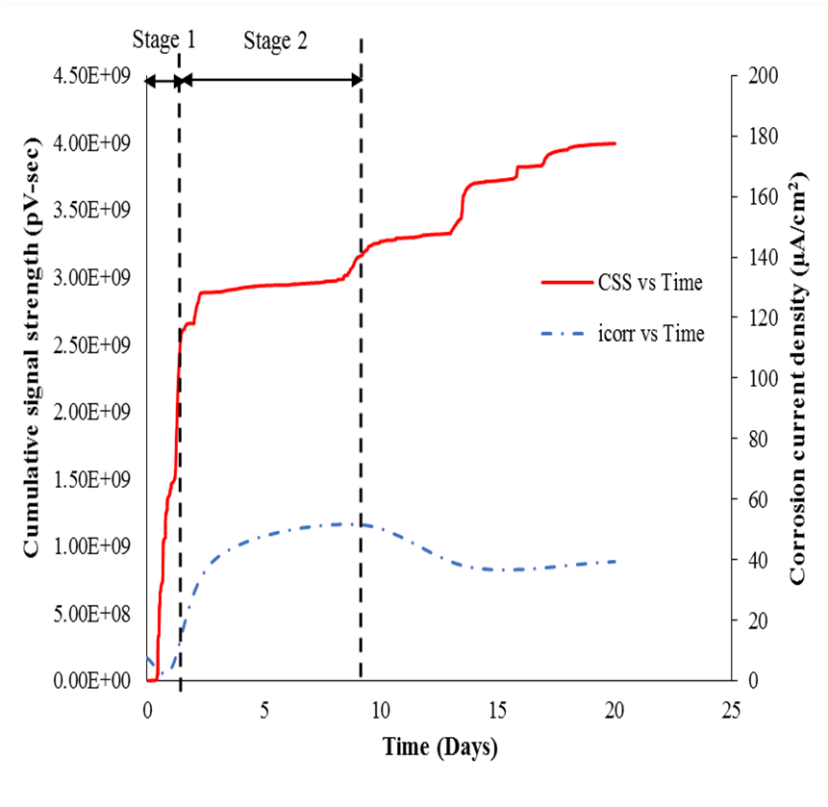

Fig. A-15. Simultaneous evolution of i_{corr} and CSS for actively corroding OT-20 SP-3 specimen

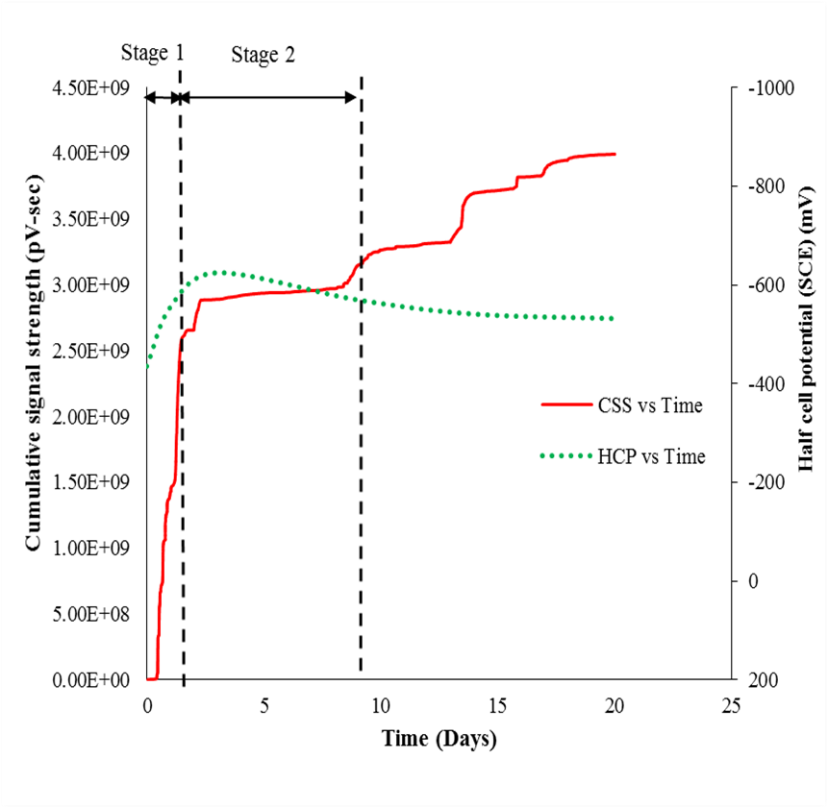

Fig. A-16. Simultaneous evolution of half-cell potential and CSS for actively corroding OT-20 SP-3 specimen

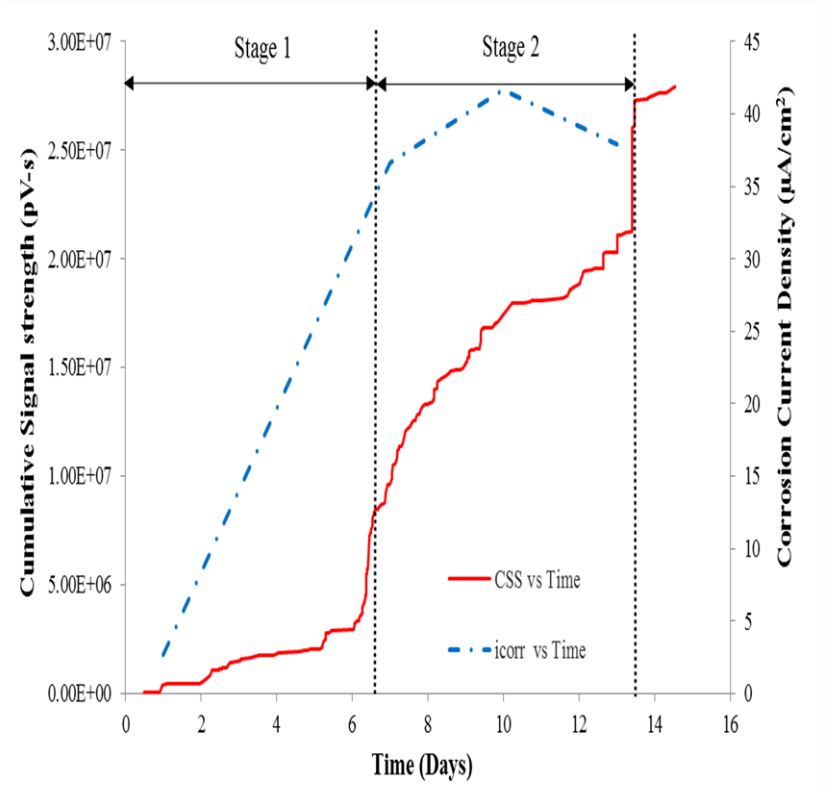

Fig. A-17. Simultaneous evolution of i_{corr} and CSS for actively corroding OC-20 SP-1 specimen

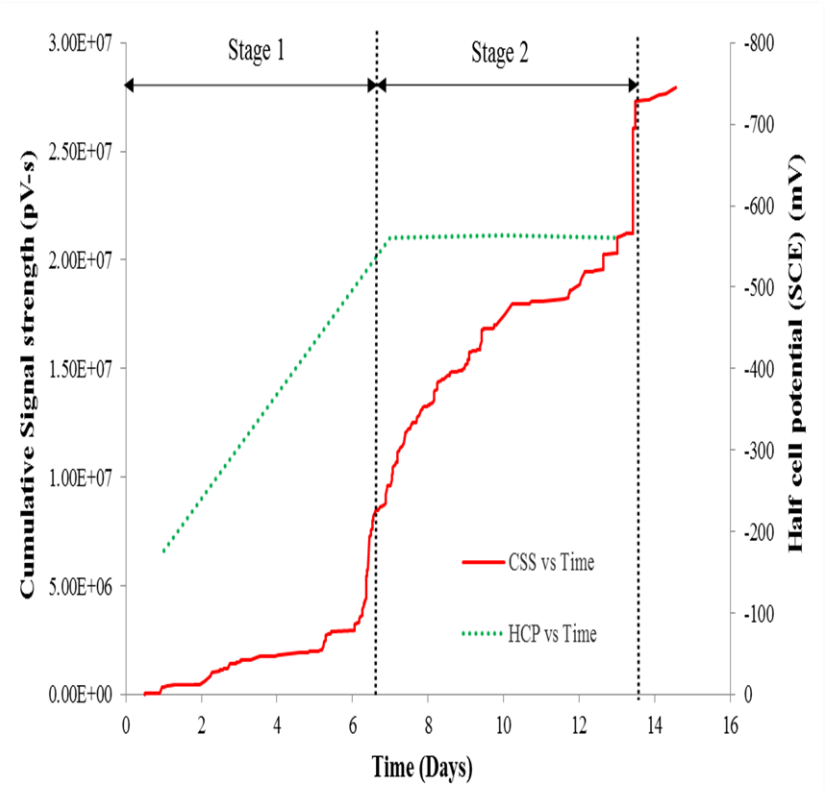

Fig. A-18. Simultaneous evolution of half-cell potential and CSS for actively corroding OC-20 SP-1 specimen

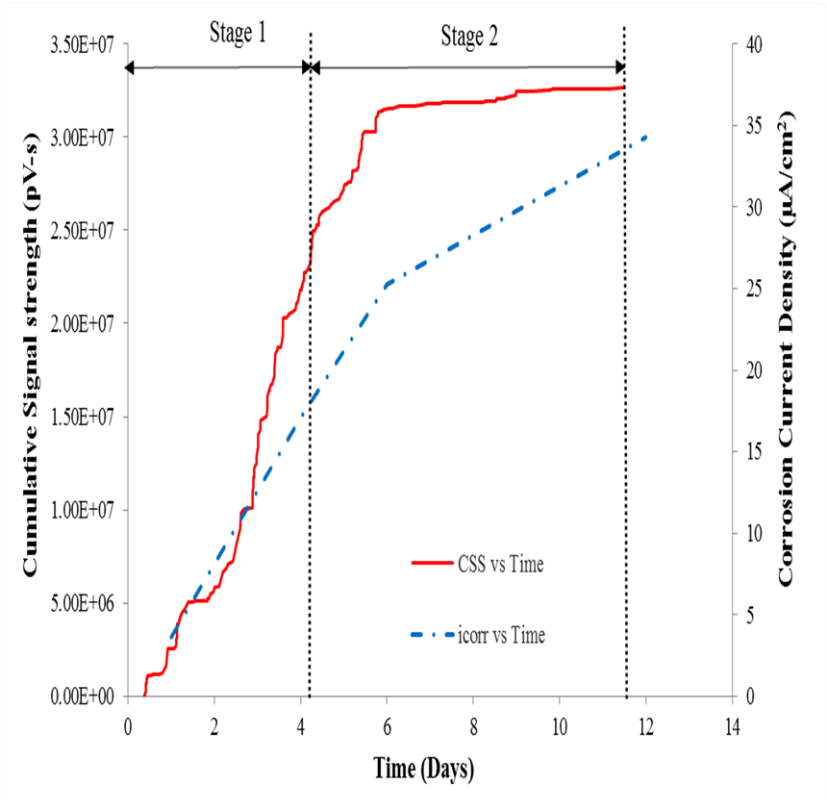

Fig. A-19. Simultaneous evolution of i_{corr} and CSS for actively corroding OC-20 SP-2 specimen

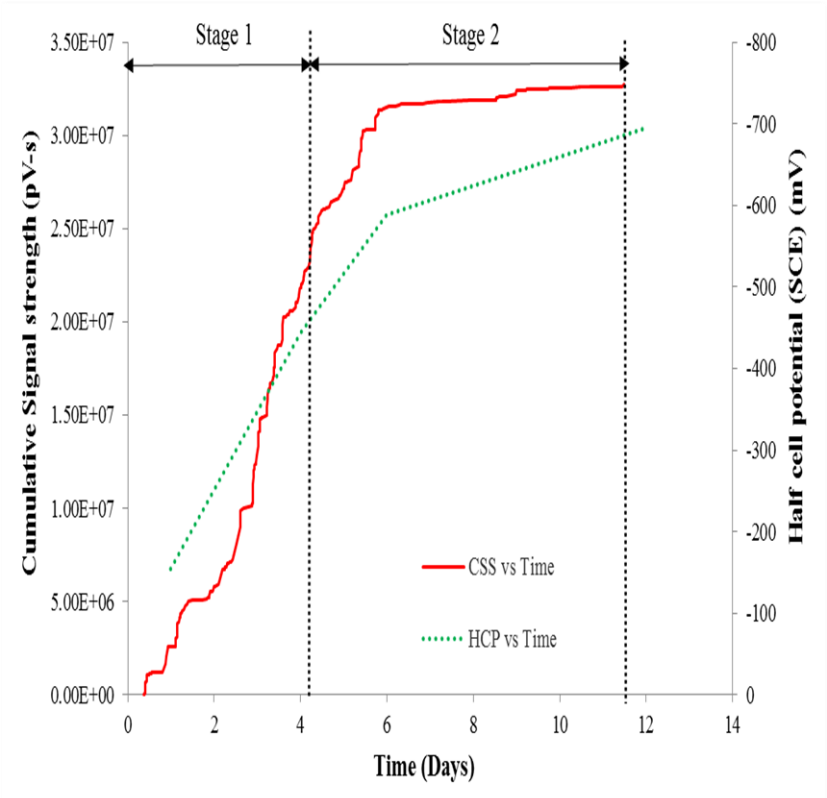

Fig. A-20. Simultaneous evolution of half-cell potential and CSS for actively corroding OC-20 SP-2 specimen

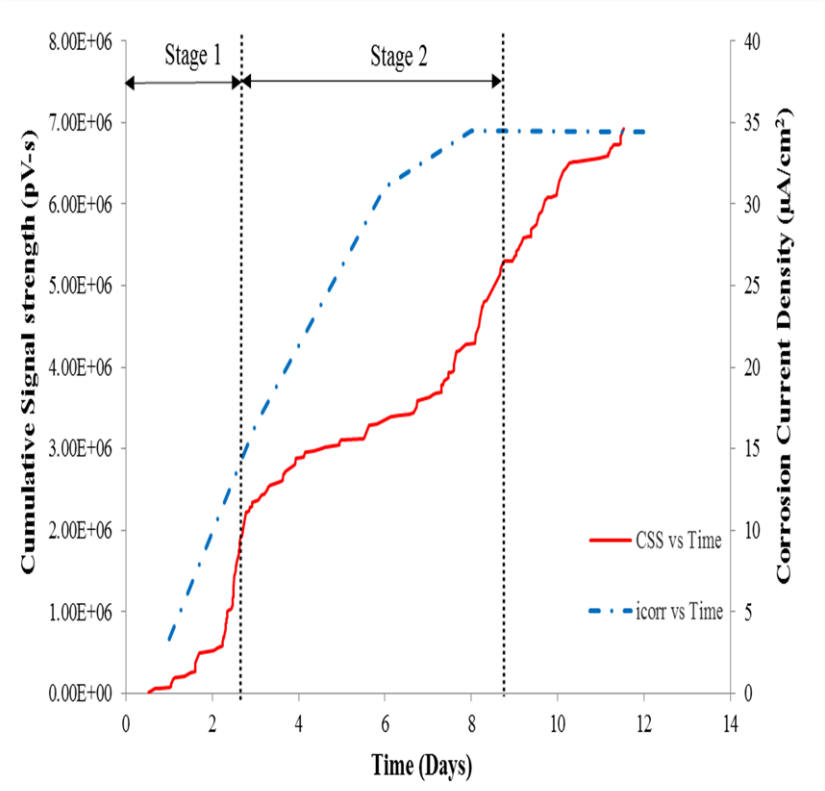

Fig. A-21. Simultaneous evolution of i_{corr} and CSS for actively corroding OC-20 SP-3 specimen

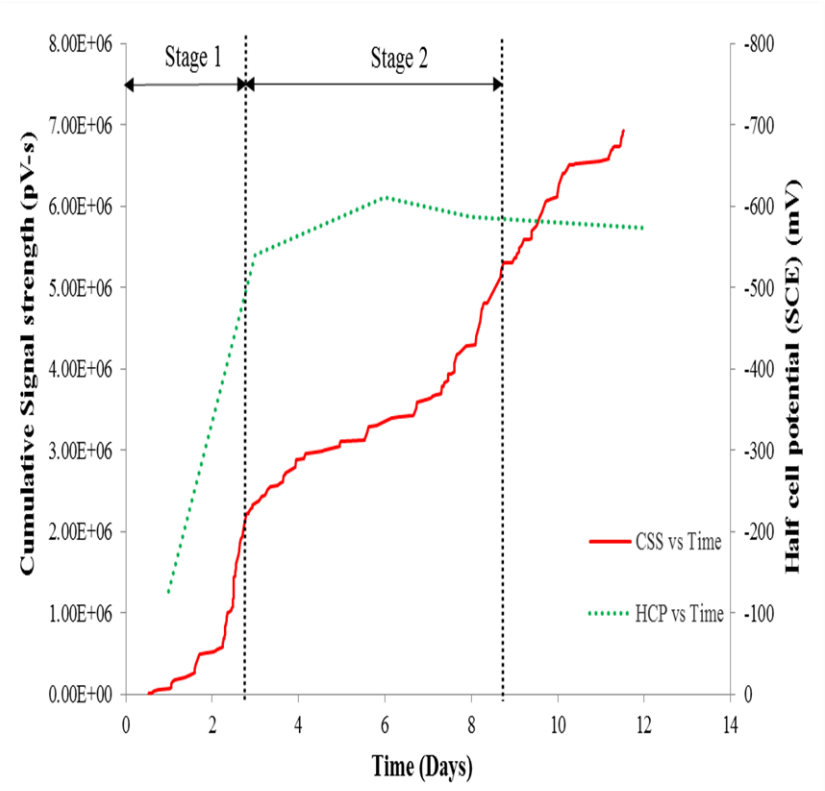

Fig. A-22. Simultaneous evolution of half-cell potential and CSS for actively corroding OC-20 SP-3 specimen

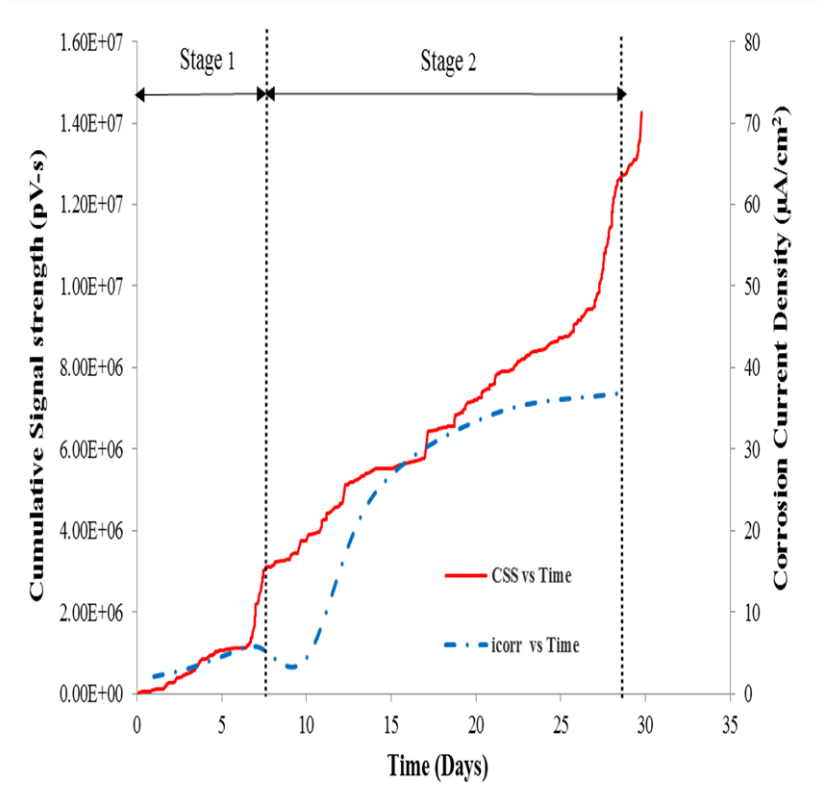

Fig. A-23. Simultaneous evolution of i_{corr} and CSS for actively corroding PT-20 SP-1 specimen

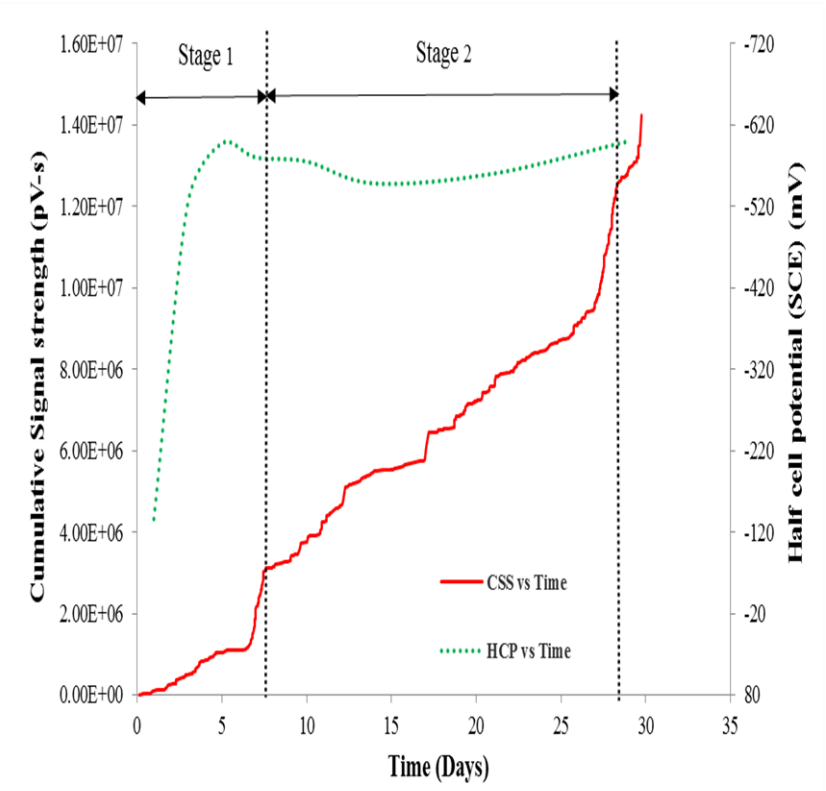

Fig. A-24. Simultaneous evolution of half-cell potential and CSS for actively corroding PT-20 SP-1 specimen

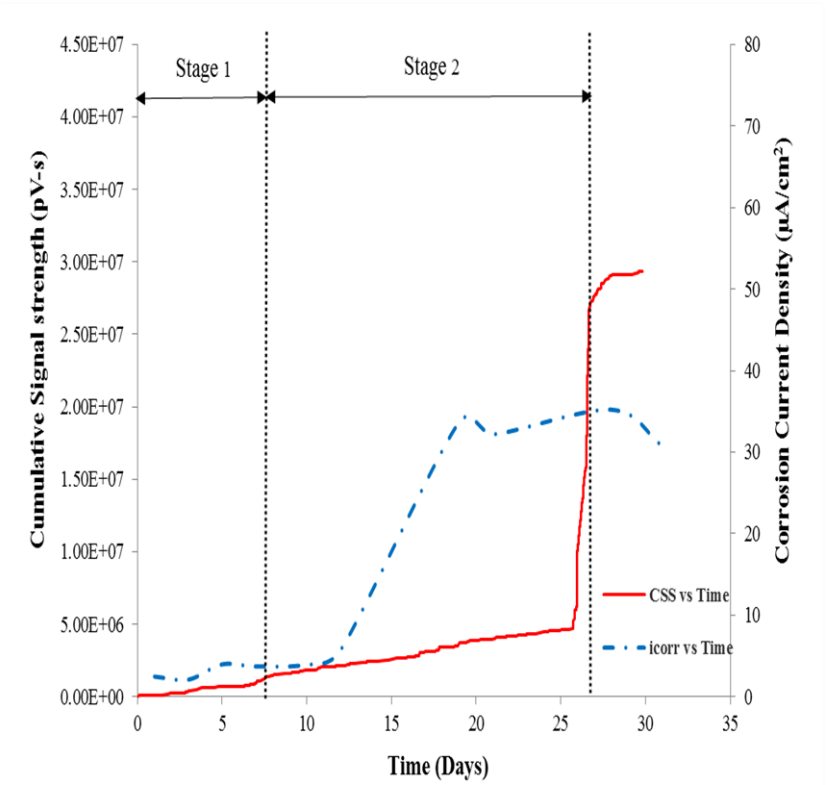

Fig. A-25. Simultaneous evolution of i_{corr} and CSS for actively corroding PT-20 SP-2 specimen

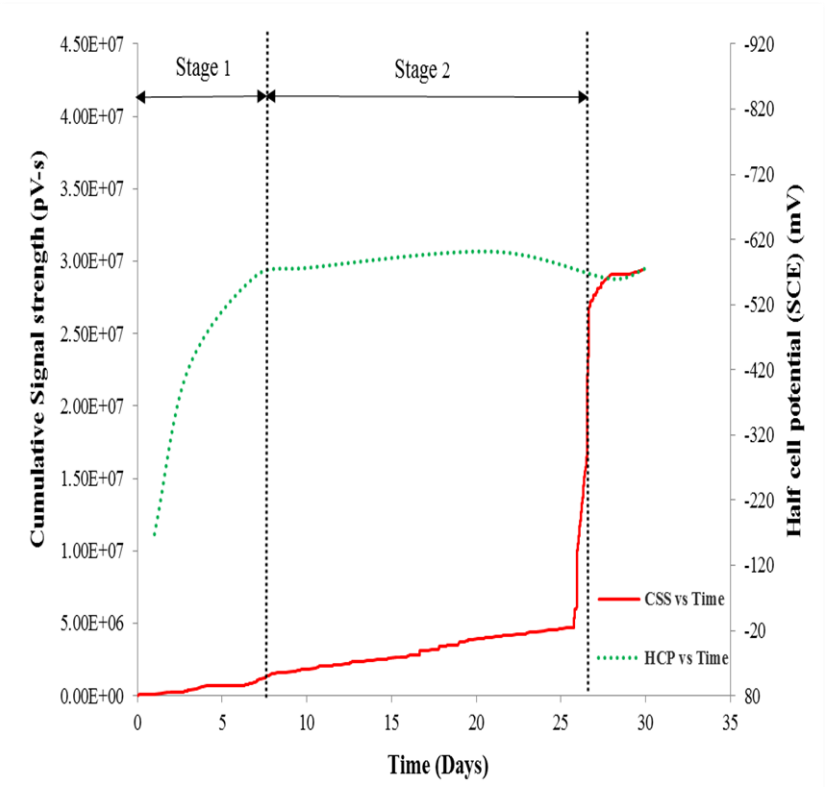

Fig. A-26. Simultaneous evolution of half-cell potential and CSS for actively corroding PT-20 SP-2 specimen

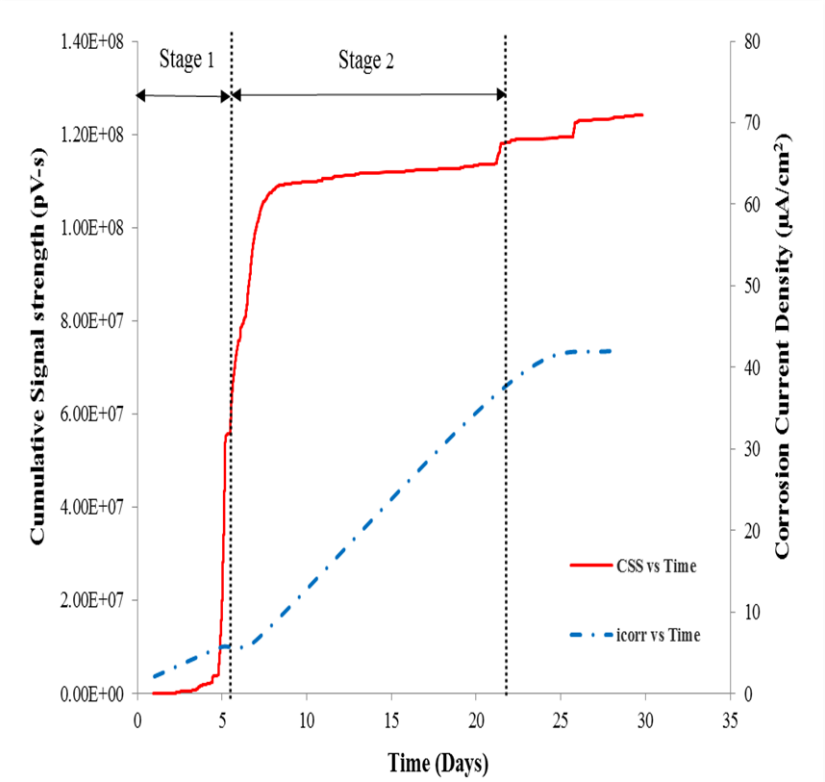

Fig. A-27. Simultaneous evolution of i_{corr} and CSS for actively corroding PT-20 SP-3 specimen

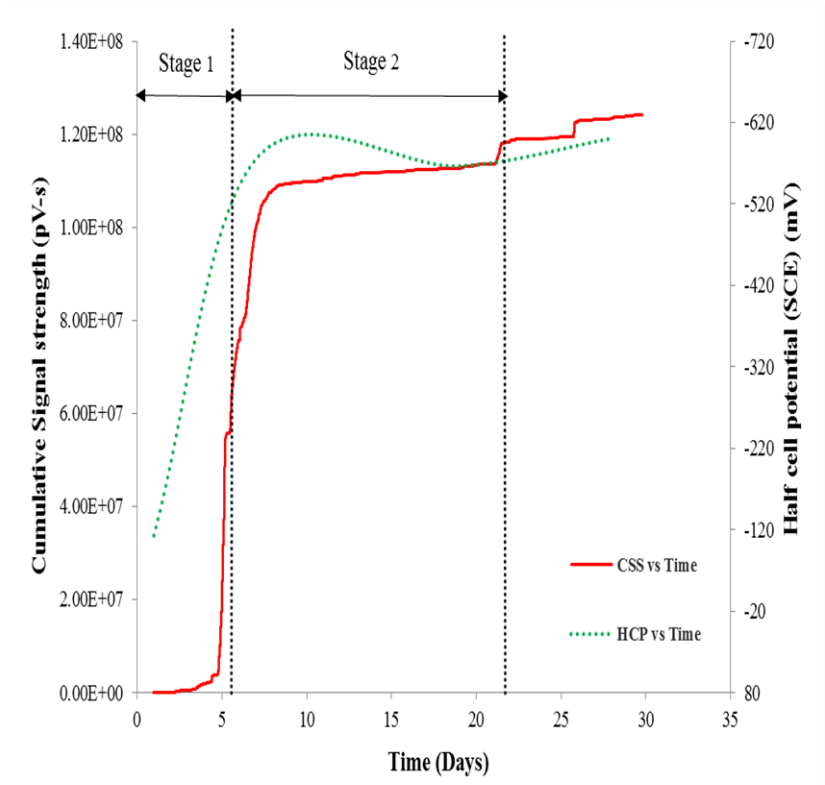

Fig. A-28. Simultaneous evolution of half-cell potential and CSS for actively corroding PT-20 SP-3 specimen

ANNEXURE – B

ANOVA TECHNIQUE

The basic principle of ANOVA is to test for differences among the means of the populations by examining the amount of variation within each of these samples, relative to the amount of variation between the samples (*Kothari C. R., 2004 and Spiegel et al. 2010).* In terms of variation within the given population, it is assumed that the values of (*Xij*) differ from the mean of this population only because of random effects i.e., there are influences on (*Xij*) which are unexplainable, whereas in examining differences between populations we assume that the difference between the mean of the j^{th} population and the grand mean is attributable to what is called a 'specific factor' or what is technically described as treatment effect.

ANOVA can be performed in two different ways:

(1) One-way ANOVA: One-way ANOVA technique is used when the data are classified on the basis of only one factor.

(2) Two-way ANOVA: Two-way ANOVA technique is used when the data are classified on the basis of two factors.

In the present investigation one-way ANOVA was performed to find the effect of variables under study on corrosion and on AE measurements. The step-by-step procedure for the same is described as below.

One-way (or single factor) ANOVA: Under the one-way ANOVA, we consider only one factor and then observe that the reason for said factor to be important is that several possible types of samples can occur within that factor. We then determine if there are differences within that factor. The technique involves the following steps:

(i) Obtain the mean of each sample i.e., obtain

$$\overline{X_1}, \overline{X_2}, \overline{X_3}, \ldots, \overline{X_k} \quad \text{(B.1)}$$

when there are *k* samples.

(ii) Work out the mean of the sample means as follows:

$$\overline{\overline{X}} = \frac{(\overline{X_1} + \overline{X_2} + \overline{X_3} + \cdots + \overline{X_k})}{\text{No.of samples (k)}} \quad \text{(B.2)}$$

(iii) Take the deviations of the sample means from the mean of the sample means and calculate the square of such deviations which may be multiplied by the number of items in the corresponding sample, and then obtain their total. This is known as the sum of squares for variance between the samples (or *SS* between). Symbolically, this can be written:

$$SS\ between = n_1(\overline{X_1} - \overline{\overline{X}})^2 + n_1(\overline{X_2} - \overline{\overline{X}})^2 + \cdots + n_k(\overline{X_k} - \overline{\overline{X}})^2 \quad \text{(B.3)}$$

(iv) Divide the result of the (iii) step by the degrees of freedom between the samples to obtain variance or mean square (MS) between samples. Symbolically, this can be written:

$$MS\ between = \frac{SS\ betweem}{(k-1)} \quad \text{(B.4)}$$

where (k – 1) represents degrees of freedom (d.f.) between samples.

(v) Obtain the deviations of the values of the sample items for all the samples from corresponding means of the samples and calculate the squares of such deviations and then obtain their total. This total is known as the sum of squares for variance within samples (or *SS* within).Symbolically this can be written:

$$SS\ within = \sum(X_{1i} - \bar{X}_1)^2 + (X_{2i} - \bar{X}_2)^2 + \cdots + (X_{ki} - \bar{X}_k)^2 \quad \text{(B.5)}$$

$$i = 1, 2, 3, \ldots$$

(vi) Divide the result of (v) step by the degrees of freedom within samples to obtain the variance or mean square (*MS*) within samples. Symbolically, this can be written:

$$MS\ within = \frac{SS\ betweem}{(n-k)} \quad \text{(B.6)}$$

where ($n - k$) represents degrees of freedom within samples,

n = total number of items in all the samples i.e., $n1 + n2 + \ldots + nk$

k = number of samples.

(vii) For a check, the sum of squares of deviations for total variance can also be worked out by adding the squares of deviations when the deviations for the individual items in all the samples have been taken from the mean of the sample means. Symbolically, this can be written:

$$SS\ for\ total\ variance = \sum\left(X_{ij} - \bar{\bar{X}}\right)^2 \quad \text{(B.7)}$$

$$i = 1, 2, 3, \ldots \ \&\ j = 1, 2, 3, \ldots$$

This total should be equal to the total of the result of the (iii) and (v) steps explained above i.e.,

SS for total variance = *SS* between + *SS* within.

The degrees of freedom for total variance will be equal to the number of items in all samples minus one i.e., ($n - 1$). The degrees of freedom for between and within must add up to the degrees of freedom for total variance i.e.,

$$(n - 1) = (k - 1) + (n - k)$$

This fact explains the additive property of the ANOVA technique.

(viii) Finally, *F*-ratio may be worked out as under:

$$F - ratio = \frac{MS\ between}{MS\ within} \quad \text{(B.8)}$$

This ratio is used to judge whether the difference among several sample means is significant or is just a matter of sampling fluctuations. For this purpose we look into the table (given in relevant text - *Kothari C. R., 2004 and Spiegel et al. 2010*) , giving the values of *F* for given degrees of freedom at different levels of significance. If the

worked out value of *F*, as stated above, is less than the table value of *F*, the difference is taken as insignificant i.e., due to chance and the null-hypothesis of no difference between sample means stands. In case the calculated value of *F* happens to be either equal or more than its table value, the difference is considered as significant (which means the samples could not have come from the same universe) and accordingly the conclusion may be drawn. The higher the calculated value of *F* is above the table value, the more definite and sure one can be about his conclusions.

ANNEXURE – C

Following are the typical photographs showing various stages in corrosion process during testing of Specimen OC-20 SP-1.

Fig. C-1. Specimen before corrosion

Fig. C-2. Condition of specimen after 2 days of testing

Fig. C-3. Condition of specimen after 4 days of testing

Fig. C-4. Condition of specimen after 6 days of testing

Fig. C-5. Condition of specimen at the end of testing

ANNEXURE – D

CASE STUDY FOR APPLICATION OF DEVELOPED MATHEMATICAL MODEL FOR REAL TIME DAMAGE ASSESSMENT OF RC STRUCTURES

INTRODUCTION

The quality assurance of new structures and characterization of structural damages as a function of time and environmental influences has become a serious concern now a days. Many factors can contribute to the deterioration of reinforced concrete structures such as; poor construction, overloading, aging, corrosion of reinforced steel, chemical reactions, natural disasters, etc. Corrosion of reinforcement is a serious problem in reinforced concrete structures and is most difficult to quantify in its early stage of development. A better understanding of the current state of an existing structure helps in maintenance scheduling and funding prioritization. Hence, structural health monitoring of in-service reinforced concrete structures is of a great importance. Continuous monitoring techniques and real time damage detection systems enable early detection of structural deficiencies and provide data to improve existing visual inspection techniques. Non-destructive testing techniques have a large potential to be part of such a system.

For corrosion assessment of real existing structures, qualitative non-destructive techniques such as half-cell potential or concrete resistivity tests are widely used in practice whereas the quantitative techniques like Tafel extrapolation technique, LPR or AC impedance spectroscopy are used for laboratory based research work. The list of various such techniques along with their uses and limitations are discussed in detail in Chapter 1. Owing to various advantages of AE technique over other nondestructive techniques, such as its high sensitivity and ability to detect

damage occurring in real-time, it is a strong candidate for serving as an efficient structural health monitoring tool. Using AE technique, the mathematical model for corrosion assessment has already been developed based on data generated in laboratory testing and is discussed in previous chapters. In the present chapter, the applicability of AE technique using the developed mathematical model for the real structural damage diagnosis is investigated. The details of the investigations are given in subsequent sections.

DAMAGE DIAGNOSIS USING NON-DESTRUCTIVE TECHNIQUES

To investigate the applicability of AE technique using the developed mathematical model for the real structural damage diagnosis, two reinforced concrete slabs were first monitored using well established and practically used non-destructive techniques viz half-cell potential technique and concrete resistivity technique. Subsequently, the same two slabs were continuously monitored using AE technique and the results were compared. The two slabs were selected based on observations collected through visual inspection.

1. **Visual Inspection:** Fig. D-1 and D-2 shows the conditions of two reinforced concrete slabs S_1 and S_2 respectively under study. The two slabs, S_1 and S_2 are located in Room No. E-001 (E- Building) and Room No. A-103 (A- Building) respectively, in the campus of Vishwakarma Institute of Information Technology, Pune.

Fig. D-1. Condition of S_1 reinforced concrete slab selected for testing

Fig. D-2. Condition of S_2 reinforced concrete slab selected for testing

From the visual inspection, it was observed that, the surface of S_1 slab was damaged. The damage was because of the leakage of water percolated from the top. Hence, it was thought that, the reinforcing steel inside this concrete, being continuously in contact with seepage water, might have been subjected to corrosion action. On the

other hand, the surface of slab S_2 was found to be free from any sign of distress. Hence, it was decided to select these two slabs, which are considered to be representative of damaged and undamaged condition of real reinforced concrete structural element respectively.

2. Non-destructive techniques for damage diagnosis:

To assess the condition of above mentioned two slabs, the non-destructive testing was performed using half-cell potential technique using copper/copper sulfate electrode (CSE) and concrete resistivity meter. The tests were performed by the well-known company, "Construction Diagnostic Centre Pvt. Ltd." situated in Pune, who provides services for structural audits. Based on visual inspection observations, it was decided to conduct both half-cell potential as well as concrete resistivity test on slab S_1 as it was found to be partly wet and damaged, whereas for slab S_2, being dry and undamaged, only concrete resistivity test was performed. Before conducting the tests, a layer of plaster above the concrete surface of slabs were removed from different locations. The different locations for testing were selected such as to cover the entire slab. Fig. D-3 and D-4 shows the schematic diagram of different locations selected for testing of slabs S_1 and S_2 respectively.

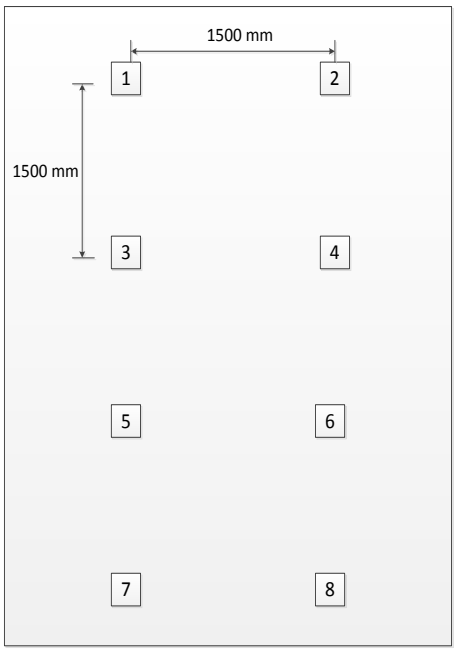

Fig. D-3. Test locations for Slab S_1

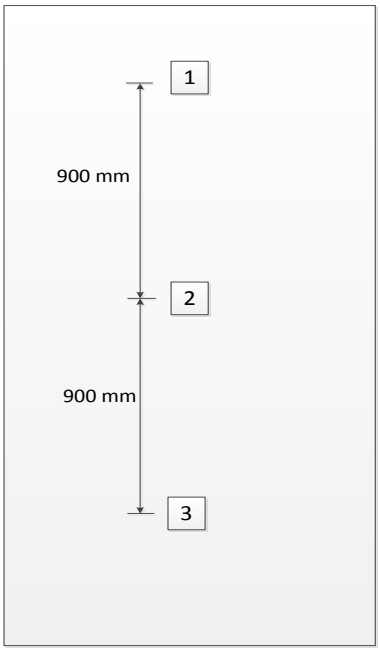

Fig. D-4. Test locations for Slab S2

The details of results of concrete resistivity test and half-cell potential test are presented in Tables D-1 and D-2 respectively.

Table D-1 Test results of Concrete resistivity test

Slab	Reading spacing (mm)	Condition of slab	Location	Resistivity (kΩ cm)	Range of Resistivity (kΩ cm)	Indication of Corrosion Rate
S_1	1500 X 1500	Partly wet, damaged	1	122.22	20 to 200	Low Corrosion Rate
			2	154.56		
			3	127.61		
			4	126.70		
			5	157.08		
			6	123.76		
			7	182.28		
			8	143.50		
S_2	900	Dry, undamaged	1	203.43	Greater than 200	Very Low Corrosion Rate
			2	166.04	20 to 200	Low Corrosion Rate
			3	213.5	Greater than 200	Very Low Corrosion Rate

Table D-2 Test results of half-cell potential technique

Slab	Reading spacing (mm)	Condition of slab	Location	Half-cell potential (mV) (w.r.t. CSE)	Range of half-cell potentials (mV) (w.r.t. CSE)	Corrosion probability
S_1	1500 X 1500	Partly wet, damaged	1	-271	-200 to -350	Uncertain corrosion activity
			2	-253		
			3	-261		
			4	-275		
			5	-260		
			6	-337		
			7	-279		
			8	-132	Less than -200	Greater than 90% probability of no corrosion
S_2	900	Dry, undamaged	Not Performed			

DAMAGE DIAGNOSIS USING AE TECHNIQUE

After completion of non-destructive testing, the two slabs were continuously monitored using AE technique. Observing the values of concrete resistivity and half-cell potentials, location no. 7 from slab S_1 and location no. 1 from slab S_2 (Fig. D-3 and D-4 respectively) were selected for AE monitoring. Two sensors with a spacing of approximately 300 mm were attached to the surface of slabs under study. To fix AE sensors firmly to the slab surface, special U-framed clamping holders were designed and fabricated as shown in Fig. D-5. Fig. D-6 shows the actual photograph of sensor firmly attached to the slab with the help of holder.

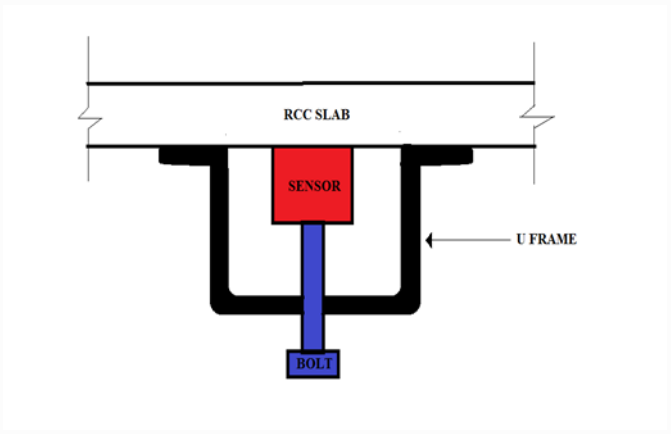

Fig.D-5. U-Shaped clamp designed for holding AE sensor

Fig.D-6. Sensors attached to the slab surface using holders

Both the slabs were monitored for 15 days using AE technique. Fig. D-7 presents the variation of CSS with time for slab S_2. Similar graphs were obtained at each location

of AE testing. Based on this data, using the developed mathematical model as derived in Chapter 5 and presented in Eq. 7.1, the probable mass loss was calculated and presented in Table D-3.

$$\text{Gravimetric mass loss} = (1.407 * \ln\text{CSS}) - 19.49 \quad (7.1)$$

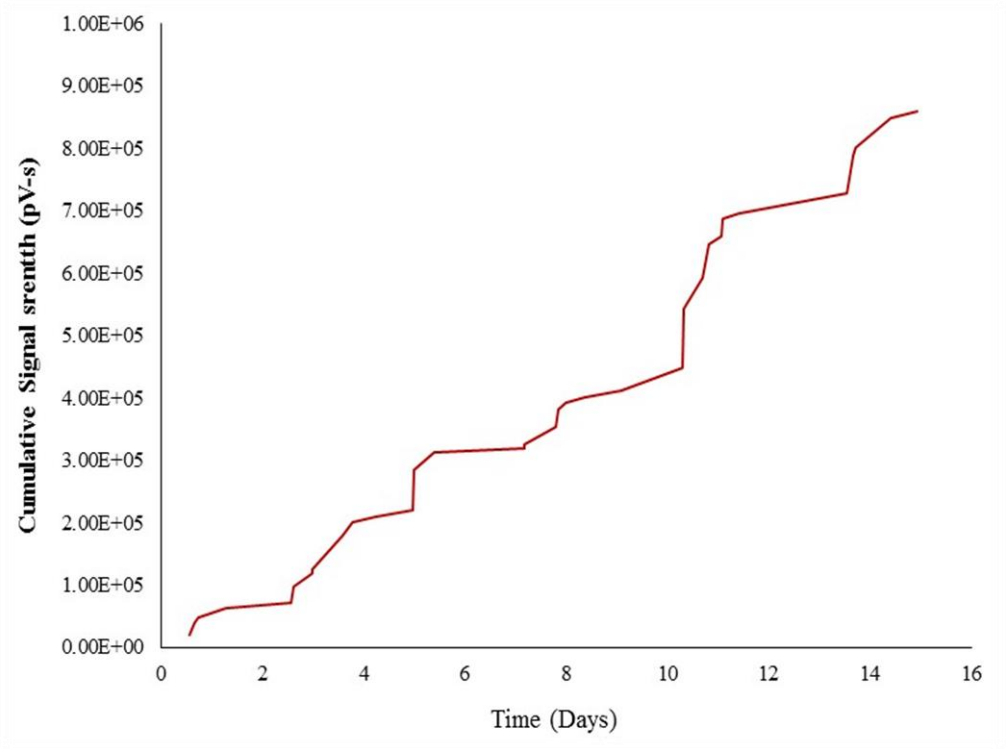

Fig. D-7. Variation of cumulative signal strength with time for reinforced concrete slab S_2

COMPARATIVE ASSESSMENT BASED ON AE AND OTHER TECHNIQUES

Table D-3 summarizes the results of all tests collectively for both these slabs.

From table D-3, it is found that, for the location no.7 on Slab S_1, the probable mass loss value ranges between 0.72 to 3.02 g which indicates the probability of active corrosion at this location. The results of half-cell potential measurements indicated uncertain corrosion activity whereas the concrete resistivity test predicted low corrosion rate. For location no.1 on Slab S_2, the developed mathematical model using AE technique predicted zero mass loss indicating very low or no corrosion activity.

For the same location, the results of concrete resistivity test predicted very low corrosion rate. Thus, from Table D-3 it can be concluded that, the results obtained from AE technique using developed mathematical model are in agreement with the results of well-established non-destructive techniques for real structural element.

Table D-3 Summary of all test results

Slab	Location	Indication of Corrosion Rate by Concrete Resistivity test	Corrosion Probability by half-cell potential test	AE sensor	Probable mass loss using developed mathematical model (g)
S_1	7	Low Corrosion Rate	Uncertain corrosion activity	1	3.02
				2	0.72
S_2	1	Very Low Corrosion Rate	Not Applicable	1	Zero
				2	Zero

CLOSING REMARKS

From the test results of real structural element monitoring using AE technique it can be concluded that, the developed mathematical model can be used appropriately to identify damage to reinforced concrete structure due to corrosion. In practice, for corrosion assessment of real existing structures, qualitative non-destructive techniques such as half-cell potential or concrete resistivity tests are widely used whereas the use of quantitative techniques like LPR, Tafel extrapolation technique or AC impedance spectroscopy is limited due to the fact that the potential scans applied to reinforcing steel during measurements may accelerate the corrosion process. Owing to this background, the use of AE technique (which is truly non-destructive technique) for corrosion assessment of real existing structures will be most helpful.

REFERENCES

1. Alonso C., Andrade C., Rodriguez J. and Diez J.M., (1998), Factors controlling cracking of concrete affected by reinforcement of corrosion. Materials and Structures, 31, 435-441.
2. Angal R. D., Principles and Prevention of Corrosion. Narosa publishing house: New Delhi: India; 2010.
3. ASNT Volume 6, Acoustic Emission Testing, Columbus, USA.2005.
4. Assouli B., Simescu F., Debicki G. and Idrissi H. (2005), Detection and identification of concrete cracking during corrosion of reinforced concrete by acoustic emission coupled to the electrochemical techniques. NDT&E International, 38, 682–689.
5. ASTM C 876-91. Standard Test Method for Half-Cell Potentials of Uncoated Reinforcing Steel in Concrete, West Conshohocken, Pennsylvania; 1999.
6. ASTM E610-82, 1991 Definition of terms related to Acoustic Emission, West Conshohocken, Pennsylvania; 1999.
7. ASTM G 1-03. Standard practice for preparing, cleaning, and evaluating corrosion test specimens. West Conshohocken, Pennsylvania, 2003.
8. ASTM G102-89. 2004. Standard Practice for Calculation of Corrosion Rates and Related Information from Electrochemical Measurements, West Conshohocken, Pennsylvania; 1999.
9. ASTM. E1316. Standard terminology for non-destructive examinations. West Conshohocken, Pennsylvania, 2010.

10. Austin S. A., Lyons R. and Ing M., (2004), Electrochemical behaviour of steel reinforced concrete during accelerated corrosion testing. Corrosion, 60 (2), 203 – 212.
11. Austin S.A., Lyons R. and Ing M.J. The Electrochemical Behaviour of Steel Reinforced Concrete Undergoing Accelerated Corrosion Testing, Corrosion, February 2004.
12. Benavent A., Castro E. and Gallego A., Evaluation of low-cycle fatigue damage in RC exterior beam-column subassemblages by acoustic emission, Construction and Building Materials, vol. 24, 2010, pp.1830–1842.
13. Broomfield J. P. Corrosion of steel in concrete, 2nd edition, Taylor and Francis, Great Britan, 2007.
14. Caré S. and Raharinaivo A., (2007), Influence of impressed current on the initiation of damage in reinforced mortar due to corrosion of embedded steel. Cement and Concrete Research, 37, 1598–1612.
15. Carino N. J., (1999), Nondestructive techniques to investigate corrosion status in concrete structures. Journal of Performance of Constructed Facilities, 13(3), 96-106.
16. Carpinteri A., Lacidogna G. and Pugno N., (2007), Structural damage diagnosis and life-time assessment by acoustic emission monitoring. Engineering Fracture Mechanics, 74, 273–289.
17. Chang C. and Liu C., (2003), Recent Research in Nondestructive Evaluation of Civil Infrastructures. Journal of Materials in Civil Engineering, 15, 298-304.

18. Chen B. and Liu J., (2008), Damage in carbon fiber-reinforced concrete, monitored by both electrical resistance measurement and acoustic emission analysis. Construction and Building Materials, 22, 2196–2201.
19. Chowdhury P.C., (2004), Strategies for resisting corrosion of reinforcement in concrete. The Indian Concrete Journal, 46-51.
20. Colombo I. S., Main I. G. and Forde M. C., (2003), Assessing Damage of Reinforced Concrete Beam Using b-value Analysis of Acoustic Emission Signals. Journal of Materials in Civil Engineering, 15 (3), 280-286.
21. Degala S., Rizzo P., Ramanathan K. and Harries K. A., (2009), Acoustic emission monitoring of CFRP reinforced concrete slabs. Construction and Building Materials, 23, 2016 – 2026.
22. Di Benedetti M., Loreto G., Matta F. and Nanni A., (2013), Acoustic emission monitoring of reinforced concrete under accelerated corrosion. Journal of Materials in Civil Engineering, 25(8), 1022–1029.
23. Di Benedetti M., Loreto G., Matta F. and Nanni A., (2013), Acoustic Emission Historic Index and Frequency Spectrum of Reinforced Concrete under Accelerated Corrosion. Journal of Materials in Civil Engineering,---, 04014059(8).
24. El-Gelany, M. A. (2001). Short-term corrosion rate measurement of OPC and HPC reinforced concrete specimens by electrochemical techniques. Materials and Structures, 34, 426-432.
25. Ervin B. L., Kuchma D. A., Bernhard J. T. and Reis H., (2008), Monitoring corrosion of rebar embedded in mortar using high-frequency guided ultrasonic waves. Journal of Engineering Mechanics, 135(1),09-19.

26. Frankel G. S., (2008), Electrochemical Techniques in Corrosion: Status, Limitations, and Needs. Journal of ASTM International, 5(2), 1-22.
27. Fricker S. and Vogel T., (2007), Site installation and testing of a continuous acoustic monitoring. Construction and Building Materials, 21, 501–510.
28. Gadve S., Mukherjee, A. and Malhotra S. N., (2009), Corrosion of steel reinforcements in FRP wrapped concrete. Construction and Building Materials, 23, 153-161.
29. Gostautas R. S, Ramirez G., Peterman R., J. and Meggers D., (2005), Acoustic emission monitoring and analysis of glass fibre-reinforced composites bridge decks. Journal of Bridge Engineering, 10(6), 713-721.
30. Grosse C. U. and Ohtsu M. (Eds.), Acoustic emission testing, Springer-Verlag Berlin Heidelberg, 2008.
31. Ha T., Muralidharan S., Bae J., Ha Y., Lee H., Park K. and Kim D. K., (2007), Accelerated short-term techniques to evaluate the corrosion performance of steel in fly ash blended concrete, Building and Environment, 42,78–85.
32. Idrissi H. and Limam A., (2003), Study and characterization by acoustic emission and electrochemical measurements of concrete deterioration caused by reinforcement steel corrosion. NDT&E International, 36, 563–569.
33. Ing M., Austin S. and Lyons R., (2005), Cover zone properties influencing acoustic emission due to corrosion, Cement and Concrete Research, 35, 284–295.
34. IS 10262-2009. Concrete mix proportioning – Guidelines. New Delhi: Bureau of Indian Standards.

35. IS 383-1970 (Reaffirmed 2002). Specification for coarse and fine aggregates from natural sources for concrete. New Delhi: Bureau of Indian Standards.
36. IS 5816 – 1999. Splitting tensile strength of concrete method of test. New Delhi: Bureau of Indian Standards.
37. IS. 516-1959. Methods of tests for strength of concrete., Bureau of Indian Standards, New Delhi.
38. IS: 12269-1999. Specification for 53 grade Ordinary Portland Cement. New Delhi: Bureau of Indian Standards.
39. IS: 1489 (Part I) – 1991. Portland Pozzolana Cement Specification. New Delhi: Bureau of Indian Standards.
40. IS: 1786 - 1990. Specification for High strength deformed steel bars and wire for concrete reinforcement. New Delhi: Bureau of Indian Standards.
41. Kawasaki Y., Tomoda Y. and Ohtsu M., (2010), AE monitoring of corrosion process in cyclic wet–dry test. Construction and Building Materials, 24(12), 2353-2357.
42. Kawasaki Y., Wakuda T., Kobarai T. and Ohtsu M., (2013), Corrosion mechanisms in reinforced concrete by acoustic emission. Construction and Building Materials, 48, 1240–1247.
43. Kelly R. G., Scully J. R., Shoesmith D. W. and Buchheit R. G., Electrochemical Techniques in Corrosion Science and Engineering, Marcel Dekker, Inc. New York, Basel, 2002.
44. Kocur G. K. and Vogel T., (2010), Classification of the damage condition of preloaded reinforced concrete slabs using parameter-based acoustic emission analysis. Construction and Building Materials, 24, 2332–2338.

45. Kothari C. R., Research Methodology - Methods and Techniques. 2nd revised edition, New age international publishers, New Delhi, India, 2004.
46. Kunisue F, Yokoyama Y, Nogami K and Ohtsu M , Quantitative evaluation of dynamic compaction process in fresh concrete, Proc. 1st fib Congress, Session 15-43, 2002.
47. Leelalerkiet V., Shimizu T., Tomoda Y., and Ohtsu M., (2005), Estimation of corrosion in reinforced concrete by electrochemical techniques and acoustic emission. Journal of Advanced Concrete Technology, 3 (1), 137-147.
48. Lura P., Couch J., Jensen O. M. and Weiss J., (2009), Early-age acoustic emission measurements in hydrating cement paste: Evidence for cavitation during solidification due to self-desiccation. Cement and Concrete Research, 39, 861–867.
49. Maaddawy T. and Soudki K., (2003), Effectiveness of impressed current technique to simulate corrosion of steel reinforcement in concrete. Journal of Materials in Civil Engineering, 15(1), 41-47.
50. Masoud S. and Soudki K., (2006), Evaluation of corrosion activity in FRP repaired RC beams, Cement & Concrete Composites, 28, 969-977.
51. Mehta P. and Monteiro Paulo J.M.,(2006), Concrete Microstructure, Properties and Materials. Tata McGraw-Hill Publishing Company Limited, New Delhi, pp. 387-446.
52. Melchers R. E. and Li C. Q., (2006), Phenomenological modeling of reinforcement corrosion in marine environments. ACI Materials Journal ,103(1), 25-32.

53. Mirmiran A. and Philip S., (2000), Comparision of acoustic emission activity in steel-reinforced and FRP-reinforced concrte beams. Construction and Building Materials, 14, 299-310.
54. Montemor, M. F., Simoes, A. M. P., and Ferreira, M. G. S. (2003). Chlorideinduced corrosion on reinforcing steel: from the fundamentals to the monitoring techniques. Cement & Concrete Composites, 25, 491-502.
55. Muralidhara S., Raghu Prasad B. K., Eskandari H. and Karihaloo B. L., (2010). Fracture process zone size and true fracture energy of concrete using acoustic emission. Construction and Building Materials, 24, 479–486.
56. Nair A. and Cai C. S., (2010), Acoustic emission monitoring of bridges: Review and case studies. Engineering Structures, 32,1704-1714.
57. Noorsuhada M. N., Azmi I., Norazura M. B., Shahiron S. and Soffian N. S., (2011), Relationship between acoustic emission signal strength and damage evaluation of reinforced concrete structure: Case studies. IEEE Symposium on Industrial Electronics and Applications 2011, 308-313.
58. Ohno K. and Ohtsu M., (2010), Crack classification in concrete based on acoustic emission Construction and Building Materials, 24(12), 2339–2346.
59. Ohtsu M. and Tomoda Y., (2008), Phenomenological model of corrosion process in reinforced concrete identified by acoustic emission. ACI Materials, Technical Paper.
60. Ohtsu M., Mori K. and Ohno K., (2009), Mechanisms of Corrosion-Induced Cracks in Concrete identified by AE Analysis. Proceedings of the SEM Annual Conference, Albuquerque New Mexico USA.
61. Pollock A. A., (2003), Acoustic emission inspection. Technical report, Physical Acoustic Corporation.

62. Pour-Ghaz1 M., Isgor O. B. and Ghods P., (2009), Quantitative Interpretation of Half-Cell Potential Measurements in Concrete Structures, Journal of Materials in Civil Engineering, 21(9), 467- 475.

63. Poursaee A. and Hansson C. M., (2009), Potential pitfalls in assessing chloride-induced corrosion of steel in concrete. Cement and Concrete Research, 39, 391–400.

64. Pradhan B. and Bhattacharjee B., (2007), Role of Steel and Cement Type on Chloride-Induced Corrosion in Concrete, ACI Materials Journal, 104-M67, 612-619.

65. Pradhan B. and Bhattacharjee B., (2009), Performance evaluation of rebar in chloride contaminated concrete by corrosion rate. Construction and Building Materials, 23, 2346–2356.

66. Pradhan B., and Bhattacharjee B., (2009), Half-Cell Potential as an Indicator of Chloride-Induced Rebar Corrosion Initiation in RC. Journal of Materials in Civil Engineering, 21(10), 543–552.

67. Raghu Prasad B. K. and Vidya Sagar R., (2008), Relationship between AE Energy and Fracture Energy of Plain Concrete Beams: Experimental Study, Journal of Materials in Civil Engineering, 20 (3), 212-220.

68. Ranjith P., Jasinge D., Song J. and Choi S., (2008), A study of the effect of displacement rate and moisture content on the mechanical properties of concrete: Use of acoustic emission. Mechanics of Materials, 40, 453–469.

69. Rens K. , Terry J. W. and Klaiber W., (1997), Review of nondestructive evaluation techniques of civil infrastructure. Journal of Performance of Constructed Facilities, 11,152 – 160.

70. Shah S. G. and Chandra Kishen J. M., Fracture behavior of concrete–concrete interface using acoustic emission technique,Engineering Fracture Mechanics, vol.77, 2010, pp.908–924.

71. Shamsad A., (2009), Techniques for inducing accelerated corrosion of steel in concrete. The Arabian Journal for Science and Engineering, 34 (2C), 95-104.

72. Shigeishi M. , Colombo K.J., Rutledge H. , Batchelor,A. J. and Forde M. C., (2001), Acoustic emission to assess and monitor the integrity of bridges. Construction and Building Materials, 15,35- 49.

73. Song H. and Saraswathy V., (2007), Corrosion Monitoring of Reinforced Concrete structures – A Review. Int. J. Electrochemical sci., Vol. 2, 1-28.

74. Soulioti D., Barkoula N., Paipetis A., Matikas T., Shiotani T. and Aggelis D., (2009), Acoustic emission behavior of steel fibre reinforced concrete under bending. Construction and Building Materials, 23, 3532–3536.

75. Spainhour L. K. and Wootton I. A., (2008), Corrosion process and abatement in reinforced concrete wrapped by fiber reinforced polymer, Cement & Concrete Composites,30, 535-543.

76. Spiegel M. R., Schiller J. J., and Srinivasan R. A. Probability and Statistics. 3rd edition, McGraw Hill education Pvt. Ltd., India, 2010.

77. Switz G., (2004), Evaluation of compliance changes in concrete beams reinforced by glass fiber reinforced plastics using acoustic emission, Journal of Materials in Civil Engineering, 16(5), 414-418.

78. Wheat H. G., (2007), Monitoring corrosion behaviour using acoustic emission techniques. Corrosion 2007. Paper no. 07291. Nashville, Tennessee: NACE International; March 2007.

79. Wootton I. A., Spainhour L. K. and Yazdani N., (2003), Corrosion of steel reinforcement in cabon fiber-reinforced polymer wrapped concrte cylinders, Journal of Composites for Construction, 7(4), 339-347.

80. www.mistrasgroup.gr

81. *www.pacndt.com*

82. Yoon D., Weiss W. and Shah S. P., (2000), Assessing damage in corroded reinforced concrete using acoustic emission. Journal of Engineering Mechanics. 126(3), 273-282.

83. Yun H., Choi W. and Seo S., (2010), Acoustic emission activities and damage evaluation of reinforced concrete beams strengthened with CFRP sheets. NDT&E International, 43,(7), 615-628.

84. Yuyama S., Yokoyama K., Niitani K., Ohtsu M. and Uomoto T., (2007), Detection and evaluation of failures in highstrength tendon of prestressed concrete bridges by acoustic emission. Construction and Building Materials, 21, 491–500.